

**„Molecular and functional alterations related to growth  
in childhood obesity“**

Dissertation  
zur Erlangung des akademischen Grades  
Dr. rer. nat.  
an der Medizinischen Fakultät  
der Universität Leipzig

eingereicht von: Elena Tamara Kempf, M. Sc.  
Geburtsdatum/ Geburtsort: 24.03.1990 in Coburg

angefertigt an der Universität Leipzig, Medizinische Fakultät, Klinik und  
Poliklinik für Kinder- und Jugendmedizin, Pädiatrisches Forschungszentrum

Betreuerin: Prof. Dr. Antje Körner  
Ko-Betreuerin: Dr. Kathrin Landgraf

Beschluss über die Verleihung des Doktorgrads vom: 22.11.2022







**Table of Contents**

Preliminary remarks .....	I
Abbreviations.....	III
1 Introduction .....	1
1.1 Childhood obesity .....	1
1.2 Linear growth and the GH axis in childhood obesity.....	2
1.3 Obesity-related AT dysfunction and growth-related factors.....	5
1.4 Monogenetic obesity and the leptin-MC4R axis .....	7
2 Aims.....	9
3 Study populations, material and methods .....	10
3.1 Study population .....	10
3.2 Material .....	12
3.2.1 Cell lines and culture media .....	12
3.2.2 Enzymes and reagents.....	14
3.2.3 Plasmids and oligonucleotides .....	16
3.2.4 Equipment and software.....	18
3.3 Methods .....	19
3.3.1 Anthropometric and laboratory measurements .....	19
3.3.2 Preparation of AT samples and assessment of AT function .....	21
3.3.3 Cell culture.....	21
3.3.4 Differentiation of SGBS cells .....	22
3.3.5 Immortalization of SVF cells .....	22
3.3.6 Proliferation and differentiation assays for SVF cells.....	22
3.3.7 siRNA-mediated knockdown of <i>ASIP</i> .....	23
3.3.8 Isolation of nucleic acids and reverse transcription.....	23
3.3.9 Gene expression analyses .....	24
3.3.10 PCR, agarose gel electrophoresis, cloning and sequencing.....	24
3.3.11 Whole genome sequencing and TruSight One Sequencing panel .....	25
3.3.12 5'-RACE PCR .....	26
3.3.13 Generation of luciferase reporter and expression vectors .....	26

## Table of Contents

---

3.3.14	Luciferase assay.....	28
3.3.15	Inhibition of the secretory pathway in SVF cells.....	28
3.3.16	Immunoblotting .....	28
3.3.17	<i>In vitro</i> lipolysis assay.....	29
3.3.18	Bioenergetic profiling .....	30
3.3.19	Statistical analyses .....	30
4	Results.....	33
4.1	Study 1: Alterations in linear growth and endocrine parameters in children with obesity.....	33
4.1.1	Children with obesity are taller until adolescence independent from parental height.....	33
4.1.2	Dynamics in growth velocity are altered in children with obesity .....	35
4.1.3	Pubertal timing and endocrine parameters are altered in childhood obesity .....	36
4.1.4	Height, growth and endocrine factors in underweight children .....	39
4.1.5	Height reference values for children with obesity.....	39
4.2	Study 2: Associations of gene expression of growth-related factors in AT with circulating levels and AT function .....	41
4.2.1	Serum levels of GHBP and IGF-1 are increased in children with overweight/obesity .....	41
4.2.2	Association between gene expression of the factors in AT cells and circulating levels.....	43
4.2.3	Association of GHBP serum levels with steatohepatosis.....	45
4.2.4	<i>GHR</i> , <i>IGF-1</i> and <i>IGFBP-3</i> gene expression is decreased in AT cells in children with overweight/obesity .....	46
4.2.5	<i>GHR</i> , <i>IGF-1</i> and <i>IGFBP-3</i> expression in AT may be related to AT function .....	47
4.2.6	<i>FGFR3</i> expression in AT is associated with obesity and metabolic parameters .....	49
4.3	Study 3: Identification of a potential novel monogenic trait for obesity and tall stature .....	50
4.3.1	Identification of a patient with ectopic <i>ASIP</i> expression.....	50
4.3.2	Identification of a heterozygous tandem duplication in the <i>ASIP</i> locus.....	56
4.3.3	The tandem duplication leads to ectopic <i>ASIP</i> expression .....	58
4.3.4	Phenotypic characterization of the patient and her father.....	60
4.3.5	Effects of <i>ASIP</i> on AT metabolism and mitochondrial function in SVF cells.....	63

4.3.6	Screening for additional patients with ectopic <i>ASIP</i> expression .....	67
5	Discussion .....	68
5.1	Linear growth and endocrine patterns are dynamically altered in children with obesity .....	68
5.2	Contribution of AT to alterations in the GH axis in childhood obesity and associations of growth-related factors with AT function.....	72
5.3	Ubiquitous <i>ASIP</i> expression as a potential monogenic trait for human obesity and tall stature .....	77
5.4	Conclusion .....	81
6	Summary .....	82
7	References .....	87
Appendix.....		V
I. Additional information on study populations.....		V
II. Additional methods .....		XIII
III. Additional results .....		XV
List of Figures .....		XXXII
List of Tables .....		XXXIII
Specification of own scientific contribution .....		XXXIV
Selbstständigkeitserklärung .....		XXXVII
Curriculum Vitae .....		XXXVIII
Publications and conference contributions.....		XL
Acknowledgement .....		XLII





---



## Preliminary remarks

This thesis consists of three studies investigating molecular and functional alterations related to growth in childhood obesity.

After analyzing linear growth and endocrine alterations in children with obesity (Study 1), we investigated if adipose tissue (AT) itself contributes to the deviations in the circulating levels of growth-related factors (Study 2). Looking more deeply into AT biology of children, we additionally examined relations of growth-related factors with AT function (Study 2) and identified a potential novel monogenic trait for human obesity and tall stature (Study 3).

Based on the three studies, I drafted three manuscripts as first author and joined one manuscript as a co-author:

### **Study 1: Alterations in linear growth and endocrine parameters in childhood obesity**

- **Kempf E**, Vogel M, Vogel T, Kratzsch J, Landgraf K, Kühnapfel A, Gausche R, Gräfe D, Sergeyev E, Pfäffle R, Kiess W, Stanik J, Körner A. Dynamic alterations in linear growth and endocrine parameters in children with obesity and height reference values. *EClinicalMedicine*. 2021; 37:100977 [1]

### **Study 2: Growth-related factors and adipose tissue function in childhood obesity**

- **Kempf E**, Landgraf K, Vogel T, Spielau U, Stein R, Raschpichler M, Kratzsch J, Kiess W, Stanik J, Körner A. Contribution of adipose tissue to alterations in the growth hormone axis in childhood obesity and associations with adipose tissue function. **Submitted**.
- Shamsi F, [6 authors], **Kempf E**, [17 authors], Tseng YH. FGF6 and FGF9 regulate *UCP1* expression independent of brown adipogenesis. *Nat Commun*. 2020; 11(1):1421 [2]

### **Study 3: Ubiquitous *ASIP* expression as a potential novel monogenic trait for obesity and tall stature**

- **Kempf E**, Stein R, Hilbert A, Jamra RA, Kühnapfel A, Tseng YH, Schöneberg T, Kühnen P, Rayner W, Zeggini E, Kiess W, Blüher M, Landgraf K, Körner A. A novel human monogenic obesity trait: severe early-onset childhood obesity caused by aberrant overexpression of agouti-signaling protein (*ASIP*). **Submitted**.

This dissertation is written as a monograph, since two of the manuscripts are not yet published. The content of the manuscripts that I drafted myself as a first author is used in this thesis without citing the manuscripts repeatedly within the text. If a figure or table of this thesis is adopted from one of the manuscript or if text is taken over literally, this will be marked by footnotes in the respective paragraph, subchapter or legend.

This dissertation is written in the “we” form, as I could not have done this work on my own. Planning and performing experiments, data analysis and interpretation as well as drafting of the manuscripts was guided by my supervisors and supported by my colleagues. My own contributions to each of the manuscripts are specified in the chapter “Specification of own scientific contribution” (see page XXXIV).

**Abbreviations**

5'-RACE-PCR	5' Rapid amplification of cDNA-ends und polymerase chain reaction
ACTB	Beta actin
ADIPOQ	Adiponectin
AGA	Appropriate for gestational age
AGRP	Agouti-related peptide
AHCY	Adenosylhomocysteinase
ALAT	Alanine aminotransferase
ASAT	Aspartate aminotransferase
ASIP	Agouti-signaling protein
AT	Adipose tissue
ATP	Adenosine triphosphate
BAT	Brown adipose tissue
BMI	Body mass index
BSA	Bovine serum albumin
cDNA	Complementary deoxyribonucleic acid
dATP	Deoxyadenoside triphosphat
dCTP	Deoxycytidine triphosphat
dGTP	Deoxyguanosine triphosphat
DHEA-S	Dehydroepiandrosterone sulphate
DNA	Deoxyribonucleic acid
dTTP	Deoxythymidine triphosphat
EDTA	Ethylenediaminetetraacetic acid
FBS	Fetal bovine serum
FCCP	Carbonyl cyanide-4 (trifluoromethoxy) phenylhydrazone
FGFR3	Fibroblast growth factor receptor 3
FGF6	Fibroblast growth factor 6
FGF9	Fibroblast growth factor 9
FSH	Follicle-stimulating hormone
FT4	Free thyroxin
gDNA	Genomic DNA
GH	Growth hormone
GHBP	Growth hormone binding protein
GHR	Growth hormone receptor
HbA1c	Glycated haemoglobin
HDL	High density lipoprotein
HOMA-IR	Homeostatic model assessment for insulin resistance
HPRT	Hypoxanthine-guanine phosphoribosyltransferase
hsCRP	High sensitivity c-reactive protein
hTERT	Human telomerase reverse transcriptase
IGF-1	Insulin-like growth factor-1
IGF1R	Insulin-like growth factor-1 receptor
IGFBP-3	Insulin-like growth factor binding protein 3
IGFBPs	Insulin-like growth factor binding proteins

## Abbreviations

---

ITCH	Itchy E3 ubiquitin protein ligase
KHCO <sub>3</sub>	Potassium bicarbonate
LDL	Low density lipoprotein
LGA	Large for gestational age
LH	Luteinizing hormone
MC1R	Melanocortin 1 receptor
MC2R	Melanocortin 2 receptor
MC3R	Melanocortin 3 receptor
MC4R	Melanocortin 4 receptor
MC5R	Melanocortin 5 receptor
MCRs	Melanocortin receptors
MRI	Magnetic resonance imaging
mRNA	Messenger ribonucleic acid
NaCl	Sodium chloride
NH <sub>4</sub> Cl	Ammonium chloride
NPY	Neuropeptide Y
OCR	Oxygen consumption rate
PBL	peripheral blood leukocytes
PBS	Phosphate buffered saline
PCR	Polymerase chain reaction
POMC	Proopiomelanocortin
PPARG	Peroxisome proliferator-activated receptor gamma
qRT-PCR	Real-time quantitative reverse transcription polymerase chain reaction
RNA	Ribonucleic acid
SD	Standard deviation
SDS	Standard deviation score
SGA	Small for gestational age
SGBS	Simpson–Golabi–Behmel syndrome
SHBG	Sex-hormone binding globulin
SVF	Stromal vascular fraction
TBP	TATA-box binding protein
TNF- $\alpha$	Tumor necrosis factor alpha
TRIS	Tris(hydroxymethyl)aminomethane
TSH	Thyroid-stimulating hormone
UCP-1	Uncoupling protein 1
WAT	White adipose tissue
$\alpha$ -MSH	alpha-melanocyte-stimulating hormone

## 1 Introduction

### 1.1 Childhood obesity

The obesity rate among children increased 10-fold in the last four decades [3] and pediatric obesity has grown to epidemic proportions worldwide [4, 5] and in Germany [6]. Even though the childhood obesity rate in Germany seemed to stabilize between the years 2005-2015, still 4-10 % of the children were obese and 10-20 % were overweight in 2015 [7]. Alarming, in the last months during the COVID-19 pandemic weight gain in children has increased again [8]. Obesity develops early in life and more than 80 % of the children, who suffered from obesity at the age of 3 years, continued suffering from obesity or overweight in adolescence [9]. In 2016, more than 650 million adults worldwide showed obesity and more than 1.9 billion exhibited overweight [10]. In Germany, in total 62.1 % of all men had overweight (44.0 %) or obesity (18.1 %) and 43.1 % of all women had overweight (28.5 %) or obesity (14.6 %) in 2017 [11].

The pathogenesis of obesity is complex and is promoted by environmental as well as by genetic factors. The fundamental cause of obesity is a long-term energy imbalance with too many calories being taken in and too few calories being expended [12]. There is a variety of environmental conditions favoring obesity, including highly energy-rich foods, growing physical inactivity, stress [12] as well as social aspects such as parental obesity or low socio-economic status [13]. However, some individuals are more susceptible to an obesogenic environment than others. Results from twin, adoption and family studies estimated genetic factors to explain 20-90 % of the body mass index (BMI) variance [14]. Most of the variance might be caused by polygenic variation [15], but also monogenic causes of obesity are described [16] and those mostly manifest early in childhood.

Overweight and obesity are associated with various comorbidities that constitute the leading causes of death, such as cardiovascular disease [17], cancer [18] and stroke [19]. Even in children with obesity, first signs of myocardial dysfunction and first metabolic and endocrine alterations are already detectable [20, 21]. The large number of children and adults affected and the deleterious health consequences highlight the need for ongoing research. We comprehensively need to recognize and understand the molecular and functional alterations causing obesity and promoting obesity-related comorbidities already in children.

One phenomenon not well understood is childhood obesity affecting linear growth. In particular, the role of adipose tissue (AT) in mediating alterations in growth dynamics is poorly known. Vice versa, it is also not fully understood how factors related to growth are involved in AT function and childhood obesity itself. A more targeted investigation of AT biology in children with obesity may not only reveal molecular drivers of altered growth, but might also give new insights into the mechanisms promoting obesity in children.

## 1.2 Linear growth and the GH axis in childhood obesity

Childhood obesity is not only a risk factor for cardio-metabolic comorbidities [22]. It has also been hypothesized that obesity during childhood affects linear growth [9, 23]. However, previous studies provided different observations, showing that growth of children with obesity was enhanced [9, 23] or blunted [24], which might derive from the distinct age ranges and developmental stages of the children investigated in those studies. Between ages 1-14 years children with obesity were taller [9] and BMI gain at ages 2-8 years was associated with increased height gain in early childhood and reduced height gain in adolescence, but not with altered final height [23, 24]. In contrast, it was also reported that in relation to parental height, final height of individuals with obesity was compromised [25]. To decipher whether, which and when exactly alterations in growth dynamics in children with obesity occur a comprehensive study spanning the entire age range from childhood to adolescence is needed.<sup>1</sup>

In general, height is an important indicator for a child's health. For clinical management and individual health surveillance, it is important to correctly assess if a child's growth deviates from the expected pattern and may hence be suggestive for other pathologies, e.g. underlying syndromic or monogenetic disorders [26]. Height reference values for children of a general population are available [23], however, as children with obesity may deviate from those patterns, height reference values specific for children with obesity might help to avoid misinterpretation and unnecessary medical diagnostic work-up for tall stature and growth acceleration in children with obesity. It also is of particular importance to recognize children with obesity being too small for their age, who may be overlooked when applying the current reference values. Therefore, height reference values specifically for children with obesity may be needed to allow clinicians an appropriate assessment of a child's height for its weight status.<sup>1</sup>

Linear growth is a tightly regulated process. The growth hormone (GH)/insulin-like growth factor-1 (IGF-1) axis is the major endocrine system regulating growth [27-29]. IGF-1 is the key regulator of postnatal longitudinal growth and its secretion is regulated by multiple players of the GH axis [30] (Figure 1). Hypothalamic GH releasing hormone and somatostatin drive the pulsatile GH secretion from the anterior pituitary gland [31]. About 50 % of GH is bound to GH binding protein (GHBP), which is the soluble form of the GH receptor (GHR) and regulates the half-life and bioavailability of GH [32]. In humans GHBP is shedded from the cell surface by the tumor necrosis factor- $\alpha$

---

<sup>1</sup> Most of this paragraph was adopted literally from the introduction section of the publication: **Kempf et al., eClinicalMedicine 2021** [1].



converting enzyme [33], while in mice GHBP is generated from an alternative splice variant [32] highlighting the limited comparability of regulation within the GH axis in mouse and man and implying the importance of human studies. When GH binds to transmembrane GHR, expression of *IGF-1* and IGF-1 binding proteins (*IGFBPs*) [34-36] in the liver, and also in several other tissues [37], is induced. Predominantly IGFBP-3 in complex with acid-labile subunit modulates the half-life and bioavailability of circulating IGF-1 [36]. By activating IGF-1 receptor (IGF-1R) IGF-1 finally induces cell proliferation and metabolic effects in target tissues, such as proliferation of chondrocyte in the growth plate of bones [38, 39].<sup>2</sup>

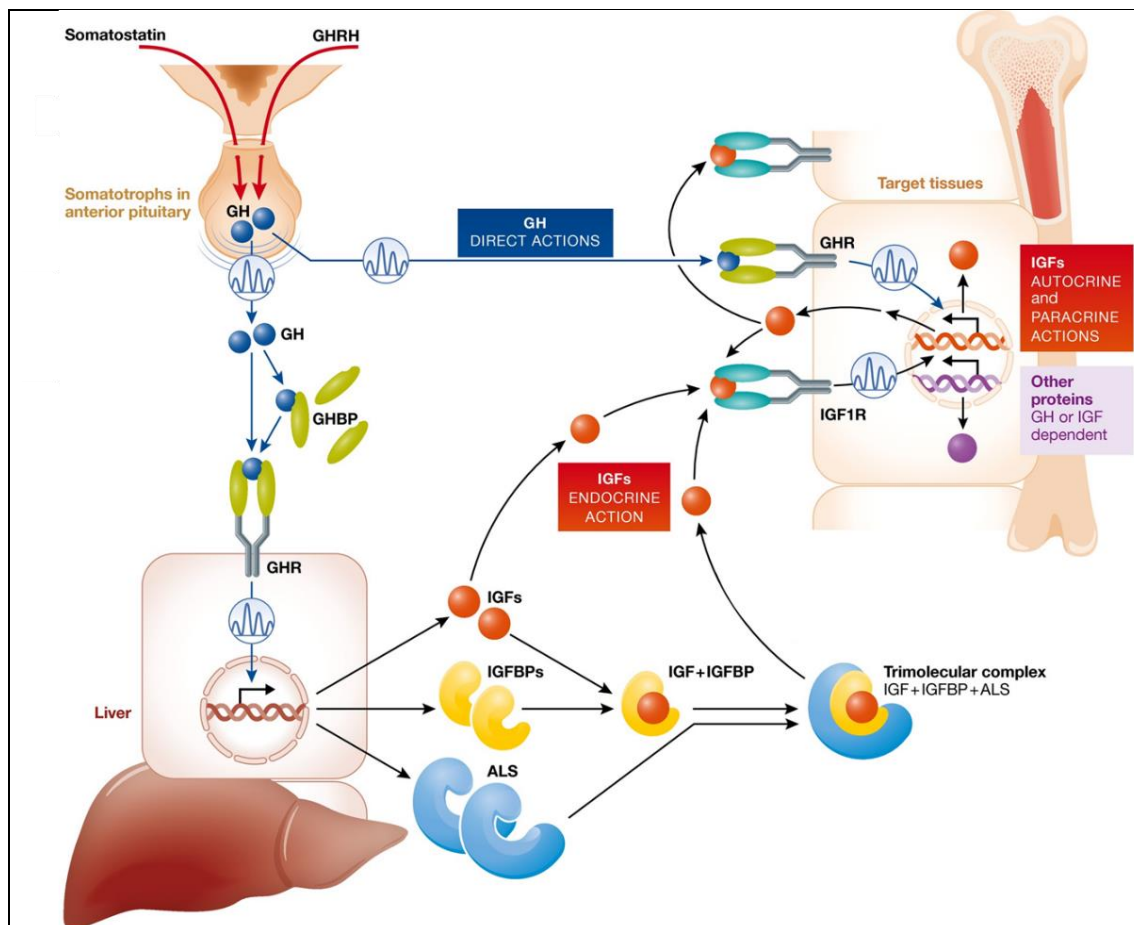


**Figure 1. The GH axis**

Upon stimulation with growth hormone (GH) releasing hormone (GHRH), GH is secreted in a pulsatile manner from the anterior pituitary gland and in part is bound by GH binding protein (GHBP) in the circulation. GH activates the GH receptor (GHR) on target tissues inducing direct effects on target cells and in the liver inducing the production of insulin-like growth factor-1 (IGF1), IGF-1 binding proteins (IGFBPs) and acid-labile subunit (ALS), which form a ternary complex. Free IGF-1 binds to its receptor on target cells and induces e.g. bone growth. This figure was adopted from Argente *et al.*, *EMBO Mol Med* 2017 [40] and modified.

<sup>2</sup> Most of this paragraph was adopted literally from the introduction section of the manuscript: **Kempf *et al.***: Contribution of adipose tissue to alterations in the growth hormone axis in childhood obesity and associations with adipose tissue function. **Submitted.**

Production, bioavailability and signaling of IGF-1 are not only modulated by IGFBPs [27], but also by thyroid hormones [39] and sex steroids [41]. Also, insulin as an anabolic hormone might affect growth through the suppression of GH secretion [27] or due to structural similarity to IGF-1 by interfering with IGF-1 signaling and IGFBPs levels [27]. Another hormone potentially accelerating growth is AT-derived leptin [27], which is linked to the GH axis, to pubertal development [42] and to bone formation [43]. Those and several other hormones are involved in the regulation of growth. With obesity the circulating levels of these growth-related factors may be altered [27, 42] and this may lead to deviations in linear growth in childhood obesity [27-29]. GH serum levels tend to be reduced in children with obesity [28], while the association of obesity with IGF-1 is inconsistent and seems to be related to age [29, 44, 45]. As most of those growth-related hormones are dynamically regulated during physical development [46], differences between normal-weight children and children with obesity are difficult to dissect as they are highly age-dependent. Anthropometric data and serum levels of the endocrine factors must be investigated throughout all ages from birth to adulthood and a high resolution of age groups is necessary in order to disentangle associations of endocrine alterations with growth in childhood obesity.<sup>3</sup>

Furthermore, it is important to investigate the mechanisms behind the deviations in growth and to ask why circulating levels of growth-related factors are changed with childhood obesity. The liver is considered to be the main source of several circulating growth factors and their binding proteins including GHBP [47, 48], IGF-1 [49, 50] and IGFBP-3 [15]. Nevertheless, these factors are additionally expressed in various other cell types, including AT cells [51-53], and there is still uncertainty about the contribution of other tissues to the circulating levels [54, 55]. Most of the studies addressing this question have been performed in mice and data regarding humans and specifically children, where the growth hormone axis is most important, are sparse.<sup>4</sup>

With obesity the endocrine function of AT is dysregulated [56], which may also affect the generation of growth-related factors. Taking into account the increased amount of fat tissue, which produces the growth-related factors, in children with obesity AT may constitute the major source contributing to the alterations in circulating levels that finally lead to deviations in linear growth.

---

<sup>3</sup> Most of this paragraph was adopted literally from the introduction section of the publication: **Kempf et al., eClinicalMedicine 2021** [1].

<sup>4</sup> Most of this paragraph was adopted literally from the introduction section of the manuscript: **Kempf et al.**: Contribution of adipose tissue to alterations in the growth hormone axis in childhood obesity and associations with adipose tissue function. **Submitted**.

### 1.3 Obesity-related AT dysfunction and growth-related factors

In humans, AT can be distinguished into two types, the white AT (WAT) and the brown AT (BAT). The function of both types of AT can be compromised with obesity. WAT is a complex organ and plays a pivotal role in the regulation of energy homeostasis. On the one hand, WAT serves as reservoir for energy storage and utilization [57]. In a high-energy state, signals like insulin promote the uptake of excess lipids and the storage as triglycerides in adipocytes in order to prevent ectopic lipid deposition leading to adverse metabolic events [58]. In a low-energy state, signals such as catecholamines trigger lipolysis in adipocytes and the release of lipids in the form of non-esterified fatty acids into the bloodstream in order to provide energy for target tissues [58]. On the other hand, WAT is an endocrine organ secreting factors, so-called adipokines, to regulate metabolism and food intake. The first classical adipokine identified was leptin, which is a long-term regulator of food intake and energy expenditure by activating the leptin-melanocortin 4 receptor (MC4R) signaling pathway in the hypothalamus resulting in satiety [16, 57] (described in detail in Introduction 1.4). Adipocytes also secrete several other adipokines such as adiponectin, interleukin 6 and tumor necrosis factor- $\alpha$  (TNF- $\alpha$ ), which regulate processes like insulin sensitivity [59] and tissue inflammation [60]. In healthy normal-weight individuals, adipokine secretion from AT is well-balanced and helps to maintain an equilibrium between energy intake and energy expenditure as well as a healthy AT plasticity.

In a long-term state of overnutrition, WAT mass is expanding due to an increase in adipocyte size (hypertrophy) or formation of new adipocytes through differentiation of resident preadipocytes (hyperplasia) or a combination of both [61]. Adipocyte hyperplasia is considered as the healthy mechanism of AT expansion, while adipocyte hypertrophy has been associated with several adverse processes such as inflammation, fibrosis, hypoxia and endocrine and mitochondrial dysfunction [57]. When adipocytes expand in size they are exposed to increased mechanical stress due to increased contact with neighboring cells and extracellular matrix components [62]. In addition, hypoxic conditions can develop with increasing adipocytes sizes approaching the limits of oxygen diffusion [62]. Both mechanisms promote AT inflammation [62]. Hypertrophic WAT is characterized by a high infiltration of immune cells and AT inflammation is associated with the development of insulin resistance and systemic inflammation [63]. This is accompanied by a shift towards enhanced production of pro-inflammatory adipokines, such as TNF- $\alpha$ , in AT and a reduction of favorable adipokines, such as adiponectin. Also leptin expression is increased in hypertrophic adipocytes [64], and leptin serum levels are increased in obesity, which can lead to leptin resistance [65]. Leptin resistance

increases the susceptibility to diet-induced obesity by reducing satiety and hence further exacerbates obesity and leptin resistance in a vicious circle [64]. In summary, with obesity the endocrine function of WAT can be disturbed, which may result in a deterioration of the obese and the metabolic state.

In addition to WAT, there is also BAT present in the human body. Even though BAT is found only in relatively small amounts in adults, it plays a profound role in non-shivering adaptive thermogenesis, a physiological process for dissipating energy in response to cold temperature, diet or  $\beta$ -adrenergic signaling [66, 67]. Brown adipocytes contain a high number of mitochondria, which express high levels of uncoupling protein 1 (*UCP-1*) in the mitochondrial inner membrane [67]. UCP-1 functions as a regulated uncoupler by dissipating the electrochemical proton gradient generated by the respiratory chain, thereby converting energy into heat instead of adenosine triphosphate (ATP) [66]. Besides the classical brown adipocytes so called 'beige' or 'brite' adipocytes can be acquired within WAT upon activation of UCP-1 by external stimuli [67]. Thus, UCP-1 activation and the recruitment of beige adipocytes became a subject of interest for therapeutically targeting obesity in the last years, in particular as it was shown, that BAT activation and thermogenesis is impaired with obesity [68]. And in turn, impaired thermogenesis may promote the progression of weight gain and metabolic disease.

Components of the GH axis, such as IGF-1 [69], as well as other growth factors, such as fibroblast growth factors (FGFs) [70], are expressed in the AT and are part of the intricate network of factors required for healthy WAT and BAT function: GHR signaling for example is known to regulate triglyceride accumulation in adipocytes [71], while IGF-1 [72, 73] and IGFBP-3 [36] are suggested to be involved in WAT expansion and adipogenic differentiation. FGFs are involved in energy homeostasis, in adipocyte development in WAT and in BAT function [70].

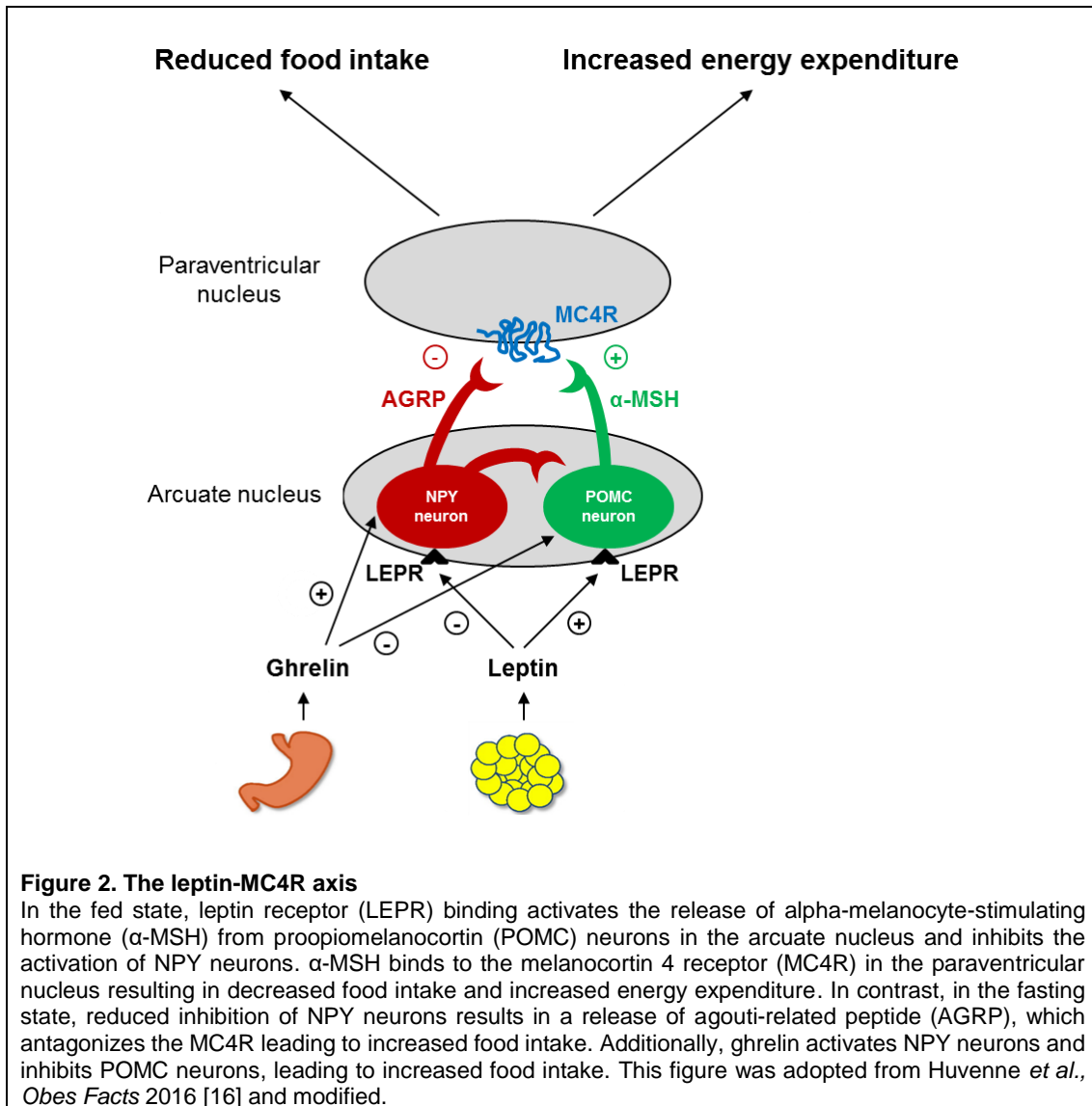
Thus, in children with obesity, altered gene expression of those growth-related factors in AT may not only affect their circulating levels and subsequently linear growth in children, but may additionally promote unhealthy AT expansion and disrupt the function of AT as reservoir for energy storage and utilization as well as its endocrine or thermogenic function.

#### 1.4 Monogenetic obesity and the leptin-MC4R axis

As already mentioned, there are monogenic forms of obesity described [16] and those monogenic forms often are associated with alterations in linear growth in children [74, 75]. Even though monogenetic forms are relatively rare [76], with novel high-throughput screening technologies new obesity-causing mutations are increasingly identified in patients [16, 77].

Patients with monogenic obesity often manifest an early-onset of obesity during childhood, which usually is associated with strongly dysregulated eating behavior. In fact, the majority of the so far described monogenic forms of obesity are based on genetic variations within the genes for leptin, leptin receptor, proopiomelanocortin (*POMC*) or *MC4R* that are coding for factors that are part of the leptin-MC4R axis. This axis centrally regulates the feeling of satiety and food intake (Figure 2). The integration of satiety signals from peripheral tissues takes place in the hypothalamus by distinct neuronal populations. In the state of long-term positive energy balance, serum levels of the satiety hormone leptin, which is secreted from AT, are increased. POMC neurons in the arcuate nucleus are activated by leptin binding to its receptor, upon which they release alpha-melanocyte-stimulating hormone ( $\alpha$ -MSH), a molecule derived from the precursor POMC.  $\alpha$ -MSH then activates MC4R in the paraventricular nucleus resulting in a satiety signal [16]. In parallel, neuropeptide Y (NPY) neurons in the arcuate nucleus are inhibited by leptin, thereby inhibiting the release of agouti-related peptide (AGRP), which is an inverse agonist of the MC4R. In a long-term fasting state circulating leptin is reduced. Hence, POMC neuron activation is reduced and inhibition of neuropeptide Y (NPY) neurons in the arcuate nucleus is diminished, promoting food intake. In addition to leptin, ghrelin, an orexigenic peptide released from the stomach, can activate NPY neurons and inhibit POMC neurons leading to increased food intake [78].

The leptin-MC4R pathway also plays a role in linear growth as patients with *MC4R* [74] and *POMC* [75] deficiency were reported to show increased growth during childhood in addition to obesity. Also mice with *Pomc* [79] or *Mc4r* [80] deficiency or *Agrp* [81] showed increased body length. In contrast, leptin or leptin receptor deficient humans [82] and mice [83] were reported to have a decreased height or body length.



Nowadays, patients with diagnosed leptin deficiency can successfully be treated with leptin supplementation [16], and there is progressive research towards therapy options for other monogenic forms of obesity. Only recently the MC4R agonist setmelanotide was approved by the U.S. Food and Drug Administration as the first pharmacotherapy for patients with *POMC* and leptin receptor deficiencies [84, 85]. Hence, as treatment options are progressively available, an early diagnosis of monogenic forms is crucial for providing targeted therapies for affected patients. However, in clinical routine not all patients with obesity are screened for monogenetic obesity [16], and not all monogenic traits for obesity may be identified yet.

## 2 Aims

In this thesis, consisting of three studies, we aimed to investigate molecular and functional alterations related to growth in childhood obesity. Specifically, we wanted to investigate deviations in linear growth as a comorbidity of childhood obesity and the role of AT in the regulation of growth. Furthermore, by analyzing AT biology in children we searched for associations of growth-related factors with AT function and searched for novel molecular alterations causing obesity and overgrowth (Figure 3).

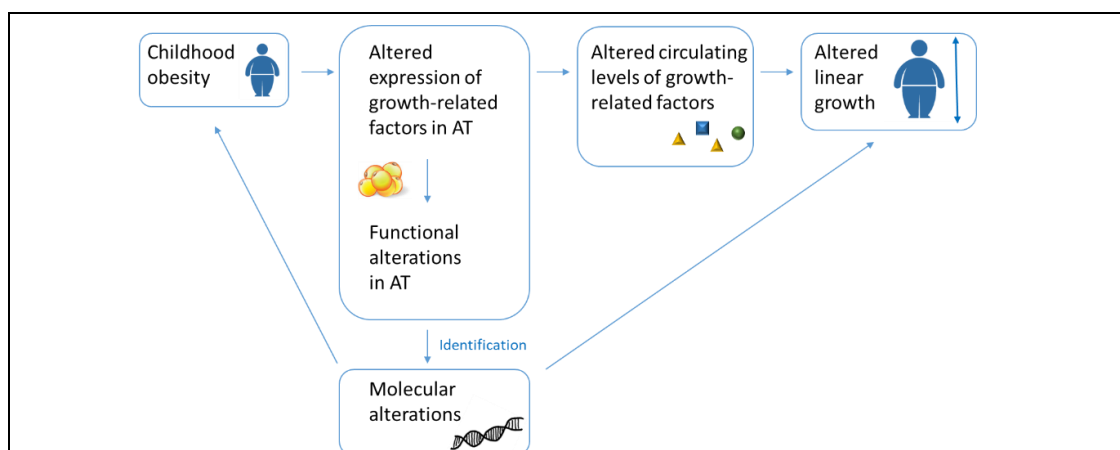


**Figure 3. Aims of this thesis**

We hypothesized that linear growth is altered in childhood obesity and that AT is involved in the regulation of circulating levels of growth-related factors. We furthermore hypothesized that gene expression of growth-related factors in AT is associated with AT function and that by analyzing AT function of children novel molecular alterations causing obesity and overgrowth can be identified.

In study 1, we hypothesized that linear growth of children and adolescents with obesity is altered compared to normal-weight peers. We were particularly interested in the temporal dynamics across age and addressed how parental height, size at birth or changes in growth-related factors are related to the alterations in growth. Additionally, we aimed to generate reference values for height specifically for children with obesity.

In study 2, we hypothesized that overweight-related alterations in circulating levels of the components of the GH axis (*GHBP*, *IGF-1* and *IGFBP-3*) are related to gene expression of these factors in AT and/or increased fat mass. Furthermore, we asked if gene expression of these factors in AT cells is related to overweight/obesity and to AT function. In addition, associations of FGF receptor 3 (*FGFR3*) expression in AT with obesity and metabolic parameters were investigated.

In study 3, we aimed to characterize AT function of a single child with extremely tall stature and severe early-onset obesity and searched for molecular alterations leading to obesity and overgrowth.

### 3 Study populations, material and methods

#### 3.1 Study population

Written informed consent was obtained from all parents (and children when older than 12 years) as well as from all adult participants by the study physicians.

##### Study 1<sup>5</sup>

The study comparing growth and endocrine parameters between children of different weight categories encompassed 8,629 children with 37,493 observations across ages 0-20 years from the population-based LIFE Child [86, 87] (44.3 % of the children) and the obesity-enriched Leipzig Obesity Childhood Cohort [88] (55.7 % of the children) recruited at the University Hospital for Children & Adolescents Leipzig in Germany from 1999 to 2018.

Based on assessment of fit in normal distribution plots (Appendix I, Figure S1), boys and girls with height standard deviation scores (SDS) between -2.5 and 4.0 and BMI SDS  $\geq$  -3.5 were included. Children suffering from diseases such as type 1 diabetes, syndromes and other conditions with severe disability (permanent immobility, cerebral palsy etc.) or with manifest precocious puberty, intracranial hypertension or valproate medication were excluded, as this could affect growth and development. Likewise, individuals taking medications affecting growth (e.g. growth hormone, systemic glucocorticoids, immunosuppressives) were excluded. Exclusively for analyzing insulin and Homeostatic Model Assessment-Insulin Resistance (HOMA-IR) or thyroid hormones, data of children taking metformin or thyroxin, respectively, were excluded (Appendix I, Figure S2). Observations of children born prematurely (gestational week < 38) were included from age at measurement  $\geq$  2.0 years onwards as by then they are supposed to have caught up in height [89]. As such, by then height SDS did not differ significantly between pre-term and full-term normal-weight children (not shown). In total 37,493 observations of 4,319 boys and 4,310 girls (total 8,629 children) were used for analyses and 4,113 children (47.7 %) had at least one follow-up visit.

An overview of the characteristics of the study sample stratified by weight categories and age groups (one observation per individual per age group) is shown in Appendix I, Table S1 and S2. The study was approved by the ethics committee of the University of Leipzig and is registered in the clinical trials data base (NCT02550236, NCT04491344).

---

<sup>5</sup> Most of this subchapter was adopted literally from the methods section of the manuscript: **Kempf et al., eClinicalMedicine 2021** [1].



Height reference values for children with obesity from 0-18 years of age were generated derived from an independent study sample from the German CrescNet registry comprising 12,703 subjects [9, 90]. Within this network, pediatricians regularly transfer pseudonymized weight and growth data from children seen for well-child visits or other consultations. The registry was approved by the Federal Saxonian Data Protection Authority and is registered at the clinical trials database (NCT03072537). Inclusion criteria for the generation of height reference values were defined according to the criteria for the study sample above and are provided in Appendix I, Figure S3. Ruth Gausche (University of Leipzig, Medical Faculty, Growth Network CrescNet, Leipzig, Germany) prepared the data from the Crescnet registry according to the inclusion criteria.

### Study 2<sup>6</sup>

The study sample comprised 306 children aged 2-18 years from the Leipzig AT Childhood Cohort (n=209) [21, 91] and the Leipzig Atherobesity Childhood Cohort (n=97) [88]. Apart from anthropometric and metabolic parameters, for the Leipzig AT Childhood Cohort parameters for AT biology and function and serum GHBP, IGF-1 and IGFBP-3 levels, and for the Leipzig Atherobesity Childhood Cohort serum GHBP and MRI data of body fat and liver fat were available. Participants were recruited at the University Hospital for Children & Adolescents, Leipzig, Germany between the years 2009-2015. We included boys and girls with a BMI SDS higher than -1.88 and a height SDS between -2.5 and 3.5. They were free of diseases (diabetes, generalized inflammation, genetic syndromes or permanent immobility) and children from the Leipzig AT Childhood Cohort were additionally free of medication potentially influencing AT biology. Subcutaneous AT samples were obtained from children undergoing elective orthopedic surgery, herniotomy/orchidopexy or other surgeries as described before [21]. The studies were approved by the local ethics committee (registration no. 265-08, 265-08-ff and 029-2006) and are registered in the National Clinical Trials database (NCT02208141, NCT01605123).

For gene expression analyses of *FGFR3*, data from n=223 children from the Leipzig AT Childhood Cohort [21, 91] were available.

---

<sup>6</sup> Most of this subchapter was adopted literally from the methods section of the manuscript: **Kempf et al.**: Contribution of adipose tissue to alterations in the growth hormone axis in childhood obesity and associations with adipose tissue function. **Submitted.**

### Study 3

The patient, her parents and control children 1-4 were enrolled in the Leipzig AT Childhood Cohort (NCT02208141) [21, 91], control children 5-8 in the Leipzig Obesity Childhood Cohort (NCT04491344). From the patient and control children 1-4 AT samples were obtained from elective surgery (Appendix I, Table S3). Screening for individuals with ectopic *ASIP* expression was performed using already available ILLUMINA HT12v4 gene expression data from blood cells from 1,020 children from the LIFE Child Cohort [99, 100].

## 3.2 Material

### 3.2.1 Cell lines and culture media

Eukaryotic cell lines and prokaryotic strains were used in this work as listed in Table 1.

**Table 1. Cells used in this work**

	Cell line	Description	Source
<b>Eukaryotic</b>	HEK293	Human embryo kidney cell line 293 (ECACC 85120602)	Sigma-Aldrich
	Phoenix-Ampho cells	Human embryo kidney 293T cell line, modified (RRID:CVCL_H716)	ATCC
	SGBS	Human preadipocyte cell line from a patient with Simpson–Golabi–Behmel syndrome	Martin Wabitsch (University of Ulm, Germany) [92]
	3T3-L1	Mouse embryonic fibroblast cell line	Peter Kovacs (University of Leipzig, Germany)
	L929	Murine fibroblast cell line	Torsten Schöneberg (University of Leipzig, Germany)
<b>Prokaryotic</b>	<i>E. coli</i> Top10 or TOP10F'	Competent <i>E.coli</i> cells	Invitrogen

Cells were cultivated and differentiated using different culture media as listed in Table 2.

**Table 2. Culture media used in this work**

Medium	Reagent	Source
Stromal vascular fraction (SVF) cell culture medium	Dulbecco's Modified Eagle's Medium (DMEM)/F-12 (ham) + L-Glutamine + 15mM 4- (2-hydroxyethyl)-1-piperazineethanesulfonic acid (HEPES) 10 % Fetal bovine Serum Superior 100 units penicillin + 0.1 mg/mL streptomycin	Gibco by Life Technologies Biochrom Sigma-Aldrich
Simpson-Golabi-Behmel (SGBS) cell culture medium	SVF cell culture medium 33 µmol/l biotin 17 µmol/l pantothenic acid	Sigma-Aldrich Sigma-Aldrich
SGBS induction medium	DMEM/F-12 (ham) + L-Glutamine + 15mM HEPES 100 units penicillin + 0.1 mg/mL streptoin 33 µmol/l biotin 17 µmol/l pantothenic acid 0.01 mg/mL human apotransferrin 20 nM insulin 100 nM hydrocortisone 0.2 nM triiodothyronine 25 nM dexamethasone 500 µM isobutyl-1-Methylxanthine (IBMX) 2µM rosiglitazone	Gibco by Life Technologies Sigma-Aldrich Sigma-Aldrich Sigma-Aldrich Sigma-Aldrich Sigma-Aldrich Sigma-Aldrich Sigma-Aldrich Sigma-Aldrich Sigma-Aldrich GlaxoSmithKline
SGBS differentiation medium	DMEM/F-12 (ham) + L-Glutamine + 15mM HEPES 100 units penicillin + 0.1 mg/mL streptomycin 33 µmol/L biotin 17 µmol/L pantothenic acid 0.01 mg/mL human apotransferrin 20 nM insulin 100 nM hydrocortisone 0.2 nM triiodothyronine	Gibco by Life Technologies Sigma-Aldrich Sigma-Aldrich Sigma-Aldrich Sigma-Aldrich Sigma-Aldrich Sigma-Aldrich Sigma-Aldrich
SVF freezing medium	DMEM/F-12 (ham) + L-Glutamine + 15mM HEPES 50 % Fetal bovine Serum Superior 10 % dimethyl sulfoxide (DMSO)	Gibco by Life Technologies Biochrom Sigma-Aldrich
Lonza differentiation medium	according to the Poietics™ human adipose-derived stem cell–adipogenesis protocol	Lonza
HEK293/L929 culture medium	DMEM - high glucose (4500mg/L glucose, +L-Glutamine, +sodium pyruvate +sodium bicarbonate) 10 % Fetal bovine Serum Superior 100 units penicillin + 0.1 mg/mL streptomycin	Sigma-Aldrich Biochrom Sigma-Aldrich
LB broth	20 g/L LB broth (Lennox)	Carl Roth
LB Agar	35 g/L LB Agar (Lennox)	Carl Roth

### 3.2.2 Enzymes and reagents

Enzymes used for digestion, ligation, PCR and reverse transcription reactions or for detaching of adherent cells are listed in Table 3.

**Table 3. Enzymes used in this work**

<b>Enzymes</b>	<b>Source</b>
Collagenase IV	Sigma-Aldrich
DNase I	Thermo Fisher Scientific
DreamTaq DNA Polymerase	Thermo Fisher Scientific
<i>EcoRI</i>	Thermo Fisher Scientific
M-MLV Reverse Transcriptase	Thermo Fisher Scientific
<i>NcoI</i>	Thermo Fisher Scientific
PfuTurbo DNA Polymerase	Agilent Technologies
RNaseOUT™ Recombinant Ribonuclease Inhibitor	Thermo Fisher Scientific
<i>SacI</i>	Thermo Fisher Scientific
T4 DNA Ligase	New England Biolabs
Trypsin-(Ethylenediaminetetraacetic acid) EDTA Solution	Thermo Fisher Scientific
<i>XbaI</i>	Thermo Fisher Scientific
<i>XhoI</i>	Thermo Fisher Scientific

Ultrapure water was prepared using the Milli-Q® Integral System from Merck. A list of reagents used for experiments is shown in Table 4. All kits, antibodies and recombinant proteins used are mentioned in section 3.3. Methods.

**Table 4. Reagents used in this work**

Reagent	Source
Agarose, wide range	Serva Electrophoresis
Ammonium chloride (NH <sub>4</sub> Cl)	Sigma-Aldrich
Ampicillin	Sigma-Aldrich
Bovine serum albumin (BSA)	Invitrogen
Brefeldin A	BioLegend
Bromophenol blue	Sigma-Aldrich
D-(+)-glucose	Sigma-Aldrich
deoxyadenoside triphosphat (dATP), deoxyguanosine triphosphat (dGTP), deoxycytidine triphosphat (dCTP) and deoxythymidine triphosphat (dTTP)	Carl Roth
Ethanol	Merck
Gelatine	Sigma-Aldrich
Geneticin	Gibco by Life Technologies
Hoechst 33342	Sigma-Aldrich
Isopropanol	Carl Roth
Kanamycin sulphate	Carl Roth
L-glutamine	Sigma-Aldrich
Methanol	J-T. Baker
Monensin	BioLegend
Nile red	Sigma-Aldrich
Oil Red O	Sigma-Aldrich
Phosphate buffered saline (PBS)	Invitrogen
Polybrene	Sigma-Aldrich
Potassium bicarbonate (KHCO <sub>3</sub> )	Merck
RedSafe Nucleic Acid Staining Solution	iNtRON Biotechnology
Roti®-Histofix 4 %	Carl Roth
Sodium chloride (NaCl)	Carl Roth
Sodium dodecyl sulphate	Carl Roth
Sodium pyruvate	Sigma-Aldrich
Ethylendiamintetraacetat (EDTA)	Sigma-Aldrich
Tris-(hydroxymethyl)-aminomethan (TRIS)	Carl Roth
Triton X-100	Sigma-Aldrich
Trypan blue solution	Sigma-Aldrich
Tween 20	Sigma-Aldrich
Xylencyanol FF	Sigma-Aldrich
β-mercaptoethanol	Sigma-Aldrich

### 3.2.3 Plasmids and oligonucleotides

Plasmids used in this work are listed in Table 5.

**Table 5. Plasmids used in this work**

Name	Method	Selection marker	Source
pBABE-neo-hTERT	Immortalization of SVF cells	Amp <sup>r</sup> ; Neo <sup>r</sup>	Addgene (1774)
pCRII-TOPO	TA-cloning vector	Amp <sup>r</sup> ; Kan <sup>r</sup>	Invitrogen
pCMV6-ASIP-Myc-DDK	<i>ASIP</i> overexpression	Kan <sup>r</sup> ; Neo <sup>r</sup>	OriGene Technologies, Inc. (RC222654)
pCMV6-ASIP	<i>ASIP</i> overexpression	Kan <sup>r</sup> ; Neo <sup>r</sup>	OriGene Technologies, Inc. (SC303053)
pCMV6-entry	control for <i>ASIP</i> overexpression	Kan <sup>r</sup> ; Neo <sup>r</sup>	OriGene Technologies, Inc. (PS100001)
pGL3-Basic	Dual-luciferase assay/ <i>ASIP</i> overexpression	Amp <sup>r</sup>	Promega (E175A)
pRL-CMV	Dual-luciferase assay	Amp <sup>r</sup>	Promega (E226A)
pASIP-EV1-L0007	<i>ASIP</i> overexpression	Kan <sup>r</sup>	Taconic Bioscience

Amp, ampicillin; neo, neomycin; kan, kanamycin

Primers used in this work have been bought as TaqMan Assays from Thermo Scientific (Applied Biosystems) (dye: FAM, quencher: MGB) (Table 6) or have been synthesized by biomers.net (Table 7). Primers target complementary deoxyribonucleic acid (DNA) (cDNA) or genomic DNA (gDNA). Primers used for colony PCR or sequencing of the *ASIP* or *ITCH* (Itchy E3 ubiquitin protein ligase) promoter regions are listed in Table 8. Primers for 5' Rapid amplification of cDNA-ends polymerase chain reaction (5'-RACE PCR) and the generation of pGL3-vector constructs are described in the Methods 3.3.12 and 3.3.12.

**Table 6. TaqMan Assays used for quantitative real-time PCR**

Target gene	TaqMan Assay	Target gene	TaqMan Assay
<i>AHCY</i>	Hs04183463_g1	<i>MC2R</i>	Hs00300820_s1
<i>IGFBP-3</i>	hs00365742_g1	<i>MC3R</i>	Hs00252036_s1
<i>ITCH</i>	Hs00395201_m1	<i>MC4R</i>	Hs00271877_s1
<i>MC1R</i>	Hs00267168_s1	<i>MC5R</i>	Hs00990431_s1

*AHCY*, adenosylhomocysteinase; *IGFBP-3*, insulin-like-growth factor-1 binding protein 3; *ITCH*, Itchy E3 ubiquitin protein ligase; *MC1/2/3/4/5R*, melanocortin 1/2/3/4/5 receptor

**Table 7. Primer sequences for quantitative real-time PCR**

Target gene	Primer, forward	Primer, reverse	Probe	Dye/Quencher or SYBR green
human primers:				
<i>ADIPOQ</i>	GGCCGTGAT GGCAGAGAT	CCTTCAGCC CCGGTACT	CGATGTCTCCCTTAGG ACCAATAAGACCTGG	FAM/TAMRA
<i>AHCY</i> Intron 3	GTCCTGACCACTG CTGAGTT	CTGCTCCAGGGA ACAACCTCT		SYBR green
<i>AP2</i>	GCTTTTGTAGGTAC CTGGAAACTTG	ACACTGATGATC ATGTTAGGTTTG G	CCTGGTGGCAAAGCC CACTCCTCAT	FAM/TAMRA
<i>ASIP</i>	CAACTCCTCTGTGA ACCTACTGGAT	TGCCGATCTGTT TGGATTCT	CCCTTCTGTCTCTATT GTGGCGCTGAAC	FAM/TAMRA
<i>ASIP</i> breakpoint	CACCCTCCATTTGT CTGCAC	GTGAGCAAGGG ACGTTTCAG	---	SYBR green
<i>GHR</i>	TTGGAATATTTGGG CTAACAGTGA	CCTCCTCTAATTT TCCTTCCTTGAG	AGGATTAATAATGCTGA TTCTGCCCCCAG	FAM/TAMRA
<i>HPRT</i>	GGCAGTATAATCC AAAGATGGTCAA	GTCTGGCTTATA TCCAACACTTCG T	CAAGCTTGCTGGTGAA AAGGACCCC	FAM/TAMRA
<i>IGF-1</i>	GCAATGGGAAAAA TCAGCAG	GAGGAGGACAT GGTGTGCA	CTTCACCTTCAAGAAA TCACAAAAGCAGCA	FAM/TAMRA
<i>IGF-1R</i>	TGCAGCGCCTCCA ACTTC	GGTCACTGGCCC AGGAAT	ATCTGCTCCTGCGGGC ATAGTCCT	FAM/TAMRA
<i>InsR-A</i>	TGAGGATTACCTG CACAACG	ACCGTCACATTC CCAACATC	TCCCCAGGCCATCT	FAM/TAMRA
<i>InsR-B</i>	CGTCCCCAGAAAA ACCTCTTC	GGACCTGCGTTT CCGAGAT	CCGAGGACCCTAGGC	FAM/TAMRA
<i>ITCH</i> breakpoint	TGGAGAAAAGGAA TCATCAGAGGA	ATGGCTGTTTAT CCCCTCC	---	SYBR green
<i>ITCH-ASIP</i> fusion	TGGAGAAAAGGAA TCATCAGAGGA	GTGGTGAAGCAAG GGACGTTTCAGC	---	SYBR green
<i>PPARG</i>	GATCCAGTGGTTG CAGATTACAA	GAGGGAGTTGG AAGGCTCTTC	TGACCTGAAACTTCAA GAGTACCAAAGTGCAA	FAM/TAMRA
<i>ACTB</i>	CGAGCGCGGCTAC AGCTT	CCTTAATGTCAC GCACGATTT	ACCACCACGCGCGAG CGG	FAM/TAMRA
<i>TBP</i>	TTGTAAACTTGACC TAAAGACCATTGC	TTCGTGGCTCTC TTATCCTCATG	AACGCCGAATATAATC CCAAGCGGTTTG	HEX/TAMRA
murine primers:				
<i>Actb</i>	GCTCTGGCTCCTA GCACCAT	GCCACCGATCCA CACCGCGT	TCAAGATCATTGCTCC TCCTGAGCGC	FAM/TAMRA
<i>Tbp</i>	AATCTTGGCTGTAA ACTTGACCTAAAG	CGTGGCTCTCTT ATTCTCATGATG	TCGTGCAAGAAATGCT GAATATAATCCCAAGC	FAM/TAMRA

Primer sequences are given in 5'-3' direction. The last column indicates the dye and quencher used for the TaqMan technology or if SYBR green technology was used. *ADIPOQ*, adiponectin; *AHCY*, adenosylhomocysteinase; *AP2*, adipocyte protein 2; *ASIP*, agouti-signaling protein; *GHR*, growth hormone receptor; *HPRT*, hypoxanthine-guanine phosphoribosyltransferase; *IGF-1*, insulin-like growth factor; *IGF-1R*, IGF-1 receptor; *InsR-A*, insulin receptor isoform A; *InsR-B*, InsR isoform B; *ITCH*, Itchy E3 ubiquitin protein ligase; *PPARG*, peroxisome proliferator-activated receptor gamma; *ACTB*, beta actin; *TBP*, TATA-box binding protein.

**Table 8. Primers used for colony PCR or sequencing**

Target	Primer, forward	Primer, reverse
<i>ASIP</i> promoter	ACTGGAGCTCGTTGAGACTGCAGTGGCC CAAGAT	GATGGAGCTGTTGACATAGGCC
<i>ITCH</i> promoter	AGGCTGGTCTCAAACCTCTG	TCTGGAAAGTCACATTTTTCAAAG
	AGGATAGTGTGGTGGCTTGA	
	GAGACAAGATTTACCATGTTGG	
	AGTGAGCTACTGCGCCCAGC	

Primer sequences are given in 5'-3' direction. *ASIP*, agouti-signaling protein; *ITCH*, itchy E3 ubiquitin protein ligase

### 3.2.4 Equipment and software

Equipment and software used in this work are listed in Table 9.

**Table 9: Equipment and software used in this work**

<b>Method</b>	<b>Equipment</b>
Quantitative PCR	QuantStudio3 real-Time PCR System (Applied Biosystems) and 7500 Real-time PCR Systems (Applied Biosystems)
Photometric measurement	CLARIOstar plate reader (BMG Labtech)
Microscopy	Keyence BZ-8000 microscope (Keyence) and EVOS FL Auto 2 (Thermo Scientific Invitrogen)
Lyophilization	ScanVac SA Speed Concentrator (Labogene)
Bioenergetic measurements	Seahorse XFe24 Analyzer (Agilent Technologies)
Transfection	Neon Transfection System (Thermo Scientific Invitrogen)
	<b>Software</b>
Data preparation, statistical analysis, graphs	Excel (Microsoft)
Data preparation, statistical analysis, graphs	GraphPad Prism 6 (GraphPad Software)
Data preparation, statistical analysis, graphs	Statistica 10 and 13 (Dell)
Data preparation, statistical analysis, graphs	R (Version 3.5.0)
Image analyses	ImageJ (National Institutes of Health)
Genetic analyses	Integrative Genomics Viewer (Broad Institute)



### 3.3 Methods

#### 3.3.1 Anthropometric and laboratory measurements

Anthropometric data, parental data, data regarding pubertal stages and laboratory data from the different study cohorts were documented by the study teams and were available for the analyses. Height, growth velocity and BMI values were transformed to sex- and age-specific national reference data and are given with SDS [23, 93].

For each observation children were classified into one of the following weight categories according to the current BMI SDS as recommended by the German Working Group for Pediatric Obesity Consensus Guideline [94]: underweight (BMI SDS <-1.28), normal-weight ( $-1.28 \leq \text{BMI SDS} \leq 1.28$ ), overweight ( $1.28 < \text{BMI SDS} \leq 1.88$ ) or obese (BMI SDS >1.88). In this thesis, the term “lean children” summarizes children with normal-weight and underweight.

Newborns were classified according to birth length SDS and birth weight SDS, into born small for gestational age (SGA;  $\leq 10^{\text{th}}$  percentiles of the cohort), appropriate for gestational age (AGA;  $< 90^{\text{th}}$  and  $> 10^{\text{th}}$  percentile) and large for gestational age (LGA;  $\geq 90^{\text{th}}$  percentiles) [95]. SDS for birth length and birth weight were calculated according to Voigt and corrected for gestational age [96]. Birth data of children born before 38<sup>th</sup> week of gestation were excluded from the analyses. Parental data were obtained from self-reports. The children’s height SDS adjusted for the mid-parental height SDS ( $\text{Height}_{\text{parental adj}} \text{ SDS}$ ) was calculated. For that, mid-parental height SDS was calculated as mean parental height +6.5 cm for boys, and -6.5 cm for girls, with subsequent standardization to SDS using the reference data for 18-years olds [23]. Height SDS adjusted to mid-parental height SDS ( $\text{Height}_{\text{parental adj}} \text{ SDS}$ ) was then calculated as the difference of the child’s height SDS and the mid-parental height SDS. Values between -2.5 and 4.0 were included.

Growth velocities for children at age  $\geq 1.5$  years (mean age between the two height observations) were calculated using consecutive follow-up data (minimum interval length of 3 months, maximum 2 years). Growth velocities <0 cm/year were excluded as well as of <1 cm/year for children aged <14 years as they were inconclusive, since children are supposed to grow at least 1 cm/year until the age of 14 years [93]. Growth velocity SDS values >10 were excluded as they were implausibly high and may result from measurement errors or undocumented disease. Assignment into weight categories was based on the weight status at the first anthropometric observation.<sup>7</sup>

---

<sup>7</sup>The text from the first four paragraphs of this subchapter and the table were adopted literally from the methods section of the publication: **Kempf et al., eClinicalMedicine 2021** [1].

Pubertal stages in study 1 were assessed according to Tanner criteria [97, 98] as shown in Appendix II, Table S4. In study 2 pubic hair stage according to Tanner was used as indicator for pubertal stage.

The MRI data used in study 2 was generated by Prof. Dr. Matthias Raschpichler (University of Leipzig, Medical Faculty, Department of Paediatric Radiology, Leipzig, Germany) and was available for these analyses. The percentage of liver fat and total body fat (MRI) was measured with localized <sup>1</sup>H Magnetic Resonance Spectroscopy and analyzed as previously described [99]. % of liver fat is presented as the mean between the right upper (one measurement) and the right lower (mean from two measurements at the same location) lobe. % of total body fat (MRI) is the sum of % of subcutaneous and visceral AT.<sup>8</sup>

Also data from laboratory measurements were already available for these studies. Blood samples obtained after an overnight fast, were instantly centrifuged and stored at -80°C. Serum levels were measured using standard laboratory protocols by the Institute of Laboratory Medicine of the University of Leipzig, Germany (Appendix II, Table S5). Homeostatic Model Assessment for Insulin Resistance (HOMA-IR) was calculated as [100]:

$$\text{HOMA-IR} = \frac{\text{Insulin [mU/l]} \times \text{Glucose [mmol/l]}}{22.5}$$

Eating behavior in study 3 was assessed by Prof. Dr. Anja Hilbert (University of Leipzig, Medical Faculty, Department of Psychosomatic Medicine and Psychotherapy, Leipzig, Germany) using validated questionnaires: The Eating Disorder Examination-Questionnaire (EDE-Q) [101, 102] was used to assess eating disorder psychopathology regarding the subscales restraint, eating concern, weight concern, shape concern and behavioral features such as binge-eating episodes. Scores from the patient were compared to a reference population of 1,354 women <44 years of age [103]. Scores from the father were compared to a reference population of 1,166 men between 44-64 years of age [103]. The Dutch Eating Behavior Questionnaire (DEBQ) [104] evaluates emotional eating, external eating and restraint using sum scores from Likert scales. Results from the patient were compared to a reference population of 1,394 women between 14-94 years of age [104].

Resting metabolic rate of the patient was examined at the age of 15 years following an overnight fast using an indirect calorimeter (Quark RMR, Cosmed Germany) according to the manufacturer's protocol and expected metabolic rate was calculated according to

---

<sup>8</sup> Most parts of this paragraph were adopted literally from the methods section of the manuscript: **Kempf et al.**: Contribution of adipose tissue to alterations in the growth hormone axis in childhood obesity and associations with adipose tissue function. **Submitted.**

her age, sex, height and body mass. This data was collected by Prof. Antje Körner (University of Leipzig, Medical Faculty, University Hospital for Children and Adolescents, Center for Pediatric Research, Leipzig, Germany).<sup>9</sup>

### 3.3.2 Preparation of AT samples and assessment of AT function<sup>10</sup>

Within the scope of the Leipzig AT Childhood Cohort [21] subcutaneous AT samples were obtained from children undergoing elective surgery and processed as described in detail by Landgraf *et al.* [21]. Data from this cohort regarding phenotype and AT function, as well as cDNA from whole AT, adipocytes and SVF cells were already available and provided for gene expression measurements. SVF cells from the patient and control children were isolated from AT samples as follows. AT was washed in phosphate buffered saline (PBS) and minced. Adipocytes and SVF cells were separated by digestion with a final concentration of 250 units/mL collagenase IV with subsequent processing through a nylon mesh with 400 µm pore size to remove connective tissue, and centrifugation (800 x g, 5 minutes). The SVF pellet was re-suspended in PBS and filtered through a nylon mesh with 30 µm pore size and centrifuged again. Remaining erythrocytes were removed by incubation of the SVF cells in erythrocyte lysis buffer (0.154 M NH<sub>4</sub>Cl, 0.01 M KHCO<sub>3</sub>, 0.1 mM EDTA). SVF cells were frozen in liquid nitrogen in SVF freezing medium. Cells were thawed and 24 hours after seeding cells were washed three times with PBS to select for adipocyte precursor cells via plastic adherence.

### 3.3.3 Cell culture

Eukaryotic cells were cultivated at 37°C and 5 % carbon dioxide and passaged every 3-4 days. SVF cells, immortalized cells and Simpson-Golabi-Behmel syndrome (SGBS) cells [23] were grown in SVF culture medium. HEK293, Phoenix-Ampho and L929 cells were grown in HEK293/L929 culture medium.

---

<sup>9</sup> Most parts of the last two paragraphs were adopted literally from the methods section of the manuscript: **Kempf et al.**: A novel human monogenic obesity trait: severe early-onset childhood obesity caused by aberrant overexpression of agouti-signaling protein (*ASIP*). **Submitted.**

<sup>10</sup> Most parts of this subchapter were adopted literally from the methods section of the manuscript: **Kempf et al.**: A novel human monogenic obesity trait: severe early-onset childhood obesity caused by aberrant overexpression of agouti-signaling protein (*ASIP*). **Submitted.**

### 3.3.4 Differentiation of SGBS cells

80.000 cells were seeded per well in 12-well plates in SGBS culture medium and grown for 2 days. Confluent SGBS cells were differentiated into mature adipocytes under serum free conditions for 12 days as previously described [105], keeping the cells in SGBS induction medium for 4 days and in SGBS differentiation medium for further 8 days. Medium was changed every second day. Cells were harvested for messenger ribonucleic acid (mRNA) analyses at days 0.25, 0.5, 1, 2, 4, 5, 6, 8, 10, 12 post-induction.

### 3.3.5 Immortalization of SVF cells

Primary SVF cells were immortalized as previously described [106, 107]. Prior to hTERT transduction primary SVF cells were cultivated for 20-25 days. Phoenix-Ampho cells (15 cm dish, 60 % confluent) were transfected with 15 µg pBABE-neo-hTERT plasmid using 45 µL PolyJet DNA *in vitro* transfection reagent (SignaGen) according to the manufacturer's protocol. Culture supernatants containing the virus were collected every 24 hours after transfection and filtered through a 0.45 µm filter, concentrated overnight using the Retro-X™ Concentrator (Takara Bio) and diluted 1:12.5 in fresh culture medium containing 2 µg/mL polybrene. The virus-conditioned medium was added to the primary cells at a confluence of 50 % with subsequent centrifugation of the cells at 800 x g and 32° C for 90 minutes. Immediately afterwards the medium was changed to SVF culture medium. This procedure was repeated twice within the next two days until the cells reached a confluence of 90 %. Successfully transduced cells were selected with 200-500 µg/mL geneticin for 14 days and were kept in 200 µg/mL geneticin for one further week.

### 3.3.6 Proliferation and differentiation assays for SVF cells<sup>11</sup>

For proliferation assays 3,500 primary or immortalized SVF cells were seeded per well in 96-well plates in 5 replicates and cultivated for 8 days. After 1 and 8 days cell viability was assessed by WST-1 assay (Roche, Applied Bioscience) according to the manufacturer's protocol. Absorbance was measured 4 hours after addition of the WST-1 reagent. Results are shown as fold change of day 8 compared to day 1. Afterwards, cells were fixed, stained with Hoechst 33342 and counted by fluorescence microscopy. The doubling time between day 1 and day 8 was calculated using the following formula [108]:

---

<sup>11</sup> Most parts of this subchapter were adopted literally from the methods section of the manuscript: **Kempf et al.**: A novel human monogenic obesity trait: severe early-onset childhood obesity caused by aberrant overexpression of agouti-signaling protein (*ASIP*). **Submitted.**

$$\text{Doubling time (days)} = \frac{\text{duration (8 days)} * \log_{10}(2)}{\log_{10}(\text{cell number per image day 1}) - \log_{10}(\text{cell number per image day 8})}$$

For differentiation assays 30,000 primary or immortalized SVF cells were seeded per well in 48-well dishes in 3 technical replicates.

Differentiated cells were fixed with Roti®-Histofix 4 %, double-stained with 10 µg/mL Nile red and 40 µg/mL Hoechst 33342 and analyzed by fluorescence microscopy. The percentage of differentiated cells was calculated by the number of counted differentiated cells divided by the total number of cells within an image for a total of three images per cell line. A cell was defined as differentiated when containing at least two lipid droplets. Additionally, the cells were stained with Oil Red O solution (0.3 % in 60 % isopropanol) for 15 minutes, washed with water and photographed. Oil red O was extracted with isopropanol and absorption was measured at 540 nm.

The number of experiments and the time points of cell seeding are indicated in the figure legends.

### 3.3.7 siRNA-mediated knockdown of *ASIP*

Primary SVF cells from the patient were transfected using the Neon Transfection System 100 µL Kit (Invitrogen) using 2 pulses with voltage 1300 V and pulse width 20 milliseconds and a cell density of  $6 \times 10^6$  cells/mL [109]. For transfection, *ASIP*-specific ON-TARGETplus SMARTpool small interfering (si)RNAs and ON-TARGETplus control non-target siRNA (Dharmacon) at a final concentration of 500 nM were used.

For assessing the effect of *ASIP* knockdown on adipogenic differentiation, 200,000 transfected primary patient SVF cells were seeded per well in 12-well format. Cells were grown to confluence for 24 to 48 hours and differentiated according to the Poietics human adipose-derived stem cell–adipogenesis protocol (Lonza) for 12 days. Knockdown efficiency was assessed using qRT-PCR at days 0, 2, 4 and 8 post-induction.

### 3.3.8 Isolation of nucleic acids and reverse transcription

Genomic DNA was extracted from EDTA blood samples using the QIAamp DNA Blood Mini Kit (Qiagen). For RNA isolation from peripheral blood leukocytes (PBL), drawn blood was stabilized in PAXgene® Blood RNA Tubes (PreAnalytix) and incubated at room temperature for two hours prior to isolation. mRNA was isolated from tissue or cells as previously described [109] using the RNeasy Mini Kit (Qiagen) including on-column DNA digestion using DNase I. 200-500 ng RNA were reverse-transcribed into cDNA using the M-MLV Reverse Transcriptase adding random hexamer primers (Promega), and 10 mM of each deoxyadenoside triphosphat (dATP), deoxyguanosine triphosphat (dGTP),

deoxycytidine triphosphat (dCTP) and deoxythymidine triphosphat (dTTP) as well as RNaseOUT™ Recombinant Ribonuclease Inhibitor. As a control one RNA sample was reverse-transcribed without adding reverse transcriptase. Additionally, a no template control was carried along.

RNA or already transcribed cDNA from different human tissues pooled from several individuals were obtained from Clontech-Takara Bio. Skin cDNA was pooled from two individuals and was kindly provided by Dr. Anja Saalbach (Department of Dermatology, Venereology and Allergology, University of Leipzig, Leipzig, Germany).

### 3.3.9 Gene expression analyses

Genome-wide expression was measured using a HumanHT-12 v4 BeadChip array (ILLUMINA) by the Core Unit for DNA technologies of the University Hospital Leipzig.

TaqMan qRT-PCR was performed using the qPCR™ Mastermix Plus - Low ROX (Eurogentec) or the Takyon™ Low Rox Probe Mastermix dTTP Blue (Eurogentec). SYBR green qRT-PCR was performed using the Maxima SYBR Green/ROX qPCR Master Mix (2x) (Thermo Fisher Scientific) and the standard or fast PCR protocol according to the manufacturer's instructions. 2 µL of 1:10 or 1:20 diluted cDNA or gDNA was used as template. Copy numbers were quantified using a standard curve with defined concentration either from a linearized plasmid containing the target sequence or from a reference cDNA. Each qRT-PCR was controlled for contamination with no template controls. Gene expression was normalized to expression of beta-actin (*ACTB*), TATA-box binding protein (*TBP*) and hypoxanthine-guanine phosphoribosyltransferase (*HPRT*) in study 2 and to *ACTB* and *TBP* in study 3. Gene expression measurements were performed in 3 technical replicates. Due to high samples sizes, measurement of *GHR*, *IGF-1* and *IGFBP-3* expression in the Leipzig AT Childhood Cohort in study 2 was performed in unicates.

The total *GHR* and *IGF-1* expression of adipocytes per kg body weight was calculated by multiplying the normalized gene expression levels in adipocytes with the total number of adipocytes (calculated by multiplying the number of adipocytes per kg AT with the total amount of AT mass in kg) and normalized to total body weight of the children.

### 3.3.10 PCR, agarose gel electrophoresis, cloning and sequencing

The human reference genome assembly from December 2013 (GRCh38/hg38) was used. PCR for cloning of DNA fragments was performed using GoTaq® Hot start Colorless Master Mix (Promega) or high fidelity polymerase PfuTurbo DNA Polymerase according to the manufacturer's instructions using primer concentrations of 500 nM each.

Agarose gel electrophoresis was performed according to Sambrook and Russell, 2001 [110]. DNA from agarose gels was purified using the QIAEX II Gel Extraction Kit (Qiagen).

For propagation, DNA fragments were cloned into the pCRII-TOPO vector using the TOPO® TA Cloning® Kit, Dual Promoter and transformed into *E. coli* TOP10F' using the provided protocol for chemical transformation. To DNA fragments amplified with PfuTurbo DNA Polymerase an A-overhang was added prior to cloning according to the manual.

Bacterial suspension was spread on LB-Agar plates containing 100 µg/mL ampicillin or 30 µg/mL kanamycin and incubated overnight at 37°C. Positive clones were selected by blue-white screening if possible. Furthermore, clones were screened for correct insertion by colony PCR performed using GoTaq® Hot start Colorless Master Mix (Promega) and a primer concentration of 900 nM or by control digestion with *EcoRI* after small scale plasmid extraction using the QIAGEN Plasmid Extraction Kit (Qiagen) from overnight cultures in LB medium containing 100 µg/mL ampicillin or 30 µg/mL kanamycin. Plasmids were extracted in large scale using the QIAGEN Plasmid Midi or Maxi Extraction Kit (Qiagen). Sanger sequencing was performed by the Core Unit for DNA technologies of the University Hospital Leipzig using primers targeting the T7 and the SP6 promoter sequences contained in the pCRII-TOPO vector.

### 3.3.11 Whole genome sequencing and TruSight One Sequencing panel<sup>12</sup>

Whole genome sequencing and bioinformatics analyses of the gDNA of the patient and her parents were performed at the DRESDEN-concept Genome Center, TU Dresden: After ultrasonic shearing of 800 ng gDNA (LE220, Covaris) the DNA library preparation was done using the Kapa HyperPlus Kit (Roche) according the manufacturer's instructions. After ligation with uniquely dual indexed adapters, non-ligated adaptors were removed by adding XP beads (Beckmann Coulter) in a ratio of 1:0.9. The DNA libraries were then size selected with XP beads to an average insert size of 300 bp and quantified by qPCR (LightCycler 480, Roche) and the Fragment Analyzer (Agilent). Libraries were sequenced paired end 2 x 150 bp to a coverage > 38X on a NovaSeq 6000 (ILLUMINA). Bioinformatic analysis was performed using the ILLUMINA DRAGEN pipeline (07.021.595.3.7.5) and the Integrated Genome Viewer.

Disease-associated regions of the exome of the patient were investigated the University of Leipzig, Medical Faculty, Institute of Human Genetics, Germany): The TruSight One

---

<sup>12</sup> Most parts of this subchapter were adopted literally from the methods section of the manuscript: **Kempf et al.**: A novel human monogenic obesity trait: severe early-onset childhood obesity caused by aberrant overexpression of agouti-signaling protein (*ASIP*). **Submitted**.

Sequencing panel has been performed after enrichment with Nextera DNA Flex Pre-Enrichment LibraryPrep and Enrichment, IDT for ILLUMINA Nextera UD Indexes and the NextSeq 500/550 High Output v2 kit (300 cycles) using the ILLUMINA NextSeq 500/550. Data were analysed using the software Varvis and Varfeed (Limbus, Rostock).

### 3.3.12 5'-RACE PCR

5'-RACE PCR was performed using the SMARTer™ RACE cDNA Amplification Kit (Clontech Laboratories). RNA from whole blood from the patient was used as template. First, 300 µg of RNA from patient PBL was reverse-transcribed according to the manufacturer's protocol. Then, the reaction was diluted with 100 µL Tricine-EDTA-buffer and 2.5 µL of this '5-RACE ready cDNA was used as template for the first PCR using the *ASIP*-specific primer 5'-TTGAGGCTGAGCACGCGGCAGGAGCAGG-3'. Next, a nested PCR using 2.5 µL of 1:50 diluted product from PCR 1 was performed using the nested *ASIP*-specific primer 5'-CTGCGGAAGAAGCGGCACTGGCAGGAGG-3'. PCR programs are shown in Table 10. PCR products were visualized and purified by agarose gel electrophoresis, cloned and sequenced.

**Table 10. PCR programs for the 5'-RACE PCR**

	Number of cycles	Temperature, duration
<b>Program 1: touch-down PCR</b>	5	94°C, 30 seconds 72°C, 3 minutes
	5	94°C, 30 seconds 70°C, 30 seconds 72°C, 3 minutes
	33	94°C, 30 seconds 68°C, 30 seconds 72°C, 3 minutes
<b>Program 2: nested PCR</b>	33	94°C, 30 seconds 68°C, 30 seconds 72°C, 3 minutes

5'-RACE-PCR, 5' Rapid amplification of cDNA-ends polymerase chain reaction

### 3.3.13 Generation of luciferase reporter and expression vectors

In order to generate pGL3-Basic vectors for luciferase assays containing the *ASIP* (NM001672.2) or *ITCH* promoter (NM031483.7) sequences upstream the luciferase reporter gene, first promoter sequences of *ASIP* and *ITCH* were cloned from gDNA of the patient using the primers listed in Table 11. Promoter sequences as well as the pGL3-Basic vector were cut with *SacI* and *XhoI* and purified. The promoter sequences were ligated into the linearized pGL3-Basic vector according to the ligation protocol for the T4 DNA Ligase (New England Biolabs).

In order to analyze if *ASIP* protein is generated from the *ITCH-ASIP* fusion construct, modified pGL3-Basic expression vectors containing the *ASIP* or the *ITCH-ASIP* mRNA



sequence under control of *ITCH* promoter or no promoter were generated. For that, the luciferase reporter gene was cut out of the pGL3-Basic vector using *NcoI* and *XbaI* and the cloned cDNA sequences were inserted. Subsequently, the *ITCH* promoter sequence was inserted into the vectors using *SacI* and *XhoI*.

**Table 11. Primers used for amplification and cloning of *ITCH* and *ASIP* sequences**

	Primer, forward	Primer, reverse	bp
<b><i>ASIP</i> promoter</b>	ACTG-GAGCTC-GTTGAGACTGCAGTGGCCCAAGAT	ACTG-CTCGAG-CTGAGTGGGACAGAGAAGGTGGTC	1,245
<b><i>ITCH</i> promoter</b>	ACTG-GAGCTC-GAAGTGGTTTTGAAAGTACTTTGCT	ACTG-CTCGAG-AAAGCGCAGGCGCCTGAGCGCG	2,868
<b><i>ASIP</i> cDNA sequence</b>	ACTG-CCATGG-GCCTCCTGGGATGGATGTCACCC	ACTG-TCTAGA-TGGGGGCGCTCAGCAGTTGAGGC	589
<b><i>ITCH-ASIP</i> cDNA fusion sequence</b>	ACTG-CCATGG-AGCTGTGGTCTGGGGCTCGGGAC	ACTG-TCTAGA-TGGGGGCGCTCAGCAGTTGAGGC	438
<b><i>ASIP</i> protein coding sequence</b>	ACTG-GGATCC-ATGGATGTCACCCGCTTACT	ACTG-CTCGAG-TCAGCAGTTGAGGCTGAGC	419

Primer sequences are given in 5'-3' direction. In the last column the size of the PCR product is indicated. bp, base pairs; *ASIP*, agouti-signaling protein; *ITCH*, itchy E3 ubiquitin-protein ligase. Each primer contains a four-nucleotide-overhang (ACTG) and a 6 nucleotide recognition sequence for restriction enzymes at the 5' end. The *ASIP* cDNA sequence comprises the full *ASIP* cDNA sequence from exon 1-3, while the *ASIP* protein coding sequence comprises only the sequence from the start to the end of translation.

A second independent expression vector containing the *ITCH-ASIP* fusion gene (*ITCH-ASIP* cDNA sequence under control of the *ITCH* promoter) was generated by Taconic Bioscience (pASIP-EV1-L0007) (Figure 4). The Taconic plasmid was constructed based on the *ITCH-ASIP* cDNA sequence from the patient identified by 5'-RACE PCR and the *ITCH* promoter sequence shown to drive expression in the luciferase assays (Table 11).

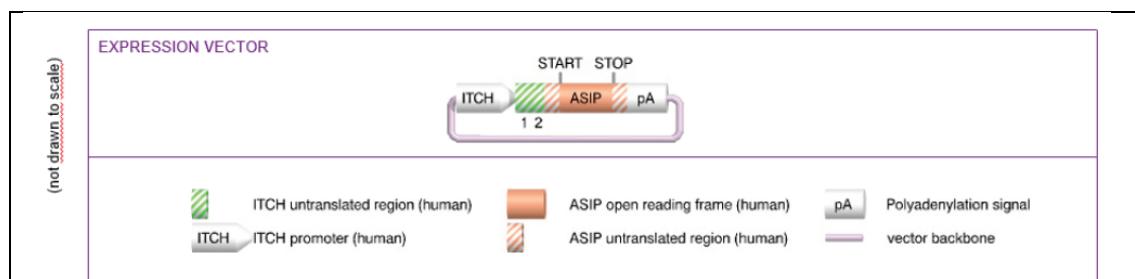


**Figure 4. Taconic expression vector**

This figure was adopted from the Taconic plasmid data sheet.

### 3.3.14 Luciferase assay<sup>13</sup>

For Luciferase reporter assays, 500,000 HEK293, 70,000 immortalized SVF (control child 1), 150,000 L929 or 80,000 3T3-L1 cells were seeded per well in 6-well plates. The cells were co-transfected 24 hours post-seeding with 1 µg of pGL3-Basic plasmid containing the firefly luciferase reporter under control of the *ITCH* or *ASIP* promoter sequence or no promoter, and 50 ng of pRL-CMV control plasmid containing the luciferase gene from *Renilla reniformis* using 3 µL Fugene HD transfection reagent (Promega). Immortalized SVF cells were transfected with 2 µg of pGL3-Basic plasmid and 100 ng of pRL-CMV using 8 µL Fugene Reagent. Luciferase activities were measured using the Dual-Luciferase Reporter Assay System (Promega) according to the manufacturer's protocol 48 hours post-transfection. Experiments were performed in technical duplicates. For normalization, the sum of firefly luciferase activity was divided by the sum of *Renilla* luciferase activity.

### 3.3.15 Inhibition of the secretory pathway in SVF cells<sup>13</sup>

For inhibition of the classical secretory pathway, 800,000 primary SVF cells were seeded on 15 cm plates. 72-96 hours post-seeding, cells were treated for 24 hours with 15 mL FBS-free medium containing penicillin, streptomycin, 0.1 % bovine serum albumin, 5 µg/mL brefeldin A (stock solved in DMSO) and 2 µM monensin (stock solved in 70 % ethanol). Medium containing the same volume of DMSO and 70 % ethanol was used as negative control. Brefeldin A is indirectly inhibiting intracellular protein transport from the endoplasmic reticulum to the Golgi complex and leads to an accumulation of proteins in the endoplasmic reticulum by preventing the recruitment of COPI coat proteins to cargo-bound receptor proteins in the membrane of the Golgi complex [111]. Monensin is a monovalent ion-selective ionophore that interacts with the Golgi membrane Na<sup>2+</sup>/H<sup>+</sup> transport and disrupts the transport of proteins from the medial to trans cisternae of the Golgi complex [112].

After 24 hours of treatment, the cells and conditioned medium were harvested for immunoblotting.

### 3.3.16 Immunoblotting<sup>13</sup>

In order to investigate ASIP protein synthesis from the different *ASIP* expression plasmids, 600,000 HEK cells were seeded per well in a 6 well plate and were transfected

---

<sup>13</sup> Most parts of this subchapter were adopted literally from the methods section of the manuscript: **Kempf et al.**: A novel human monogenic obesity trait: severe early-onset childhood obesity caused by aberrant overexpression of agouti-signaling protein (*ASIP*). **Submitted**.

24 hours later with 2 µg of plasmid using 8 µL using Fugene HD transfection reagent (Promega). Medium was changed 24 hours post-transfection. Cells and supernatants were harvested 48 hours post-medium change.

For *ASIP* knockdown, 600,000 cells transfected with siRNA were seeded on 10 cm plates and harvested 72 hours post-transfection.

For Immunoblotting, cells were washed in PBS and lysed in RIPA lysis buffer (50mM Tris pH7.5, 150mM NaCl, 1 % Triton X-100, 0.1 % SDS, 1 cOmplete™ Mini Protease Inhibitor Cocktail Tablets (Roche, Sigma-Aldrich) per 10 mL) with additional break up via QiaShredder Homogenizer Columns (Qiagen). Conditioned medium was centrifuged for 5 minutes at 800 x g, lyophilized and resuspended in H<sub>2</sub>O. Protein concentration was measured using the Pierce™ BCA Protein Assay Kit (Thermo Fisher Scientific). Equal amounts of protein were resolved by 12 % sodium dodecyl sulphate-polyacrylamide gel electrophoresis according to Sambrook and Russell, 2001 [110] and detected using an anti-*ASIP* antibody (PA5-77052, Invitrogen). Equal loading was confirmed by detection of β-actin with an anti-β-actin antibody (ab8227, Abcam). Protein signal was quantified by the area under the curve method and normalized to β-actin.

### **3.3.17 *In vitro* lipolysis assay**

SGBS cells were seeded in a density of 200,000 cells per well in 6-well plates and induced for adipocyte differentiation the following day as described in 3.3.4. Successful adipogenic differentiation was documented with microscopic images. At day 12 of differentiation, cells were starved in 1 mL FBS-free medium containing 0.1 % BSA for 4 hours before 100 nM human recombinant *ASIP* protein (9094-AG, Research And Diagnostic Systems) or PBS was added to the wells. One hour later isoproterenol, or medium for the controls, was added to the cells to receive a final concentration of 10 µM in order to stimulate lipolysis. After 23 hours the conditioned medium was harvested and glycerol release of the cells was measured using Free Glycerol Reagent (Sigma-Aldrich). Glycerol concentration was normalized to the amount of protein extracted from the washed cells as described in 3.3.16.

### 3.3.18 Bioenergetic profiling<sup>14</sup>

Mitochondrial function was assessed using the Seahorse XF Cell Mito Stress Test Kit (Agilent Technologies) using 2  $\mu$ M oligomycin, 3  $\mu$ M carbonyl cyanide-4 (trifluoromethoxy) phenylhydrazone (FCCP) and 1  $\mu$ M rotenone/antimycin A. In this assay, oxygen consumption rate of cells is measured i) on basal condition, ii) after injection of oligomycin (inhibitor of the ATP synthase), iii) after injection of FCCP (uncoupling agent disrupting the mitochondrial membrane gradient) leading to uninhibited electron flow through the electron transport chain so that the oxygen consumption reaches the maximum, and iiiii) after injection of rotenone and antimycin A, which fully shut down mitochondrial respiration. Wells of XFe24 plates were gelatine-coated prior to cell seeding. For assessing mitochondrial function of SVF cells from the patient and control children, 15,000 SVF cells were seeded per well in XFe24 well format. For assessing the effect of *ASIP* knockdown on mitochondrial function, primary patient SVF cells were transfected with siRNA as described in section 3.3.7 and 30,000 transfected cells were seeded per well in XFe24er-well plates.

Measurements were performed in 3-4 technical replicates 48-72 hours post-transfection using XF Base Medium (Agilent Technologies) containing 2 mM pyruvate, 10 mM glucose and 2 mM glutamine. Results were normalized to total protein per well ( $\mu$ g) by lysing the cells in 30  $\mu$ L of 50 mM NaCl solution with subsequent protein quantification using the Pierce™ BCA Protein Assay Kit (Thermo Fisher Scientific).

### 3.3.19 Statistical analyses

For all studies *p*-values  $p < 0.05$  were considered statistically significant.

### Study 1<sup>15</sup>

For the study comparing growth and endocrine parameters between children of different weight categories, children were allocated to age groups according to their rounded age (e.g. age group 1:  $\geq 0.5$  and  $< 1.5$  years; age group 2:  $\geq 1.5$  and  $< 2.5$  years etc.). Children older than 17.5 years were allocated to the group 18+. To avoid bias by several observations of an individual within one age group, only the first observation of an individual per age group was included. For visualization, data of the normal-weight and obese subgroups were presented for boys and girls by age group as mean with standard

---

<sup>14</sup> Most parts of this subchapter were adopted literally from the methods section of the manuscript: **Kempf et al.**: A novel human monogenic obesity trait: severe early-onset childhood obesity caused by aberrant overexpression of agouti-signaling protein (*ASIP*). **Submitted**.

<sup>15</sup> Most parts of the text were adopted literally from the methods section of the publication: **Kempf et al.**, *EClinicalMedicine* 2021 [1].

error in a cross-sectional manner. Sex/age group/weight strata with sample size <6 were excluded from the charts. Differences between normal-weight and obese groups were assessed by multiple t-tests combined with a Holm-Šidák multiple comparison test if not indicated otherwise.

For the generation of height reference values and percentiles for German girls and boys with obesity, one randomly selected observation of each child with obesity from the CrescNet registry was used. Reference values were estimated for ages 0 to 18 years using the LMS-method [113] and using the same modeling parameter as Kromeyer-Hauschild *et al.* 2001 [23]. Those calculations were performed by Dr. Mandy Vogel (University of Leipzig, Medical Faculty, LIFE–Leipzig Research Center for Civilization Diseases, Leipzig, Germany).

Ruth Gausche (University of Leipzig, Medical Faculty, Growth Network CrescNet, Leipzig, Germany), Dr. Mandy Vogel and Dr. Daniel Gräfe (University of Leipzig, Medical Faculty, Pediatric Radiology, Leipzig, Germany) provided the online tools for the height reference values and percentiles.

### Study 2<sup>16</sup>

Only one observation of each child is included to this study. When not normally distributed, data were log<sub>10</sub>-transformed for statistical analyses. Multiple regression analyses were performed using a stepwise forward model stopping at a *p*-value of 0.05. The most significant variable at each step was determined according to the smallest *p*-value. Lean and overweight/obese groups were compared by unpaired student's t-test (two-sided) or Chi<sup>2</sup>-tests. In order to assess correlations, Pearson correlation and partial correlations were applied as indicated in the legends.

Prior to the analyses of *FGFR3* expression in AT, ILLUMINA gene expression data was pre-processed using the R package limma by Dr. Andreas Kühnapfel (University of Leipzig, Medical Faculty, Institute for Medical Informatics, Statistics and Epidemiology, Leipzig, Germany).

---

<sup>16</sup> Most parts of the text were adopted literally from the methods sections of the manuscript: **Kempf *et al.***: Contribution of adipose tissue to alterations in the growth hormone axis in childhood obesity and associations with adipose tissue function. **Submitted.**

### **Study 3<sup>17</sup>**

To test for statistical significance student's t-test or one-way-ANOVA with multiple comparison test with Holm-Šídák correction was performed.

Genome-wide expression in SVF cells was analyzed using the R package limma to perform pre-processing (background correction, quantile normalization) as well as differential gene expression analyses [114]. Fold changes were log<sub>2</sub>-transformed and *p*-values were adjusted for multiple testing using Benjamini-Hochberg procedure (False Discovery Rate, FDR). Those analyses have been performed by Dr. Andreas Kühnapfel (University of Leipzig, Medical Faculty, Institute for Medical Informatics, Statistics and Epidemiology, Leipzig, Germany).

---

<sup>17</sup> Most parts of the text were adopted literally from the methods section of the manuscript: **Kempf et al.**: A novel human monogenic obesity trait: severe early-onset childhood obesity caused by aberrant overexpression of agouti-signaling protein (*ASIP*). **Submitted.**

## 4 Results

### 4.1 Study 1: Alterations in linear growth and endocrine parameters in children with obesity<sup>18</sup>

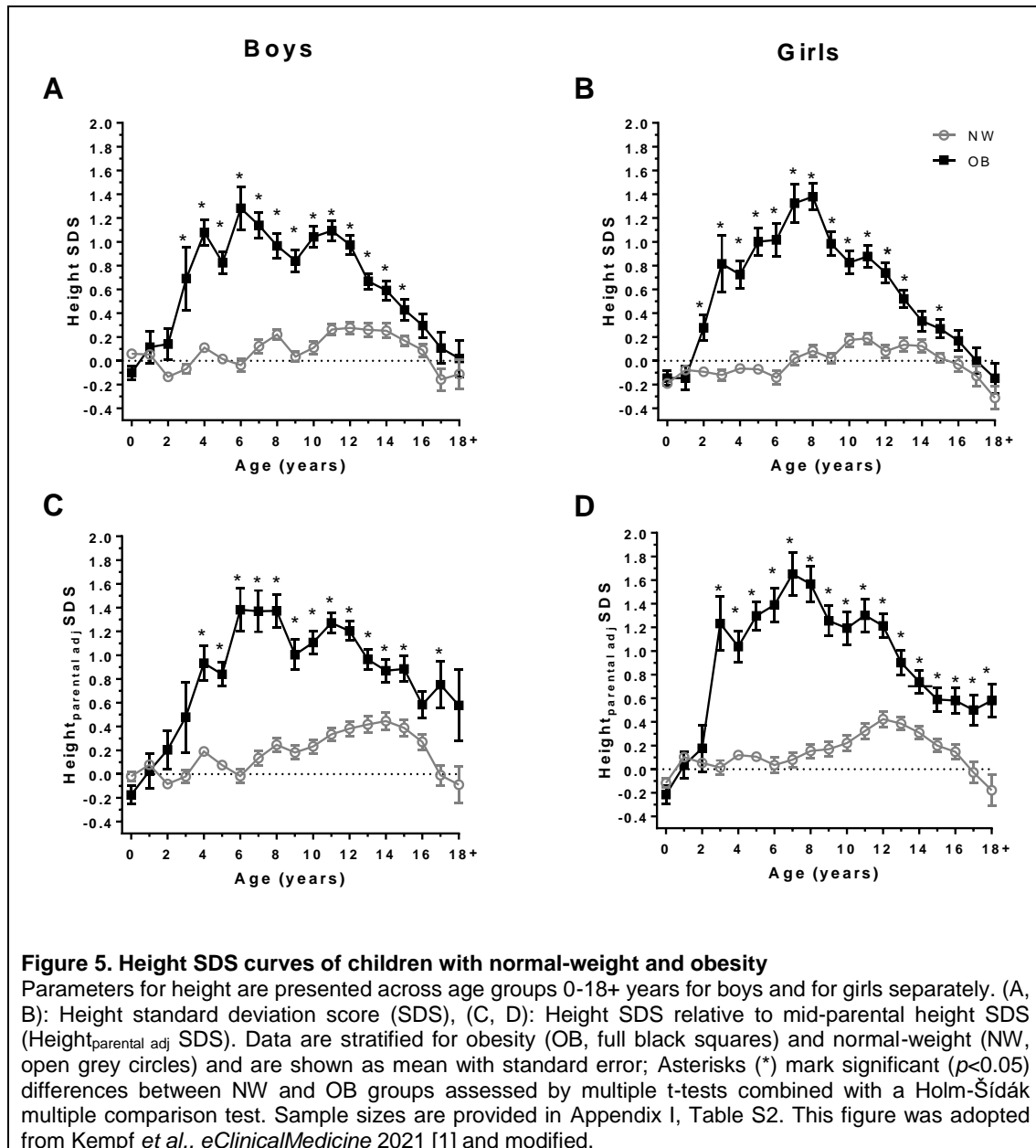
#### 4.1.1 Children with obesity are taller until adolescence independent from parental height

Searching for differences in linear growth, we found that children with obesity were significantly taller than their normal-weight peers. While the normal-weight group showed a height SDS around the expected 0 SDS throughout childhood, the obese group had an elevated height SDS around 1 SDS indicating relative tall stature (Figure 5 A, B). The most pronounced difference appeared around the age of 6 years in boys and 8 years in girls, accounting for a total difference in height of 6.8 and 7.6 cm, respectively. Beyond the age of 12 years in boys and 9 years in girls, the height SDS curves of obese and lean groups converged and there were no significant differences in final height. The analyses were repeated with exclusion of all data from prematurely-born children and the same results were obtained (not shown).

As familial predisposition is a major determinant for height, we corrected for mid-parental height ( $\text{Height}_{\text{parental adj}} \text{ SDS}$ ) and found a similar pattern indicating that children with obesity were taller independent of familial predisposition (Figure 5 C, D). However, when corrected for parental height, individuals with obesity had an increased final height compared to normal-weight peers. We did notice, however, that the parents of children with obesity in our study were slightly shorter than parents of normal-weight children (Appendix IIIA, Figure S4).

---

<sup>18</sup> The figures, the tables and most parts of the text of this subchapter were adopted literally from the results section of the publication: **Kempf et al., eClinicalMedicine 2021** [1].



Next, we investigated the influence of birth weight and length on later heights, as we observed that, independent from weight status, height SDS of 4-14 years old children were lower in previously small (SGA) than in appropriate (AGA) and particularly large for gestational age (LGA) born children (Appendix IIA, Figure S5).

Particularly girls with obesity had already been heavier at birth by >110 g and also birth length was higher compared to their normal-weight peers (Appendix IIIA, Table S6).



#### 4.1.2 Dynamics in growth velocity are altered in children with obesity

In a subcohort of children with growth velocities available, we assessed whether the obesity-related increase in height in early childhood was due to accelerated growth velocities. The height SDS patterns of this subgroup were not different from the entire cohort (not shown). Indeed, growth velocity (SDS) was slightly higher at ages 2-11 for boys with obesity and at ages 2-10 for girls with obesity compared to normal-weight children, with an increase of approximately 1 cm/year (Figure 6).

In the normal-weight group, the increase in growth velocity during pubertal growth spurt was evident at the age of 13 years in boys and 11 years in girls, as expected. However, in children with obesity, such a prominent growth spurt was lacking, further reflected by significantly lower growth velocities with reductions by up to 25 % in boys aged 13-14 and by 22 % in girls aged 12-13 years compared with their normal-weight peers.

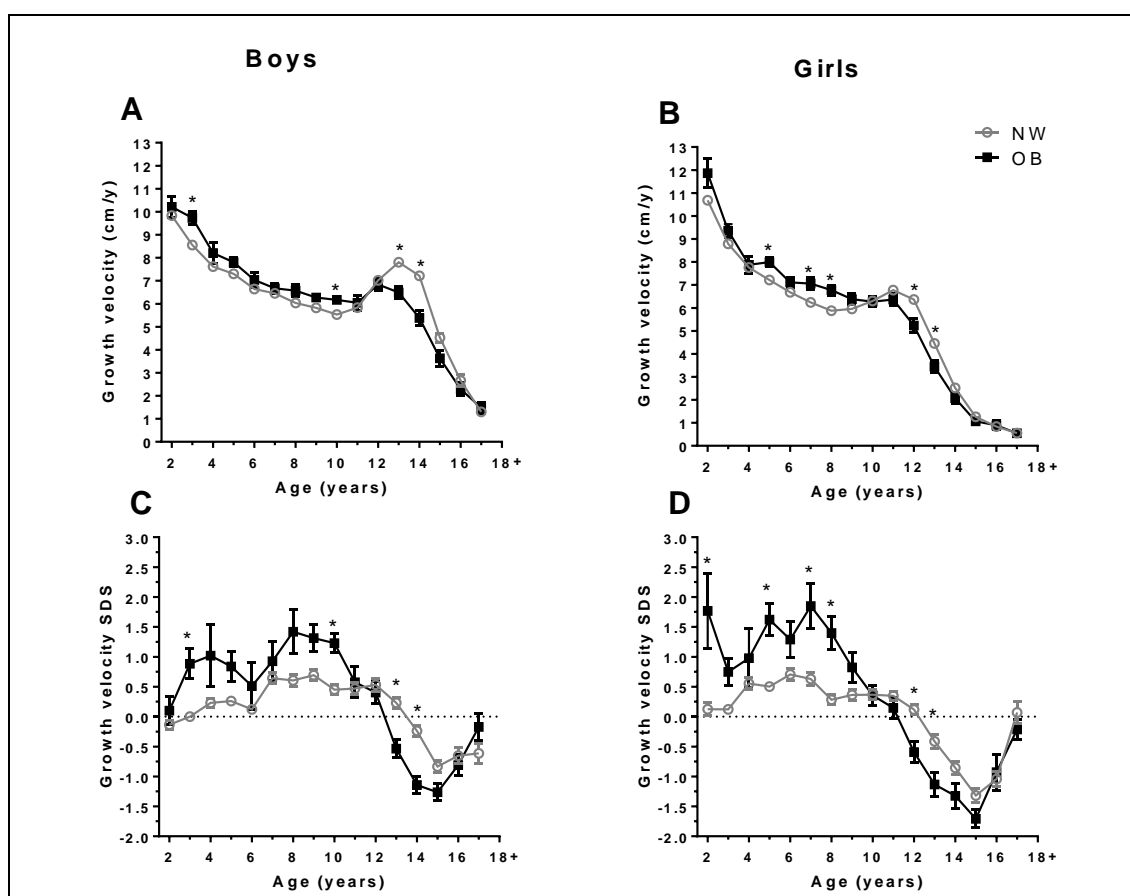


**Figure 6. Growth velocities of children with normal-weight and obesity**

Growth velocities are depicted for obese (OB, full black squares) and normal-weight (NW, open grey circles) groups of boys and girls for age groups 2-18+ years. Sample sizes are provided in Appendix I, Table S2. (A, B): Total growth velocities in cm per year (cm/y); (C, D): Growth velocity standard deviation scores (SDS); Data are shown as mean with standard error; Asterisks (\*) mark significant ( $p < 0.05$ ) differences between NW and OB groups assessed by multiple t-tests combined with a Holm-Šidák multiple comparison test. This figure was adopted from Kempf *et al.*, *eClinicalMedicine* 2021 [1].

#### 4.1.3 Pubertal timing and endocrine parameters are altered in childhood obesity

Boys with obesity were on average 6.6 months older than normal-weight boys when entering puberty (Appendix IIIA, Table S7). In contrast, girls with obesity were 9.1 months younger and experienced menarche 8.9 months earlier than normal-weight girls.

Serum levels of IGF-1 or IGFBP-3, sex hormones, metabolic factors and thyroid hormones were available in subcohorts (Appendix I, Table S2). Growth velocities of the subcohorts are shown in the graphs and were similar to those of the entire cohort.

IGF-1 levels were elevated in children with obesity at ages 6-9 years, corresponding to the elevated growth velocities (Figure 7 A, B). In contrast, during pubertal age IGF-1 levels decreased by up to 17 %. There were no major differences in IGFBP-3 levels between the weight groups (Figure 7 C, D).

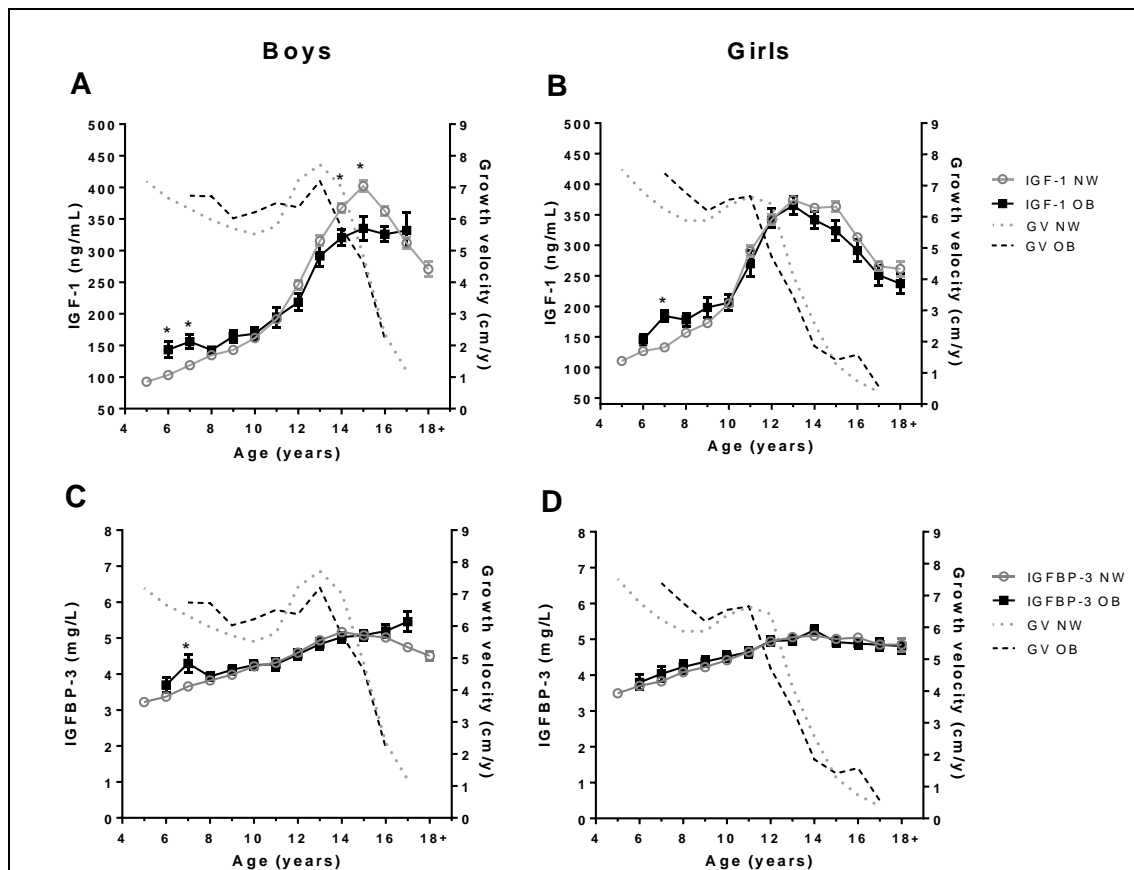


**Figure 7. Serum IGF-1 and IGFBP-3 levels of children with normal-weight and obesity**

Serum hormone levels of obese (OB, full black squares) and normal-weight (NW, open grey circles) groups of boys and girls are presented for age groups 5-18+ years. Data are shown as mean with standard error. The grey dotted-lined curves presents the growth velocities (GV) in cm per year (cm/y) of normal-weight individuals from whom insulin-like growth factor-1 (IGF-1) or IGF-binding protein 3 (IGFBP-3) measurements were available. The black dashed-lined curves show growth velocities from individuals with obesity from whom IGF-1 or IGFBP-3 measurements were available. Growth velocities are presented as mean without standard error. Sample sizes for the IGF-1 or IGFBP3 subcohort are provided in Appendix I, Table S2: (A, B): Serum IGF-1 in ng/mL; (C, D): Serum IGFBP-3 in  $\mu$ g/mL. Asterisks (\*) mark significant ( $p < 0.05$ ) differences between NW and OB groups assessed by multiple t-tests combined with a Holm-Šidák multiple comparison test. This figure was adopted from Kempf *et al.*, *eClinicalMedicine* 2021 [1].

Regarding sex steroid levels (Figure 8), during puberty, we found testosterone to be reduced by up to 62 % in boys with obesity compared to normal-weight boys, along with decreased LH levels (Appendix IIIA, Figure S6). Pubertal girls with obesity, in contrast, presented higher testosterone levels, but up to 37 % reduced estradiol serum levels in late puberty (Figure 8). FSH levels were similar between normal-weight and obese groups, while DHEA-S was increased in pre-pubertal children with obesity (Appendix IIIA, Figure S6). SHBG and FT4 were reduced, and TSH tended to be elevated in children with obesity throughout childhood and adolescence (Appendix IIIA, Figure S6, 7). During puberty, differences in growth velocity between obese and normal-weight groups corresponded to differences in testosterone levels in boys and in estradiol in girls and resembled the pattern of the IGF-1 levels. We did not observe any obvious association with growth velocity for FSH, SHBG, DHEA-S, TSH or FT4 (Appendix IIIA, Figure S6, 7).

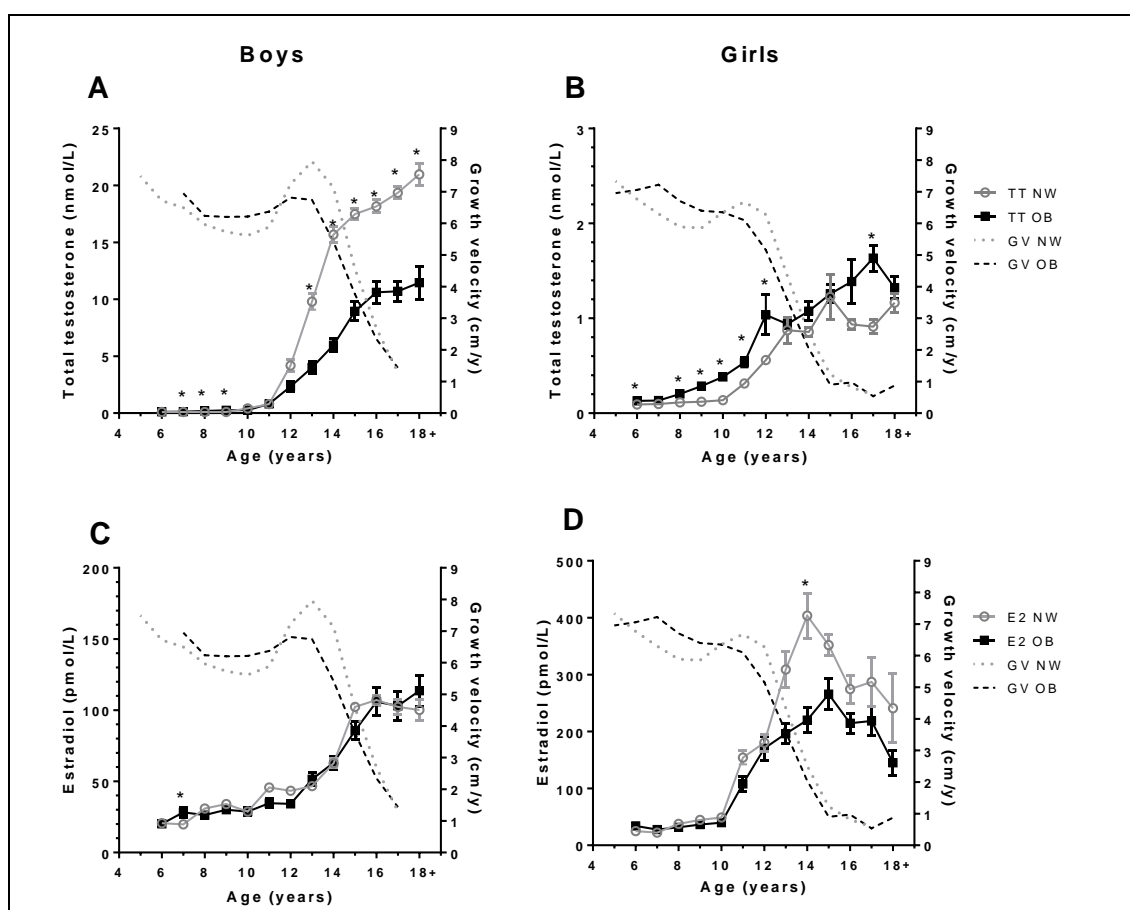


**Figure 8. Sex hormone levels of children with normal-weight and obesity**

Serum sex hormone levels of obese (OB, full black squares) and normal-weight (NW, open grey circles) groups of boys and girls are presented for age groups 5-18+ years. Data are shown as mean with standard error. The grey dotted-lined curves presents the growth velocities (GV) in cm per year (cm/y) of normal-weight individuals from whom sex steroid measurements were available. The black dashed-lined curves show growth velocities from individuals with obesity from sex steroids measurements were available. Growth velocities are presented as mean without standard error. Sample sizes of the sex steroid subcohort are provided in Appendix I, Table S2. (A, B): Serum testosterone (TT) in nmol/L; (C, D): Serum estradiol (E2) in pmol/L. Asterisks (\*) mark significant ( $p < 0.05$ ) differences between NW and OB groups assessed by multiple t-tests combined with a Holm-Šidák multiple comparison test. This figure was adopted from Kempf *et al.*, *eClinicalMedicine* 2021 [1].

Serum leptin, insulin, and HOMA-IR were significantly elevated in obese compared to normal-weight groups during childhood. However, there was no particular similarity to the pattern of growth or growth velocity (Figure 9).

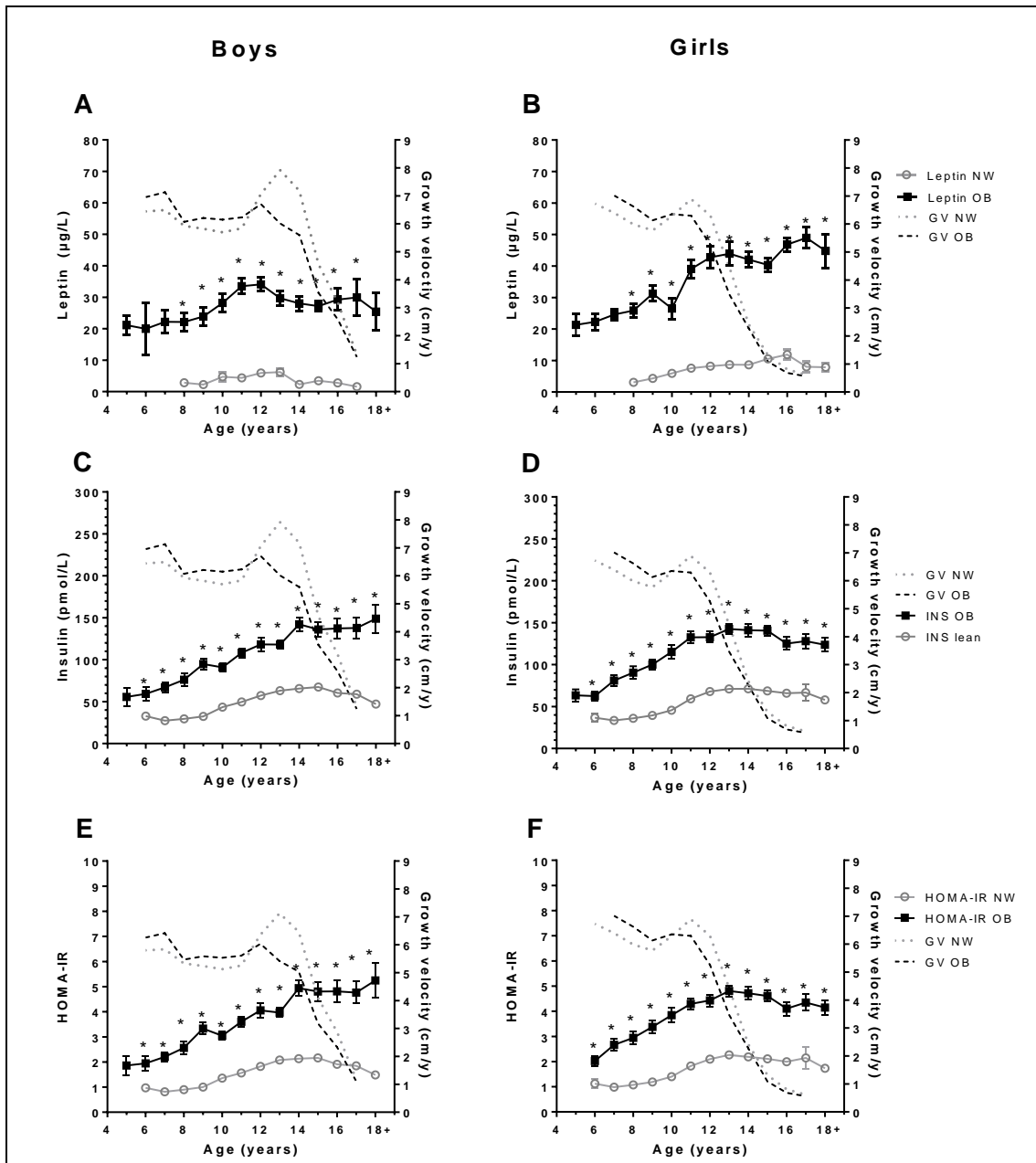


**Figure 9. Metabolic parameters of children with normal-weight and obesity**

Metabolic parameters of obese (OB, full black squares) and normal-weight (NW, open grey circles) boys and girls are depicted for age groups 5-18+ years. Data are shown as mean with standard error. The grey dotted-lined curves presents the growth velocities (GV) in cm per year (cm/y) of normal-weight individuals from whom metabolic measurements were available. The black dashed-lined curves show growth velocities from individuals with obesity from whom metabolic measurements were available. Growth velocities are presented as mean without standard error. Sample sizes of the metabolic factor subcohort are provided in Appendix I, Table S2. (A, B): Serum leptin in µg/L; (C, D): Serum fasting insulin in pmol/L. (E, F): Homeostatic Model Assessment for Insulin Resistance (HOMA-IR). Asterisks (\*) mark significant ( $p < 0.05$ ) differences between NW and OB children assessed by multiple t-tests combined with a Holm-Sídák multiple comparison test. This figure was adopted from Kempf *et. al.*, *eClinicalMedicine* 2021 [1].

#### 4.1.4 Height, growth and endocrine factors in underweight children

The group of underweight children was shorter before puberty, followed by catch-up growth and finally reaching similar heights as the other weight groups (Appendix IIIA, Figure S8-13). This delayed pubertal growth spurt was even more apparent when analyzing growth velocities and was accompanied by lower levels of IGF-1. Sex steroid levels also appeared slightly lower than in normal-weight children, whereas SHBG levels were higher showing the most distinct dependence on weight group. Hence, the observed effects of weight on growth dynamics and hormones were consistent across the weight categories, with underweight children presenting a delay in growth and pubertal development.

#### 4.1.5 Height reference values for children with obesity

As growth curves of children with obesity strongly differ from those of normal-weight children, we need specific height reference values for children with obesity. Using data from a second, independent population-based study sample of  $n=12,703$ , the CrescNet registry [9, 90], we generated height curves for the 3rd, the 50th and the 97th percentile for boys and girls with obesity (Figure 10). Height curves deviate from the percentile curves from the German references by Kromeyer-Hauschild *et al.* [23], which represent mostly normal-weight children and are comparable to the height curves of our normal-weight children of the CrescNet registry (not shown). As shown in our LIFE Child and Leipzig Childhood Obesity cohorts, children with obesity were taller until puberty, the pubertal growth spurt appeared to be blunted, hence reassuringly confirming the alterations in growth patterns in an independent populational cohort. The novel reference values are available open-access at the CrescNet website [115], the Ped(Z) Pediatric Calculator app [116] and via an R package [117].

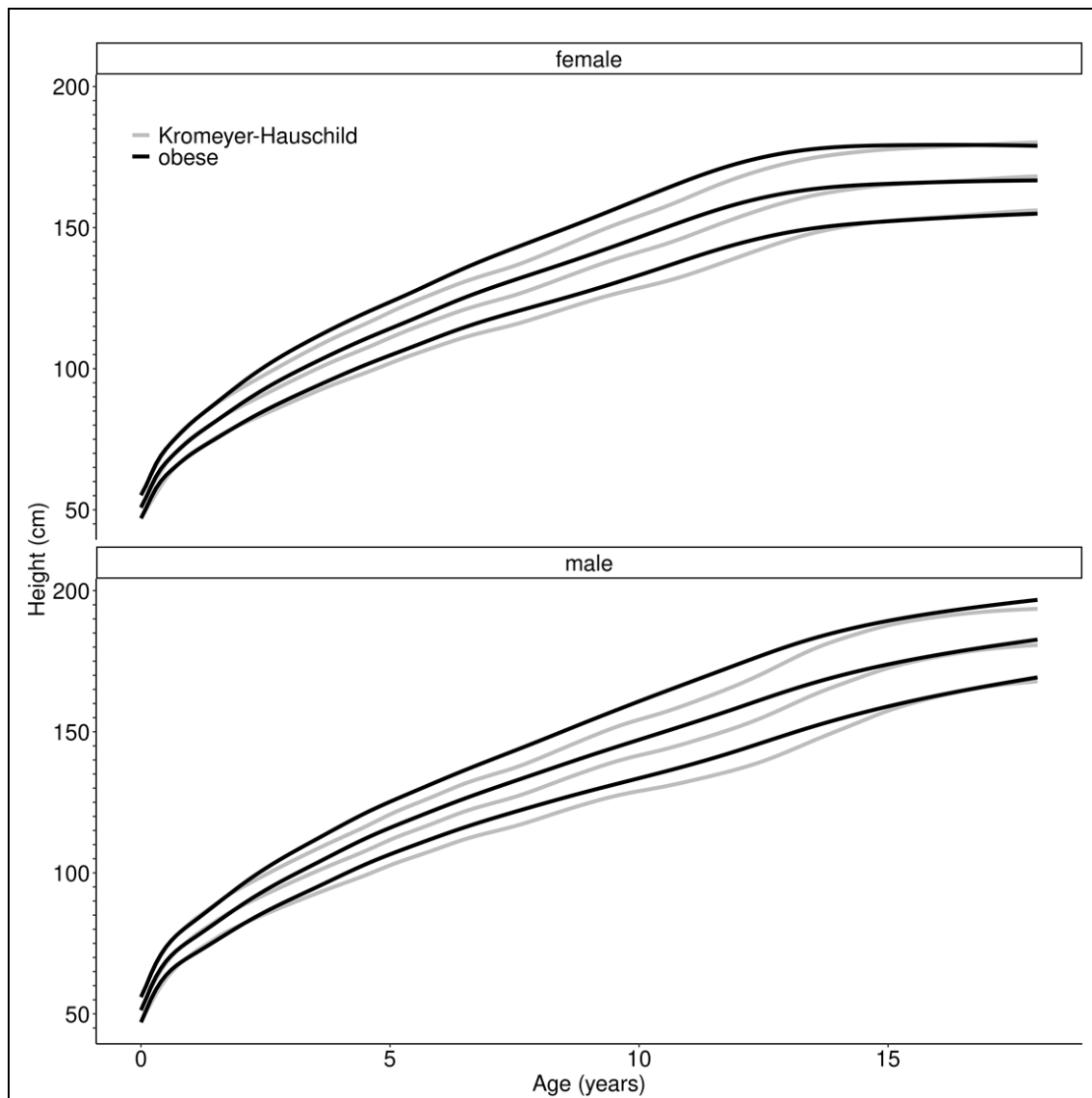


**Figure 10. Height percentiles for children with obesity compared to population-based reference values**

Height percentile curves in cm for children with obesity (BMI SDS  $\geq 1.88$ ) for boys and girls from ages 0 to 18 years derived from the CrescNet registry are presented (black lines) and compared to the height reference values according to Kromeyer-Hauschild [23] (grey lines). For each the 3rd, the 50th and the 97th height percentiles are presented. This figure was generated by Mandy Vogel and adopted from Kempf *et. al.*, *eClinicalMedicine* 2021 [1].

## 4.2 Study 2: Associations of gene expression of growth-related factors in AT with circulating levels and AT function<sup>19</sup>

In study 1, we found that circulating levels of components of the GH axis are altered in children with obesity [1]. As some of those factors are known to be also expressed in AT, in study 2, we investigated if AT might be involved in the regulation of the circulating levels in children with overweight or obesity.

We focused on circulating levels of IGF-1 and included IGFBP-3, as this is highly correlated with IGF-1 [118, 119], and GHBP, as this is a parameter previously observed to be increased in children with obesity [120]. Furthermore, we investigated associations between the expression of those growth-related factors in AT with overweight/obesity and AT function.

### 4.2.1 Serum levels of GHBP and IGF-1 are increased in children with overweight/obesity

306 children of the Leipzig AT Childhood Cohort (n=209) and the Leipzig Atherobesity Childhood Cohort (n=97) were included into this study. Anthropometric, laboratory and gene expression data as well as parameters for AT were compared between lean children and children with overweight/obesity (Appendix IIIB, Table S8 and S9). There was no significant difference in distribution of sex, but children with overweight/obesity were slightly older, taller and more advanced in puberty than their lean peers. When stratified for pubertal stage, children with overweight/obesity were taller than their lean peers, whereas age was not different between the two weight groups from pubertal stage 2 onwards pointing towards an obesity-associated gain in height (Figure 11 A, B), as already observed in study 1 [1].

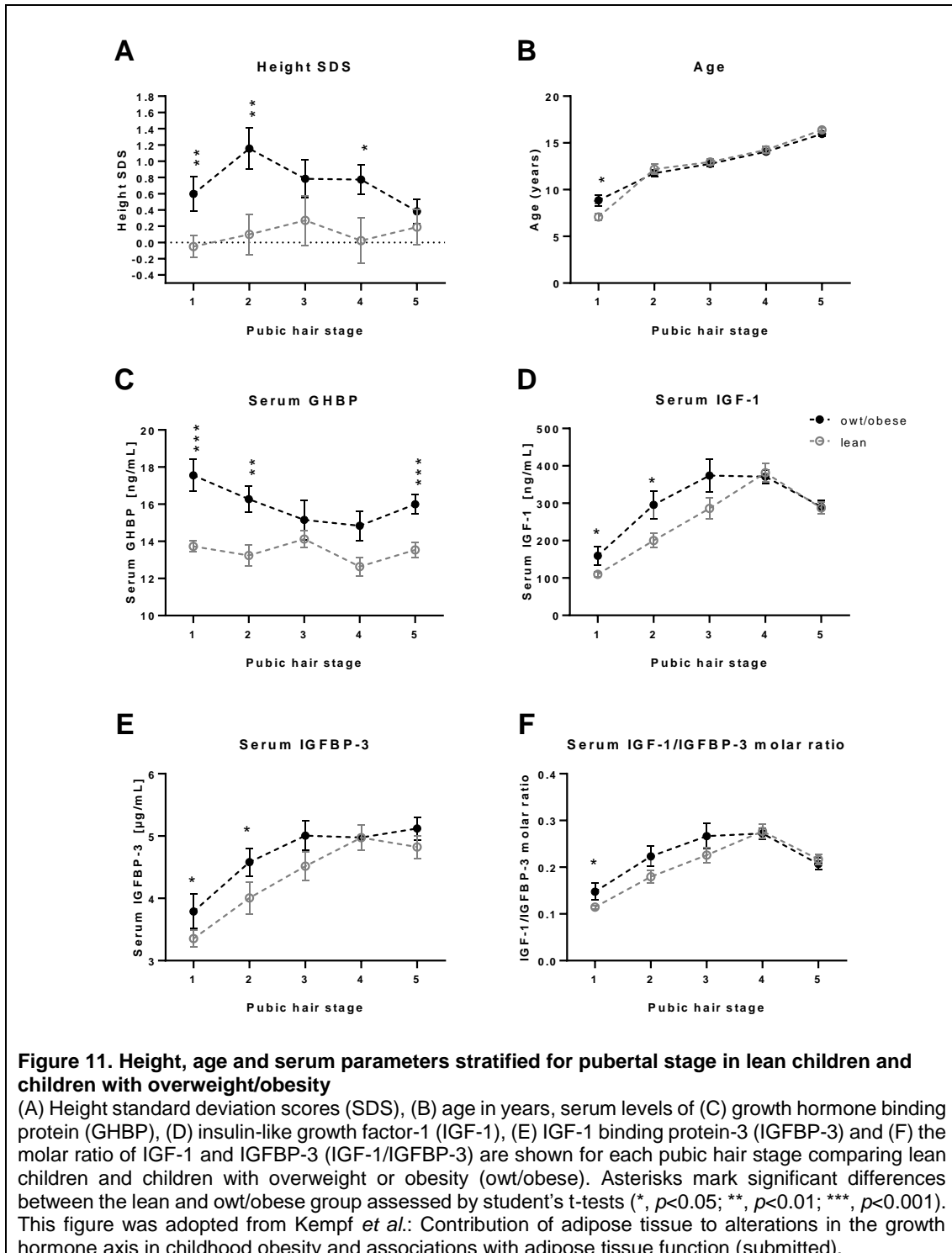
Similar to previous studies [21, 88, 121], the children with overweight/obesity presented an increased percentage of liver fat and total body fat (MRI) as well as obesity-related alterations in metabolic and inflammatory serum parameters such as triglycerides, cholesterol, HDL and LDL, hsCRP, ALAT, adiponectin, leptin, insulin as well as HOMA-IR (Appendix IIIB, Table S8).

The obesity-associated gain in height was accompanied by increased serum levels of GHBP, IGF-1 and IGFBP-3 in the children with overweight/obesity (Appendix IIIB, Table S8). When children were further stratified according to pubertal stage, GHBP serum levels were increased in individuals with overweight/obesity throughout childhood and

---

<sup>19</sup> The figures, the tables and most parts of the text of this subchapter were adopted literally from the results section of the manuscript: **Kempf et al.**: Contribution of adipose tissue to alterations in the growth hormone axis in childhood obesity and associations with adipose tissue function. **Submitted.**

adolescence (Figure 11 C), while IGF-1 and IGFBP-3 levels were increased in pre-puberty and early puberty (Figure 11 D, E) and the IGF-1/IGFBP-3 molar ratio was increased only in pre-pubertal children (Figure 11 F). As IGF-1 and IGFBP-3 levels followed an approximately linear pattern below the age of 11 years (Appendix IIIB, Figure S14) (in the following designated to 2-10 years), only children within this age range were included in the following statistical analyses of associations of IGF-1 and IGFBP-3 with obesity-related parameters.





Multiple regression analyses restricted to healthy lean children showed that serum GHBP levels were not associated with age, sex or height SDS, while serum IGF-1 and IGFBP-3 and the IGF-1/IGFBP-3 molar ratio were significantly associated with age and/or sex (Appendix IIIB, Table S10), confirming the relation to physiological development during childhood.

To determine the impact of obesity on serum levels we performed multiple regression analyses in the entire cohort showing that higher BMI SDS was the strongest predictor of increased serum GHBP. For IGF-1 and IGF-1/IGFBP-3, BMI SDS did also independently contribute to variance, although to a minor degree, while IGFBP-3 was not affected by BMI SDS (Table 12). Hence, particularly increased serum GHBP is predominantly related to overweight in children.

**Table 12. Multiple regression analysis on the effect of BMI SDS on serum levels of GHBP, IGF-1 and IGFBP-3**

Ages included	Dependent variable	Step	Independent variable	$\Delta r^2$	$\beta \pm SE$	<i>p</i>
2-18 y	<b>Serum GHBP</b> ( $r^2=0.133$ ; $p < 0.001$ ; $n=285$ )	1	BMI SDS	0.133	$0.364 \pm 0.055$	<b>&lt;0.001</b>
2-10 y	<b>Serum IGF-1</b> ( $r^2 = 0.509$ ; $p < 0.001$ ; $n=74$ )	1	Age	0.397	$0.500 \pm 0.090$	<b>&lt;0.001</b>
		2	Sex	0.062	$-0.269 \pm 0.087$	<b>0.003</b>
		3	BMI SDS	0.051	$0.233 \pm 0.086$	<b>0.009</b>
2-10 y	<b>Serum IGFBP-3</b> ( $r^2 = 0.405$ ; $p < 0.001$ ; $n=74$ )	1	Age	0.351	$0.527 \pm 0.095$	<b>&lt;0.001</b>
		2	Sex	0.054	$-0.241 \pm 0.095$	<b>0.014</b>
2-10 y	<b>IGF-1/IGFBP-3</b> ( $r^2 = 0.432$ ; $p < 0.001$ ; $n=74$ )	1	Age	0.421	$0.459 \pm 0.097$	<b>&lt;0.001</b>
		2	BMI SDS	0.045	$0.254 \pm 0.093$	<b>0.008</b>
		3	Sex	0.038	$-0.210 \pm 0.094$	<b>0.028</b>

As independent variables age, sex and BMI SDS were included. For IGF-1, IGFBP-3 and IGF-1/IGFBP-3, exclusively children until the age of 10 years were included in the statistical analyses as until this age serum levels followed an approximately linear pattern (Appendix IIIB, Figure S14). *P*-values <0.05 are highlighted in bold. BMI SDS, body mass index standard deviation score; GHBP, growth hormone binding protein; IGF-1, insulin-like growth factor-1; IGFBP-3, IGF-1 binding protein-3; IGF-1/IGFBP-3, IGF-1 IGFBP-3 molar ratio;  $\Delta r^2$ , *r* square change;  $\beta \pm SE$ , standardized beta and standard error; y, years. This table was adopted from Kempf *et al.*: Contribution of adipose tissue to alterations in the growth hormone axis in childhood obesity and associations with adipose tissue function (submitted).

#### 4.2.2 Association between gene expression of the factors in AT cells and circulating levels

Given the association of increased serum GHBP and IGF-1 levels with increasing BMI SDS in children, we assessed if by gene expression AT cells might contribute to the increase in serum levels observed with overweight/obesity. For this, we assessed whether gene expression levels of *GHR* and *IGF-1* in adipocytes and SVF cells were associated with the circulating levels in children. There was no positive correlation between gene expression and any of the serum parameters (Figure 12). The only

correlations observed were negative associations between *GHR* expression in SVF cells and serum GHBP (Figure 12 B).

However, it must be considered that children with overweight/obesity have an increased AT mass and a higher number of adipocytes [21] (Appendix IIIB, Table S8) expressing *GHR* and *IGF-1*. To take this into account, we calculated the total expression from adipocytes per kg body weight per individual. Nonetheless, there again was no correlation with the serum levels (GHBP:  $r=-0.13$ ,  $p=0.482$ ; IGF-1:  $r=-0.19$ ,  $p=0.574$ ) indicating that, regarding the gene expression, adipocytes may not constitute the major source of elevated circulating GHBP and IGF-1 levels in children with obesity.

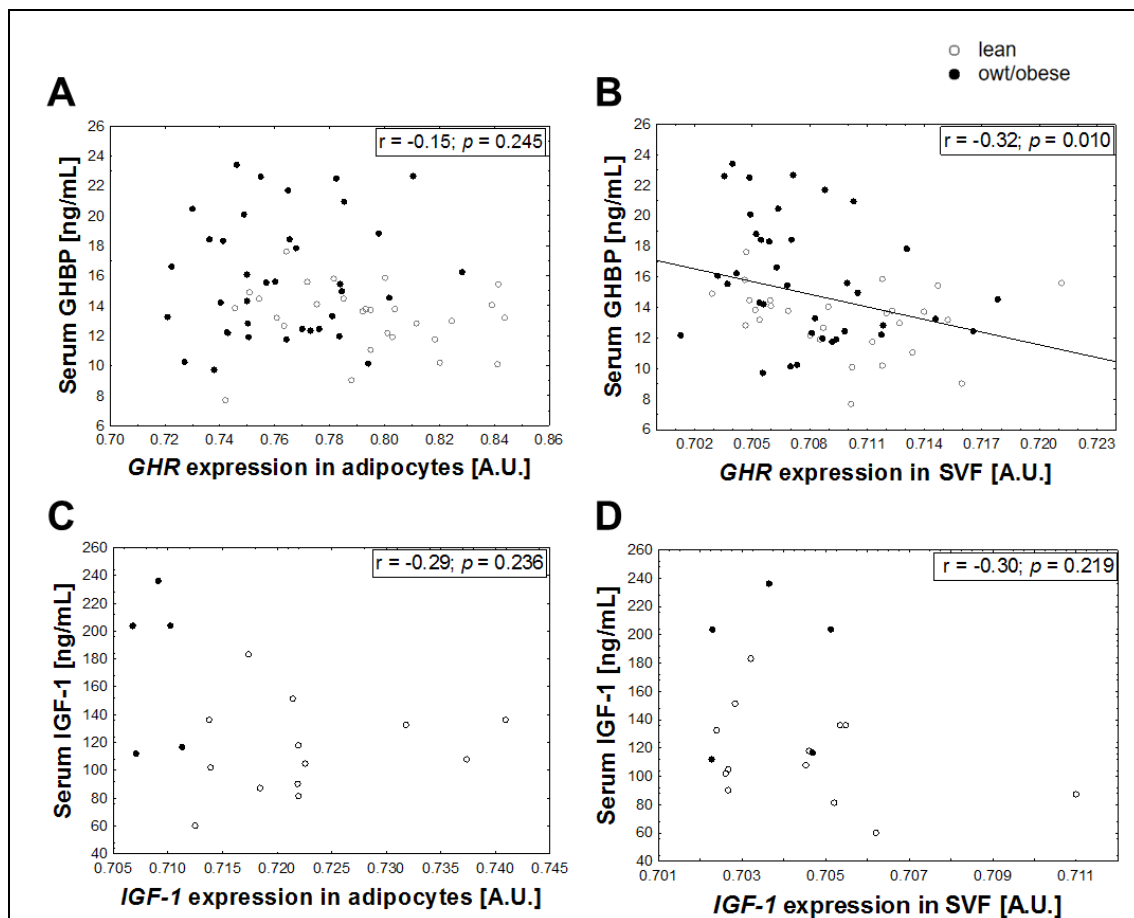


**Figure 12. Associations of gene expression of *GHR* and *IGF-1* in adipocytes and SVF cells with serum levels**

The relation of serum growth hormone binding protein (GHBP) (shedded from the growth hormone receptor (GHR)) with gene expression of *GHR* in (A) adipocytes and (B) stromal vascular fraction (SVF) cells and the relation of serum insulin-like growth factor-1 (IGF-1) with gene expression of *IGF-1* in (C) adipocytes and (D) SVF cells are shown. Regression coefficient  $r$  and  $p$ -value are given and significant correlations are marked with a regression line. For IGF-1 exclusively children until the age of 10 years were included to the analyses as until this age serum levels followed an approximately linear pattern (Appendix IIIB, Figure S14). For GHBP data from 2-18 years are included. Gene expression data were  $\log_{10}$ -transformed. This figure was adopted from Kempf *et al.*: Contribution of adipose tissue to alterations in the growth hormone axis in childhood obesity and associations with adipose tissue function (submitted).

### 4.2.3 Association of GHBP serum levels with steatohepatosis

We further observed that in children with overweight/obesity not only the percentage of total body fat (MRI) was increased, but they also already had an increased percentage of liver fat (MRI) (Appendix IIIB, Table S8). Since the liver is supposed to be the primary source of circulating GHBP, we assessed whether there was an association between the serum levels and liver parameters. Unfortunately, IGF-1 and IGFBP-3 serum levels were not available in the subcohort, in which MRI data was available. Multiple regression analyses revealed that an increased percentage of liver fat is a strong predictor for increased serum GHBP accounting for 35 % of serum GHBP variability in this model, while the percentage of total body fat (MRI) did not contribute to the model (Table 13).

**Table 13. Multiple stepwise regression analysis in order to identify predictors for GHBP serum levels**

Ages Included	Dependent variable	Step	Independent variable	$\Delta r^2$	$\beta \pm SE$	$p$
2-18 y	<b>Serum GHBP</b> ( $r^2=0.436$ ; $p<0.001$ ; $n=47$ )	1	% Liver fat *	0.352	$0.580 \pm 0.132$	<b>&lt;0.001</b>
		2	Age	0.051	$0.193 \pm 0.123$	0.124
		3	% Total body fat (MRI)	0.032	$0.197 \pm 0.126$	0.127

As independent variables age, sex, % total body fat (MRI) and % liver fat were included. % liver fat was  $\log_{10}$ -transformed prior to analyses as indicated with an asterisk (\*).  $P$ -values  $<0.05$  are highlighted in bold. GHBP, growth hormone binding protein; y, years;  $\Delta r^2$ ,  $r$  square change;  $\beta \pm SE$ , standardized beta and standard error. This table was adopted from Kempf *et al.*: Contribution of adipose tissue to alterations in the growth hormone axis in childhood obesity and associations with adipose tissue function (submitted).

We looked for further correlations with parameters associated with liver function [122]. Indeed, we observed positive correlations of serum GHBP with liver aminotransferases ALAT, ASAT, as well as TNF- $\alpha$  and the lipid parameters total cholesterol, LDL cholesterol and triglyceride levels independently from BMI SDS and developmental parameters, (Table 14) confirming a potential association of increased serum GHBP with increased liver fat content.

**Table 14. Association of serum GHBP with metabolic and liver parameters**

Parameter	n	r	p
ALAT, $\mu\text{kat/L}$ *	97	0.506	<b>&lt;0.001</b>
ASAT, $\mu\text{kat/L}$ *	97	0.460	<b>&lt;0.001</b>
Adiponectin, $\text{mg/L}$ *	181	-0.033	0.658
Leptin, $\text{ng/mL}$ *	189	0.044	0.592
TNF- $\alpha$ , $\text{pg/mL}$ *	180	0.181	<b>0.016</b>
hsCRP $\text{mg/L}$ *	176	0.112	0.125
Cholesterol, $\text{mmol/L}$ *	279	0.3391	<b>&lt;0.001</b>
LDL cholesterol, $\text{mmol/L}$ *	280	0.323	<b>&lt;0.001</b>
HDL cholesterol, $\text{mmol/L}$ *	297	0.133	0.079
Triglycerides, $\text{mmol/L}$ *	93	0.405	<b>&lt;0.001</b>
Glucose, $\text{mmol/L}$ *	184	-0.124	0.100
Insulin, $\text{pmol/L}$ *	181	0.002	0.983
HOMA-IR *	179	0.016	0.839

Analyses were performed using partial correlation with adjustment for age, sex and BMI SDS. *P*-values <0.05 are highlighted in bold. Data of children from age 2-18 years are included. Asterisks (\*) indicate that this parameter was  $\log_{10}$ -transformed for statistical analysis. GHBP, growth-hormone binding protein; ALAT, alanine aminotransferase; ASAT, aspartate aminotransferase; hsCRP, high sensitive C-reactive protein; HDL, high-density lipoprotein; LDL, low density lipoprotein; TNF- $\alpha$ , tumor necrosis factor alpha; HOMA-IR, Homeostasis Model Assessment for Insulin Resistance. This table was adopted from Kempf *et al.*: Contribution of adipose tissue to alterations in the growth hormone axis in childhood obesity and associations with adipose tissue function (submitted).

#### 4.2.4 *GHR*, *IGF-1* and *IGFBP-3* gene expression is decreased in AT cells in children with overweight/obesity

In order to assess the role of growth-related factors *GHR*, *IGF-1* and *IGFBP-3* in AT, we first compared the gene expression of these factors between mature adipocytes and SVF cells isolated from subcutaneous AT of lean children. *GHR* expression was almost 10-fold increased in adipocytes compared to SVF cells (Figure 13 A) and *IGF-1* approximately 4-fold higher in adipocytes than in SVF cells (Figure 13 B), while *IGFBP-3* expression was around 13-fold lower in adipocytes (Figure 13 C). In line with that, during human adipocyte differentiation of SGBS cells, and particularly in late stages of differentiation and subsequent to the *PPARG* increase (Appendix IIIB, Figure S15 A), *GHR* and *IGF-1* expression in differentiated SGBS cells increased >300-fold and >800- fold, respectively, compared to undifferentiated cells (Appendix IIIB, Figure S15 B, C). In contrast, *IGFBP-3* expression was decreased to 38 % in differentiated cells (Appendix IIIB, Figure S15 D). Expression of *IGF-1R* was not different in differentiated cells, while isoforms A and B of the insulin receptor (*INSR*) were around 7- and 5-fold increased, respectively (Appendix IIIB, Figure S15 E, F).

Interestingly, gene expression of *GHR*, *IGF-1* and *IGFBP-3* was diminished in children with overweight/obesity compared to lean children (Figure 13).

In line with this, after adjusting to the confounding parameters age and sex (Appendix IIIB, Table S11), gene expression of *GHR* and *IGF-1* in adipocytes as well as *IGFBP-3* expression in SVF cells decreased with increasing BMI SDS (Appendix IIIB, Table S12).

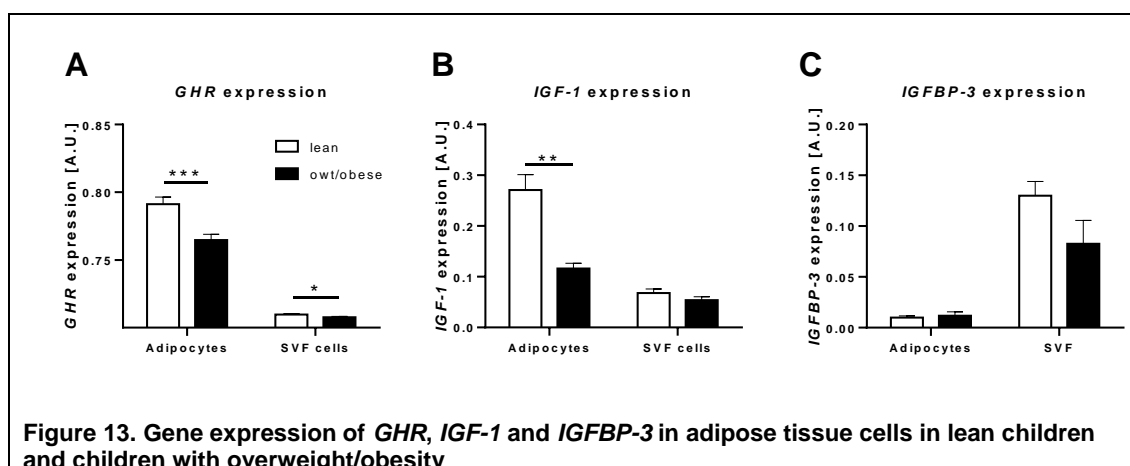


**Figure 13. Gene expression of *GHR*, *IGF-1* and *IGFBP-3* in adipose tissue cells in lean children and children with overweight/obesity**

For adipocytes and stromal vascular fraction (SVF) cells gene expression levels of (A) growth hormone receptor (*GHR*), (B) insulin-like growth factor-1 (*IGF-1*) and (C) IGF-1 binding protein-3 (*IGFBP-3*) are shown. For *IGF-1* and *IGFBP-3* expression, data from children between ages 2-10 years are included. For *GHR* expression data from 2-18 years are included. Asterisks mark significant differences between lean children and children with overweight/obesity (owt/obese) assessed by student's t-tests (\*,  $p < 0.05$ ; \*\*,  $p < 0.01$ ; \*\*\*,  $p < 0.001$ ). For statistical analyses gene expression data were  $\log_{10}$ -transformed. This figure was adopted from Kempf *et al.*: Contribution of adipose tissue to alterations in the growth hormone axis in childhood obesity and associations with adipose tissue function (submitted).

#### 4.2.5 *GHR*, *IGF-1* and *IGFBP-3* expression in AT may be related to AT function

As children with overweight/obesity showed reduced gene expression of *GHR*, *IGF-1* and *IGFBP-3* in subcutaneous adipocytes and SVF cells, we next analyzed if local expression of these factors in adipocytes and SVF cells was associated with parameters of AT function.

We found that reduced *GHR* expression in adipocytes and *IGF-1* expression in SVF cells was associated with a larger diameter of adipocytes and a reduced number of adipocytes per g AT independently of age, sex and BMI SDS (Table 15), hence indicative for adipocyte hypertrophy. Additionally, reduced *IGFBP-3* expression in adipocytes showed a relation to a lower number of adipocytes per g AT. Regarding parameters indicative of AT inflammation, we observed an inverse correlation of *IGFBP-3* expression in adipocytes with the number of macrophages. Furthermore, gene expression of *IGFBP-3* in SVF cells was slightly lower in AT samples interspersed with crown-like structures (CLS) than in samples without. We did not find an association of *GHR* or *IGF-1* expression with macrophage infiltration or formation of CLS in AT.

There was no BMI-independent association of *GHR*, *IGF-1* and *IGFBP-3* expression in AT cells with basal or isoproterenol-stimulated lipolysis of adipocytes or with the proliferative and adipogenic potential of SVF cells *in vitro*. Also, we did not observe any association with serum adiponectin, leptin or fasting glucose levels, but *GHR*, *IGF-1* and *IGFBP-3* expression in SVF cells seemed to inversely correlate with serum insulin.

**Table 15. Association of *GHR*, *IGF-1* and *IGFBP-3* expression in adipocytes and SVF cells with AT function**

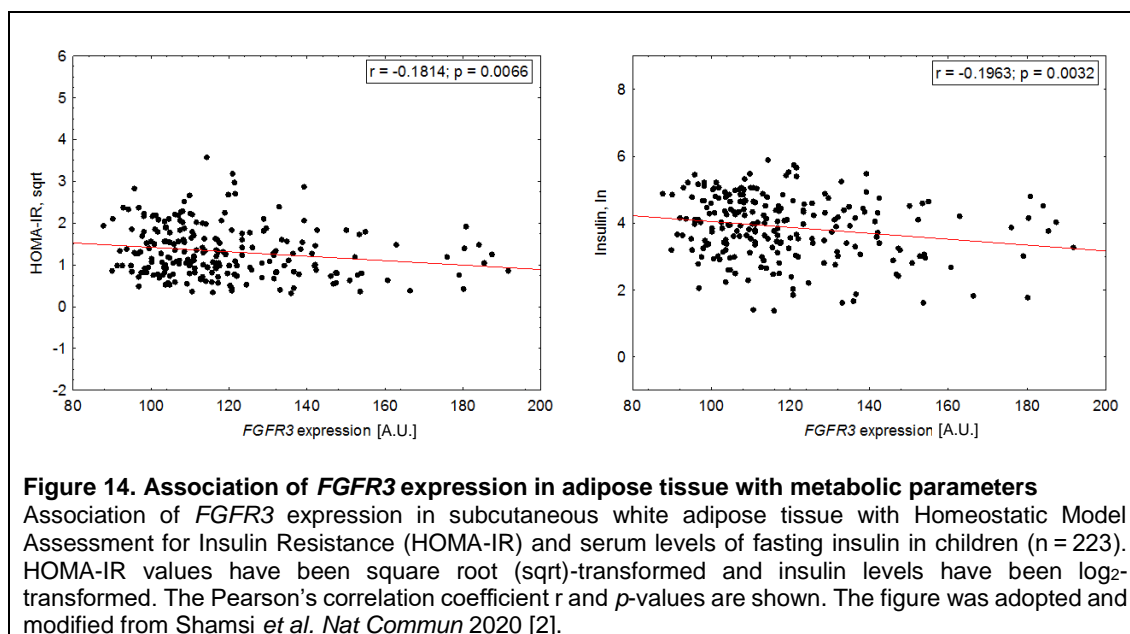
	n		<i>GHR</i> *		<i>IGF-1</i> *		<i>IGFBP-3</i> *	
			Adipocyte	SVF	Adipocyte	SVF	Adipocyte	SVF
<b>AT composition</b>								
Adipocyte diameter, $\mu\text{m}$	49	r	-0.338	-0.274	-0.136	-0.506	-0.238	-0.214
		p	<b>0.033</b>	0.087	0.403	<b>0.001</b>	0.139	0.185
Number of adipocytes per g ATx10 <sup>6</sup> *	49	r	0.364	0.262	0.299	0.402	0.359	0.221
		p	<b>0.021</b>	0.103	0.061	<b>0.010</b>	<b>0.023</b>	0.170
<b>AT inflammation</b>								
Macrophages per 100 adipocytes*	57	r	-0.128	-0.201	-0.029	-0.049	-0.297	-0.227
		p	0.377	0.161	0.842	0.738	<b>0.036</b>	0.114
Crown-like structures <sup>b</sup>	32 absent	mean $\pm$ SD	1.070 $\pm$ 0.416	0.118 $\pm$ 0.051	0.216 $\pm$ 0.12	0.062 $\pm$ 0.03	0.009 $\pm$ 0.006	0.103 $\pm$ 0.057
	25 present	mean $\pm$ SD	0.893 $\pm$ 0.487	0.103 $\pm$ 0.048	0.168 $\pm$ 0.089	0.059 $\pm$ 0.022	0.008 $\pm$ 0.006	0.069 $\pm$ 0.038
		p	0.125	0.256	0.105	0.706	0.524	<b>0.011</b>
Serum hsCRP*	61	r	-0.075	-0.276	0.035	0.113	-0.093	0.049
		p	0.584	<b>0.040</b>	0.797	0.406	0.494	0.722
<b>AT function</b>								
Basal lipolysis in adipocytes	18	r	0.049	0.136	0.167	-0.126	0.172	0.248
		p	0.826	0.629	0.552	0.654	0.540	0.373
Stimulated lipolysis in adipocytes*	19	r	0.426	0.201	0.441	-0.005	0.424	0.390
		p	0.100	0.456	0.087	0.985	0.101	0.135
Doubling time of cells, hours*	33	r	-0.330	-0.250	0.105	0.124	-0.135	-0.041
		p	0.100	0.218	0.611	0.547	0.510	0.844
Differentiation of SVF cells, %	30	r	-0.075	0.132	0.021	-0.085	-0.123	0.183
		p	0.721	0.529	0.922	0.685	0.560	0.382
<b>Serum parameters</b>								
Adiponectin, mg/L*	64	r	0.119	0.046	0.109	0.035	0.148	0.177
		p	0.370	0.728	0.413	0.790	0.264	0.181
Leptin, ng/mL*	63	r	-0.051	-0.222	-0.003	0.171	0.134	-0.100
		p	0.706	0.094	0.981	0.201	0.316	0.453
Glucose, mmol/L*	66	r	-0.078	-0.053	0.154	-0.047	-0.138	-0.224
		p	0.546	0.681	0.228	0.712	0.281	0.077
Insulin, pmol/L*	64	r	-0.174	-0.306	0.053	-0.318	-0.093	-0.265
		p	0.179	<b>0.017</b>	0.686	<b>0.012</b>	0.476	<b>0.039</b>

Asterisks (\*) indicate that this parameter was log<sub>10</sub>-transformed for statistical analysis. *P*-values <0.05 are highlighted in bold. Data from children age 2-18 years were analyzed using partial regression analyses adjusting for age, sex and BMI SDS. Gene expression of crown-like structure positive and negative tissues was compared using student's test (b). BMI SDS, body mass index standard deviation score; *GHR*, growth hormone receptor; *IGF-1*, insulin-like growth factor-1; *IGFBP-3*, IGF-1 binding protein; AT, adipose tissue; SVF, stromal vascular fraction; hsCRP, high sensitive C-reactive protein. This table was adopted from Kempf *et al.*: Contribution of adipose tissue to alterations in the growth hormone axis in childhood obesity and associations with adipose tissue function (submitted).

#### 4.2.6 *FGFR3* expression in AT is associated with obesity and metabolic parameters<sup>20</sup>

In collaboration with the research group of Dr. Yu-Hua Tseng (Joslin Diabetes Center, Section on Integrative Physiology and Metabolism, Harvard Medical School, Boston, MA, USA), we contributed to investigating factors from a different family of growth factors, the fibroblast growth factors. It was discovered that the fibroblast growth factors FGF6 and FGF9, both expressed in adipocytes, can induce UCP-1 activation and hence thermogenesis in AT, in part through binding to the fibroblast growth factors receptor 3 (FGFR3) [2].

Using already available ILLUMINA array gene expression data from AT from 223 individuals of the Leipzig AT Childhood Cohort, we found that *FGFR3* expression in subcutaneous AT was negatively associated with parameters of obesity such as BMI SDS ( $r = -0.134$ ,  $p = 0.021$ ) and the percentage of body fat ( $r = -0.209$ ,  $p = 0.009$ ) as well as with HOMA-IR and fasting plasma insulin levels (Figure 14). The negative correlation with fasting plasma insulin persisted adjustment for BMI SDS ( $r = -0.142$ ,  $p = 0.030$ ), indicating that the relation between *FGFR3* expression and insulin sensitivity may be independent of body weight. Hence, FGFR3 may be another growth-related factor involved in AT function that is dysregulated in children with obesity [2].



<sup>20</sup> The content and the figure of this subchapter were adopted from the manuscript Shamsi *et al. Nat Commun* 2020 [2].

### 4.3 Study 3: Identification of a potential novel monogenic trait for obesity and tall stature<sup>21</sup>

So far the relations between common childhood obesity and linear growth were investigated. However, in rare cases severe obesity can be caused by mutations in genes of the leptin-MC4R axis and those monogenic forms of obesity often are accompanied by tall stature of the patients. By using a bottom-up approach investigating AT function in a girl suffering from severe early-onset obesity and extremely tall stature, in study 3, we identified a potential novel trait for monogenic obesity and overgrowth.

#### 4.3.1 Identification of a patient with ectopic *ASIP* expression

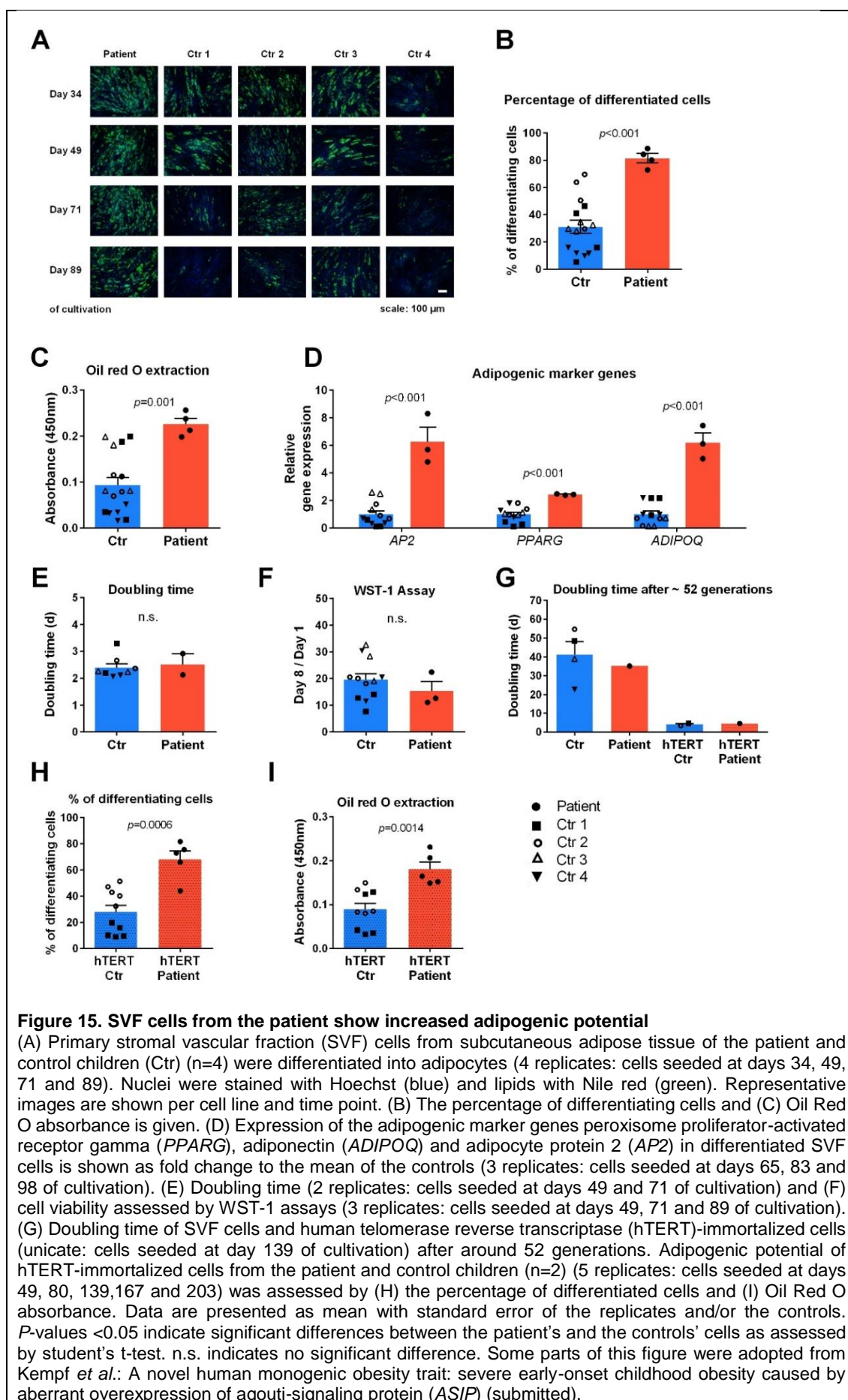
At the age of 12.4 years, a girl suffering from severe obesity (156 kg, BMI SDS 3.7) and tall stature (181 cm, height SDS 3.34) underwent bariatric surgery and subcutaneous AT samples were obtained.

Using *in vitro* approaches we characterized the function of primary AT-derived SVF cells from the girl and from age-matched control children also suffering from obesity or overweight (Appendix II, Table S3). Interestingly, compared to the control children adipogenesis of SVF cells from the patient was enhanced, even in cells long-term cultivated for up to 89 days (Figure 15 A), as quantified as 2.7-fold increase in the percentage of differentiating cells (Figure 15 B) and Oil Red O absorbance (Figure 15 C). In line with this, adipogenic gene expression was increased up to 6-fold in differentiated cells from the patient compared to the controls (Figure 15 D). However, doubling time (Figure 15 E) and cell viability (Figure 15 F) was not different and SVF cells of the patient entered senescence at similar age as the control cells after around 52 generations (Figure 15 G). SVF cells from the patient and from two of the control children were immortalized by introducing the human telomerase reverse transcriptase gene (*hTERT*) to the cells in order to generate a stable cell line. As expected, the immortalized cells (hTERTs) continued to proliferate when primary cells already became senescent (Figure 15 G). After immortalization the cells lost some of their adipogenic capacity, however, the cells of the patient still differentiated better compared to the immortalized control cells (Figure 15 H, I).

---

<sup>21</sup> Some parts of the text, of the figures and of the tables of this subchapter were adopted from the manuscript: **Kempf et al.**: A novel human monogenic obesity trait: severe early-onset childhood obesity caused by aberrant overexpression of agouti-signaling protein (*ASIP*). **Submitted.**





In order to identify potential causes for the enhanced adipogenesis in the patient's versus the controls' cells, we searched for differentially expressed genes using ILLUMINA gene expression arrays. Particularly one gene, coding for the agouti-signaling protein (*ASIP*), was significantly and highly overexpressed in pre-passaged, undifferentiated (fold change (FC): 116.8; false discovery rate (FDR) = 0.002) as well as in differentiated (FC: 64.2; FDR = 0.008) primary SVF cells from the patient (Figure 16 A, B).

*ASIP* is an inverse agonist of melanocortin receptors [123] and physiologically *ASIP* is expressed in the skin regulating hair pigmentation. Interestingly, ubiquitous overexpression of the murine *ASIP* homologue *agouti* in mice leads not only to yellow fur, but also to obesity by increasing food intake and lipid storage in adipocytes and by decreasing thermogenesis [124-127]. Accordingly, ubiquitous expression of *ASIP* might be a novel trait for monogenetic obesity in humans.

We confirmed *ASIP* overexpression in several cell types (Figure 16 C-G) of the patient including AT cells and PBL suggesting an ubiquitous overexpression. Even after immortalization SVF cells maintained the *ASIP* overexpression (Figure 16 G). Regarding expression in tissues of healthy humans, high *ASIP* expression was observed in skin (Figure 16 H). Apart from that, *ASIP* was comparably low expressed in human tissues (Figure 16 I).

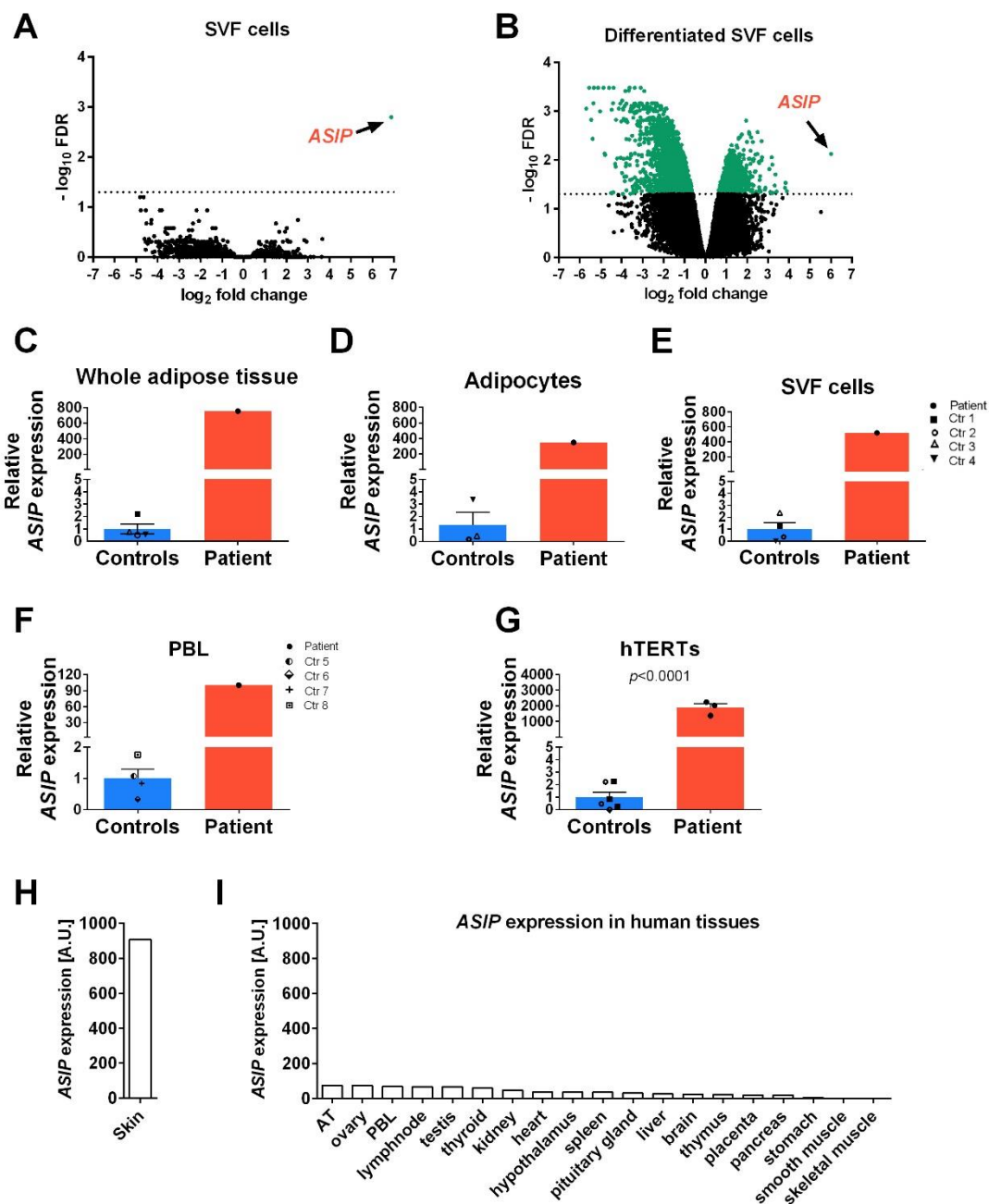


**Figure 16. ASIP expression in the patient and in human tissues**

Differentially expressed genes in pre-passaged, (A) undifferentiated stromal-vascular fraction (SVF) cells and (B) differentiated SVF cells between the patient and control children ( $n=4$ ) are given as the  $\log_2$  of the fold change of the gene expression across the  $-\log_{10}$  of the false discovery rate (FDR). Differentially expressed genes with  $FDR < 0.05$  are highlighted in green. Agouti-signaling protein (*ASIP*) expression is shown in (C) whole AT, freshly isolated (D) SVF cells and (E) adipocytes, (F) peripheral blood leukocytes (PBL) and (G) immortalized SVF cells (hTERTs) (3 replicates) from the patient and controls. As from control children 1-4 RNA from PBL was not available, measurements were performed in the additional control children 5-8 (Appendix I, Table S3). *ASIP* expression in (H) skin and (I) human tissues pooled from several subjects is shown. In C-G gene expression is given as fold change (mean controls=1). Data are presented as mean with standard error of replicates and/or the controls.  $P$ -values  $< 0.05$  indicate significant differences between the patient cells and the controls as assessed by student's t-test. Some parts of this figure were adopted from Kempf *et al.*: A novel human monogenic obesity trait: severe early-onset childhood obesity caused by aberrant overexpression of agouti-signaling protein (*ASIP*) (submitted).

The finding of ectopic *ASIP* expression was further confirmed by analyzing ASIP protein levels in SVF cells. By cloning and sequencing we confirmed that the *ASIP* protein coding sequence in the patient was identical to the reference sequence (GRCh38/hg38) (Figure 17 A).

For ASIP protein detection by immunoblotting, first an anti-ASIP-antibody was tested for specificity: In HEK293 cells transfected with a pCMV6-ASIP-Myc-DDK vector the artificially expressed ASIP protein tagged with Myc-DDK was detected in cell lysates and conditioned medium, but not in cells transfected with a control vector (pCMV6-entry) (Figure 17 B). The same bands were detected using an anti-Myc antibody, showing that the anti-ASIP antibody binds specifically to ASIP.

Performing immunoblotting of ASIP in cell lysates from immortalized SVF cells and conditioned medium the amount of ASIP protein was strongly increased in the patient compared to two controls (Figure 17 C).

siRNA-mediated knockdown of *ASIP* in the patient further validated that the anti-ASIP-antibody specifically detects the ASIP protein, as the ASIP signal was almost absent in the *ASIP* knockdown cells and mirrors the knockdown efficiency of 95 % as assessed by gene expression analyses (Figure 17 D).

Inhibition of the classical secretory pathway using brefeldin A and monensin leads to a retention of ASIP in the patient's cells further confirming that the ectopic ASIP is secreted via the classical secretory pathway just like the endogenous protein [128] (Figure 17 E).



#### 4.3.2 Identification of a heterozygous tandem duplication in the *ASIP* locus

Ubiquitous overexpression of the murine *ASIP* homologue *agouti* has already been observed in mice. In some cases the underlying genetic alterations is the emergence of cryptic promoter elements, upstream of the *agouti* coding exons, thereby resulting in constitutive and ubiquitous *ASIP* expression [125]. Another mutation seen in mice is a 170 kbp-deletion upstream of the *agouti* gene leading to a fusion of the *ASIP* coding region to the promoter of the ubiquitously expressed *RALY* gene [129].

In order to investigate if an alteration in the *ASIP* promoter region causes the ectopic *ASIP* expression in the patient, whole genome sequencing of the patient's gDNA was performed, revealing a heterozygous 183 kbp-tandem duplication on chromosome 20 encompassing the genes *ASIP*, *AHCY* (adenosylhomocysteinase) and *ITCH* (Figure 18 A). The duplication leads to fusion of the *ITCH* promoter region and the *ITCH* 5' UTR (exons 1-2) to the *ASIP* protein coding region, as confirmed by cloning and sequencing of the *ITCH-ASIP* fusion gDNA sequence of the patient (Figure 18 B). As there is an overlap of 6 nucleotides present at the breakpoint sites of both, the *ITCH* and the *ASIP* sequences, it is not possible to define the exact duplication breakpoints.

The heterozygous duplication was further confirmed by quantifying gDNA copy number. For this we established qPCR for 3 regions: The region of *AHCY* intron 3 was supposed to be duplicated, while the region 5' of *ASIP* and *ITCH* intron 2 were not supposed to be affected by the duplication. As expected, the copy number of *AHCY* intron 3 was around 50 % increased (Figure 18 C) in patient SVF cells compared to control cells and copy numbers of the 5' *ASIP* and *ITCH* intron 2 sequences were unchanged. Finally, the duplication-specific *ITCH-ASIP* fusion sequence was quantified by qPCR showing a high copy number in the patient and no signal in the controls.

In line with this, gene expression of *AHCY* (Figure 18 D), but not *ITCH* (Figure 18 E), was by ~50 % increased in undifferentiated and differentiated SVF cells from the patient confirming the heterozygous tandem duplication in the patient.

Analyses of *ASIP* expression in PBL of the parents revealed that the father, but not the mother, also had an ectopic *ASIP* expression (Figure 18 F). Accordingly, the father possessed the duplication-specific *ITCH-ASIP* breakpoint sequence, thereby confirming that the mutation was inherited from the father (Figure 18 G). This was validated by whole genome sequencing.

Further clinically relevant variants or copy number variations in genes related to obesity (such as *MC4R*, *POMC* or leptin receptor) or other diseases in the patient were excluded by TruSight One panel sequencing.

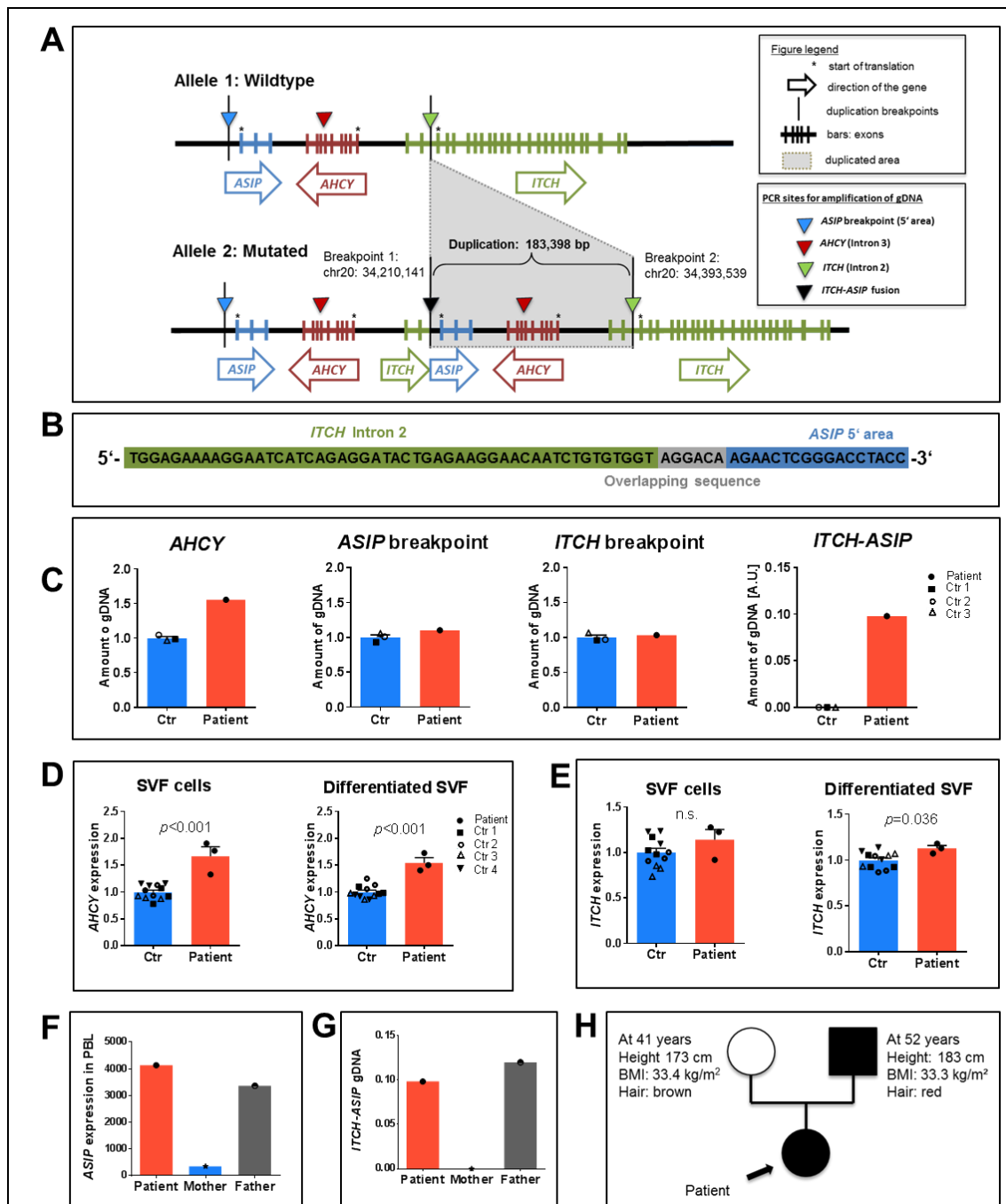


**Figure 18. A heterozygous tandem duplication at the *ASIP* locus**

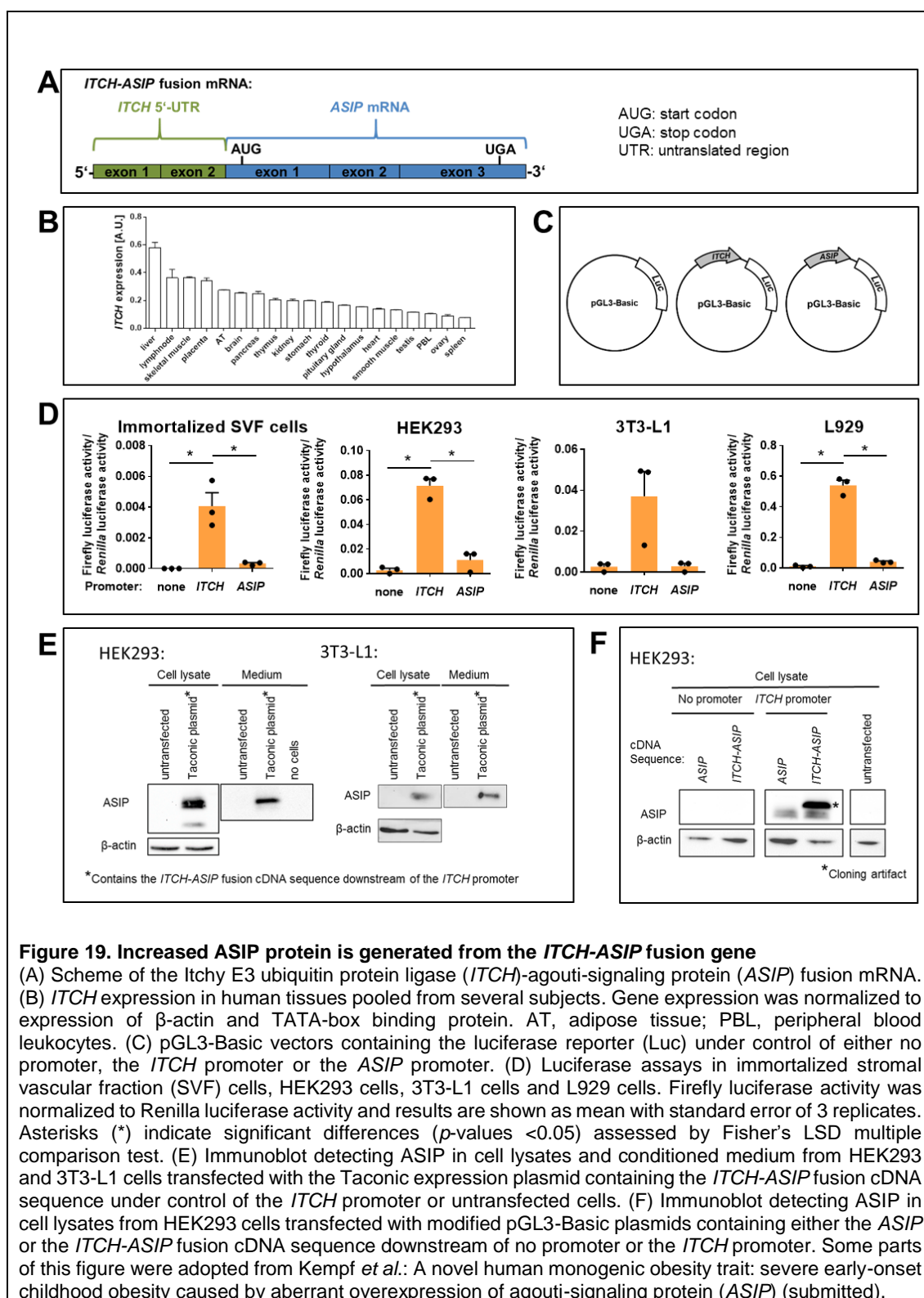
(A) Scheme of the wildtype and the mutated allele with the duplication spanning the genes agouti signaling protein (*ASIP*), adenosylhomocysteinase (*AHCY*) and itchy E3 ubiquitin protein ligase (*ITCH*). (B) Excerpt from the *ITCH-ASIP* fusion gDNA sequence. (C) gDNA copy numbers of *AHCY* intron 3 (red triangle in (A)), region 5' of *ASIP* (blue triangle) and *ITCH* intron 2 (green triangle) and *ITCH-ASIP* fusion (black triangle) sequences are shown as the fold change to the mean of the controls ( $n=3$ ) with standard error. (D) Gene expression of *ITCH* and (E) *AHCY* in undifferentiated and differentiated SVF cells from the patient and controls ( $n=4$ ) (performed in 3 replicates) are presented as fold change to the mean of the controls with standard error. (F) *ASIP* expression in peripheral blood leukocytes (PBL) and (G) gDNA copy numbers of *ITCH-ASIP* fusion gDNA in the patient and her parents. gDNA copy numbers were normalized to those of  $\beta$ -actin.  $P$ -values  $<0.05$  indicate significant differences assessed by student's  $t$ -test. n.s. indicates no statistical significance. Some parts of this figure were adopted from Kempf *et al.*: A novel human monogenic obesity trait: severe early-onset childhood obesity caused by aberrant overexpression of agouti-signaling protein (*ASIP*) (submitted).

### 4.3.3 The tandem duplication leads to ectopic *ASIP* expression

To answer the question if the *ITCH-ASIP* fusion gene drives the ectopic *ASIP* expression in the patient, 5'-RACE-PCR was performed. Indeed, we verified that the tandem duplication promotes an *ITCH-ASIP* fusion transcript consisting of the first two non-coding *ITCH* exons (5'-UTR) and the *ASIP* coding exons (Figure 19 A). In contrast to *ASIP* (Figure 16 J), *ITCH* is ubiquitously expressed in human tissues (Figure 19 B). The duplication placing *ASIP* under control of the ubiquitous *ITCH* promoter hence explains the ubiquitous expression of *ASIP* in the patient. Performing luciferase assays with modified pGL3-Basic plasmids (Figure 19 C), we showed that the genomic region located 2.8 kbp upstream of *ITCH* exon 1 (the *ITCH* region fused to the *ASIP* coding exons) constitutes a functional promoter as it is capable to drive gene expression in human and murine cells (Figure 19 D). The 1.2 kbp *ASIP* promoter only drove weak expression, however, we could not reassure that this *ASIP* promoter fragment is sufficient and functional, as we could not test it in cells physiologically expressing *ASIP*.

Next, we reconstructed an artificial fusion gene by placing the *ITCH-ASIP* fusion cDNA sequence under control of the 2.8 kbp-*ITCH* promoter and confirmed that this leads to increased synthesis and secretion of *ASIP* protein in HEK293 and 3T3-L1 cells (Figure 19 E). Finally, we tested whether the *ITCH* 5'-UTR contained in the *ITCH-ASIP* cDNA affects *ASIP* protein synthesis. However, we did not detect any obvious differences in presence or absence of this region (Figure 19 F). Thus, here we show that the chromosomal rearrangement in the patient, positioning *ASIP* under the control of the *ITCH* promoter, causes ectopic *ASIP* expression.





#### 4.3.4 Phenotypic characterization of the patient and her father

We performed a more detailed characterization of the patient. As the daughter of non-consanguineous parents of European ancestry the patient presented first at the age of 1.9 years, already suffering from overgrowth (95.1 cm, height SDS 2.7) (Figure 20 A) and severe early onset obesity (24.7 kg, BMI SDS 4.9) (Figure 20 B). From the age of around 2 years onwards, she maintained a height and BMI above the 97th percentile (Figure 20 A, B). Even when applying the height reference values specific for girls with obesity (generated in study 1 [1]), the patient maintained a height above the 97th percentile, being suggestive for an underlying genetic disease. Another characteristic of the patient's physical appearance is her red hair color and bright skin with freckles (Figure 20 C).

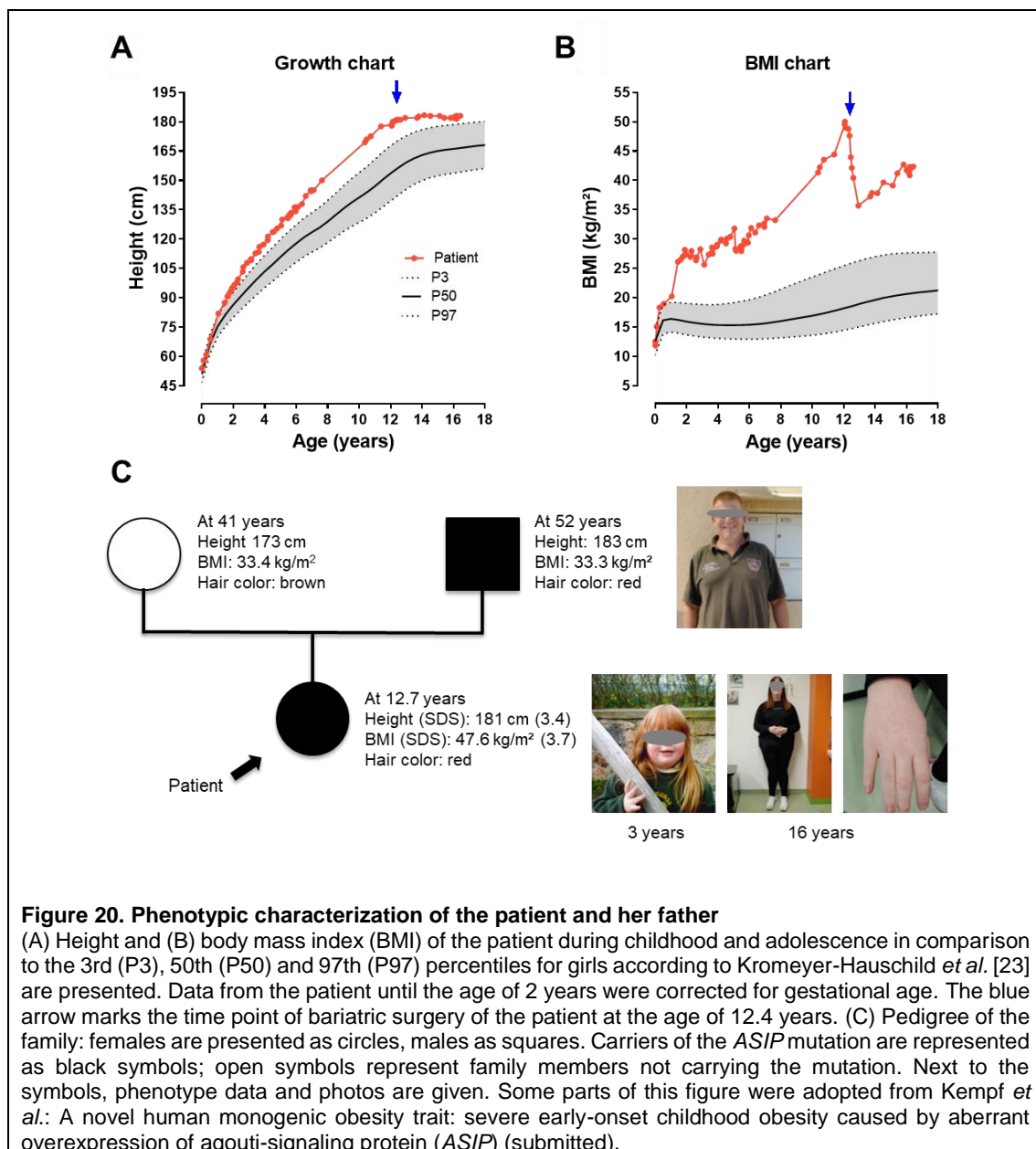


**Figure 20. Phenotypic characterization of the patient and her father**

(A) Height and (B) body mass index (BMI) of the patient during childhood and adolescence in comparison to the 3rd (P3), 50th (P50) and 97th (P97) percentiles for girls according to Kromeyer-Hauschild *et al.* [23] are presented. Data from the patient until the age of 2 years were corrected for gestational age. The blue arrow marks the time point of bariatric surgery of the patient at the age of 12.4 years. (C) Pedigree of the family: females are presented as circles, males as squares. Carriers of the *ASIP* mutation are represented as black symbols; open symbols represent family members not carrying the mutation. Next to the symbols, phenotype data and photos are given. Some parts of this figure were adopted from Kempf *et al.*: A novel human monogenic obesity trait: severe early-onset childhood obesity caused by aberrant overexpression of agouti-signaling protein (*ASIP*) (submitted).

Already in early childhood (2 years of age onwards) the patient showed first signs of formation of hepatic steatosis indicated by serum ALAT levels above the 97th percentile (Figure 21 A), while serum ASAT levels were elevated only later around the age of 10 years (Figure 21 B). Furthermore, she presented high fasting glucose levels (Figure 21 C) starting from the age of 7 years and developed insulin resistance (Figure 21 D) as seen from high levels of fasting insulin with a peak >1200 pmol/L at the age of 12.4 years and a HOMA-IR above 50 (Figure 21 E). Also the glycated haemoglobin (HbA1c) (Figure 21 F) reached the critical value of 5.7 % at the age of 12 years and was accompanied by high 2 hour glucose levels (Figure 21 G).

At the age of 12.4 years with a height of 181 cm (height SDS 3.34) and a weight of 156 kg (BMI SDS 3.7) she underwent bariatric surgery and lost around 40 kg of body weight within the following year, however, still remaining above the 97th percentile of BMI SDS (Figure 20 B). The liver parameters as well as the metabolic parameters improved (Figure 21). Around the age of 13 years she slowly started regaining weight. Currently, at the age of 16 years, she is 183.1 cm tall (height SDS 2.5) and weighs 142 kg (BMI SDS 3.75) (Figure 20 A, B).

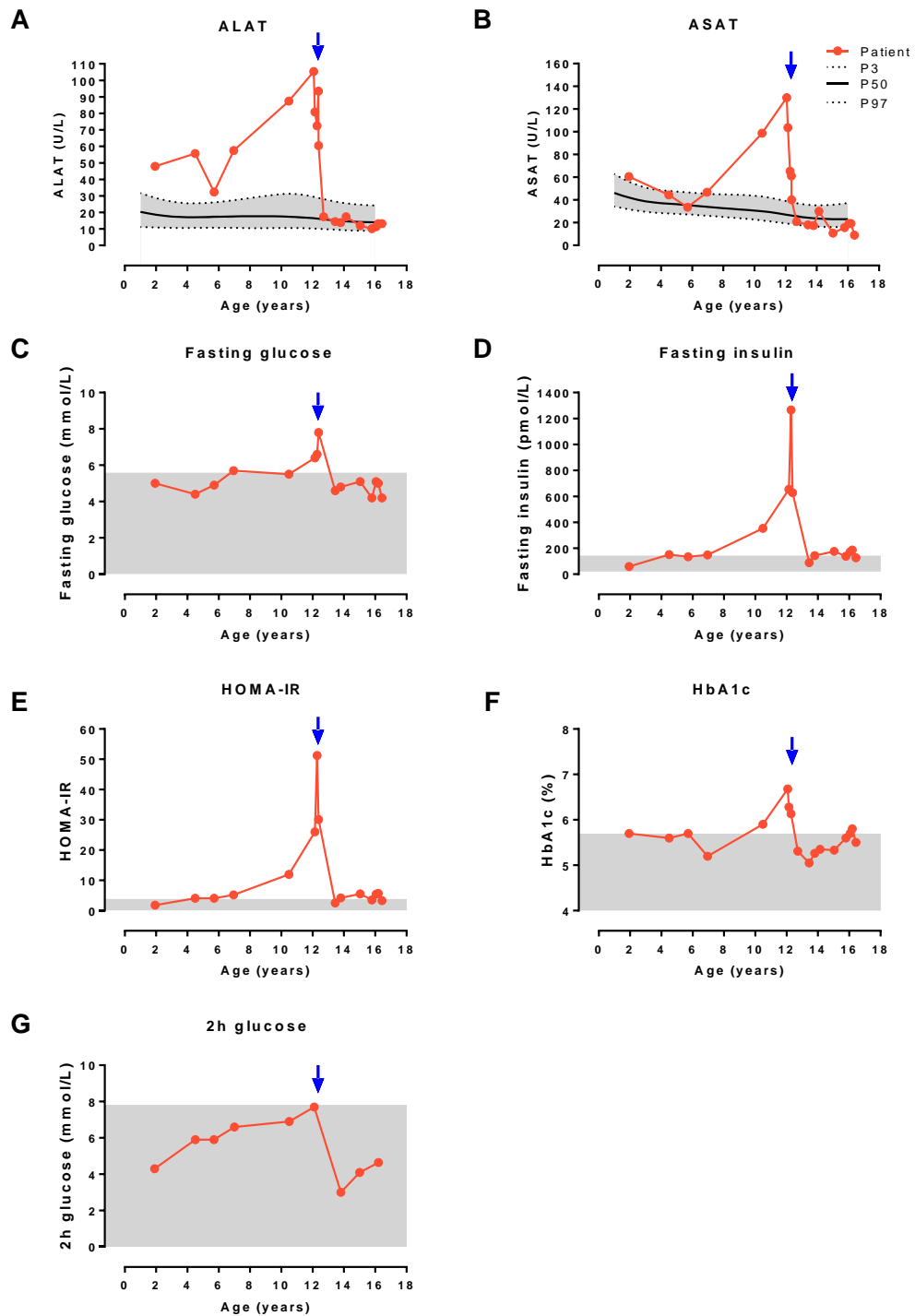


**Figure 21. Liver and metabolic parameters of the patient**

Liver and metabolic parameters of the patient during childhood and adolescence are presented. For the liver parameters (A) alanine aminotransferase (ALAT) and (B) aspartate aminotransferase (ASAT) are presented in comparison to the 3rd (P3), 50th (P50) and 97th (P97) percentiles according to Bussler *et al.* [117]. The metabolic parameters (C) fasting glucose, (D) fasting insulin, (E) Homeostatic Model Assessment for Insulin Resistance (HOMA-IR), (F) glycated haemoglobin (HbA1c) and (G) 2 hour (2h) glucose are presented. Reference ranges according to the local hospital laboratory, the American Diabetes Association [130] or Allard *et al.* [131] are indicated in grey. The blue arrow marks the time point of bariatric surgery of the patient at the age of 12.4 years. Some parts of this figure were adopted from Kempf *et al.*: A novel human monogenic obesity trait: severe early-onset childhood obesity caused by aberrant overexpression of agouti-signaling protein (*ASIP*) (submitted).

During childhood, the patient reported being continuously hungry, except after eating very large amounts of food, and trying to consciously control food intake. At the age of 16, she scored high at the Eating Disorder Examination-Questionnaire (EDE-Q) and the Dutch Eating Behavior Questionnaire showing high cognitive restraint (>85 percentile) as well as extreme eating, weight and shape concern (>95 percentile). She did not report binge eating, external (<5 percentile) or emotional eating (<25 percentile).

In a clinical exploration, a remarkably low physical activity was noted. Furthermore, indirect calorimetry revealed a reduced resting metabolic rate of 1,660 kcal/day accounting for only 77.4% of the expected 2,145 kcal/day.

Similarly, the patient's father, who is carrying the same mutation, also has red hair, bright skin and freckles (Figure 20 C). According to self-reports, from birth on he was taller and weighed more than his peers. At the age of 10 years, he engaged in professional athletics sports and lost some weight. Nonetheless, he reported to have weighed 125 kg at the age of 18 years (BMI: 36 kg/m<sup>2</sup>). At the age of 52 years, he still suffered from obesity (height 185 cm, weight 114 kg, BMI 33.3 kg/m<sup>2</sup>) as well as asthma, allergies, diabetes mellitus type II, hypertonia and gout. He did however not score conspicuously in eating questionnaires at the age of 52 years.

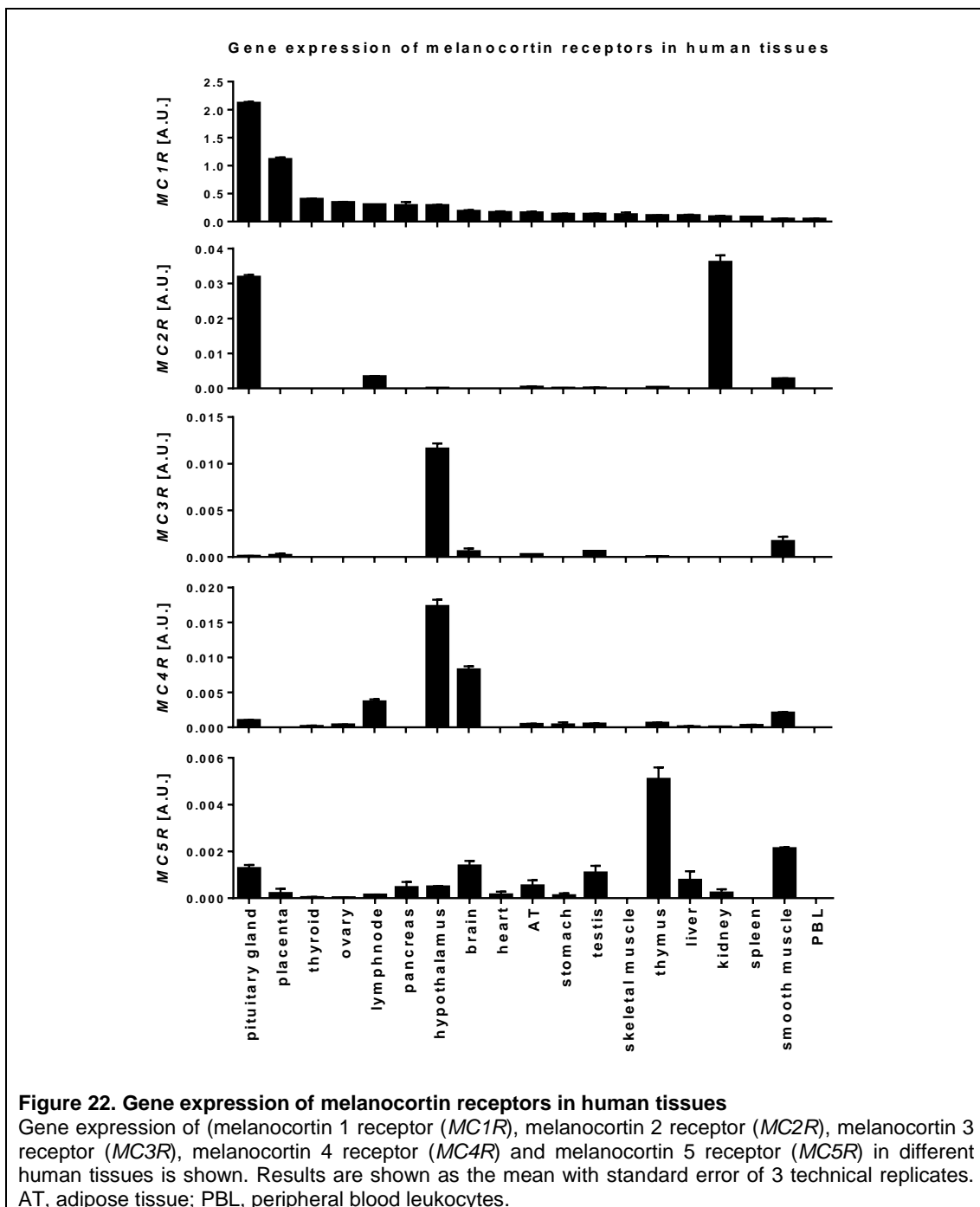
We confirmed by whole genome sequencing that both, the patient and her father, do not carry any genetic variant known to be associated with red hair [132], e.g. in the *MC1R* (Appendix IIIC, Table S13), indicating that the identified *ASIP* mutation is likely to be responsible for the red hair color.

#### 4.3.5 Effects of *ASIP* on AT metabolism and mitochondrial function in SVF cells

The obesity phenotype of mice ubiquitously overexpressing *agouti* (in the following called *agouti* mice), was suggested to result at least in part from altered metabolic processes on AT level such as decreased lipolysis or increased adipogenesis [133, 134]. In line with that, we observed that the patient SVF cells differentiated better than SVF cells from control children (Figure 15).

As *ASIP* is supposed to exert obesity-promoting effects by antagonizing melanocortin receptors [123], we first investigated expression of the different melanocortin receptors in human tissues. *MC1R* was moderately expressed in all examined tissues, with highest expression in the pituitary gland and placenta (Figure 22). *MC2R* expression was absent in most tissues except for kidney and pituitary gland and in lower amounts the lymph node and smooth muscle. Expression in AT was detectable, however, was very low. *MC3R* expression also was absent in many tissues, but was highly expressed in the

hypothalamus and in lower amounts in the smooth muscle, brain and AT. Similarly, *MC4R* was expressed in the hypothalamus and brain and only in lower amounts in other tissues. *MC5R* was mainly expressed in the thymus and at lower levels in smooth muscle, brain, pituitary gland, testis, liver, AT, hypothalamus, pancreas, kidney, placenta, lymph node, stomach, thyroid and ovary. In summary, in AT all melanocortin receptors appeared to be expressed, however, except for *MC1R* in comparably low amounts. Similarly, SVF cells from the patient and the controls as well as SGBS cells expressed *MC1R* but not *MC2R-MC5R* (not shown).



Additionally, there are previous studies suggesting MCR-independent effects of ASIP on lipolysis [135]. This may explain our observation that differentiated SGBS cells treated with recombinant ASIP protein had a slightly decreased basal and isoproterenol-stimulated lipolytic rate compared to untreated cells (Figure 23 A).

However, when we knocked down *ASIP* expression in patient SVF cells and differentiated them into adipocytes, we did not observe a difference in adipogenic capacity compared to control cells (Figure 23 B), although knockdown efficiency was 91-97 % and *ASIP* knockdown was also shown to result in reduced *ASIP* protein synthesis (Figure 17 D).

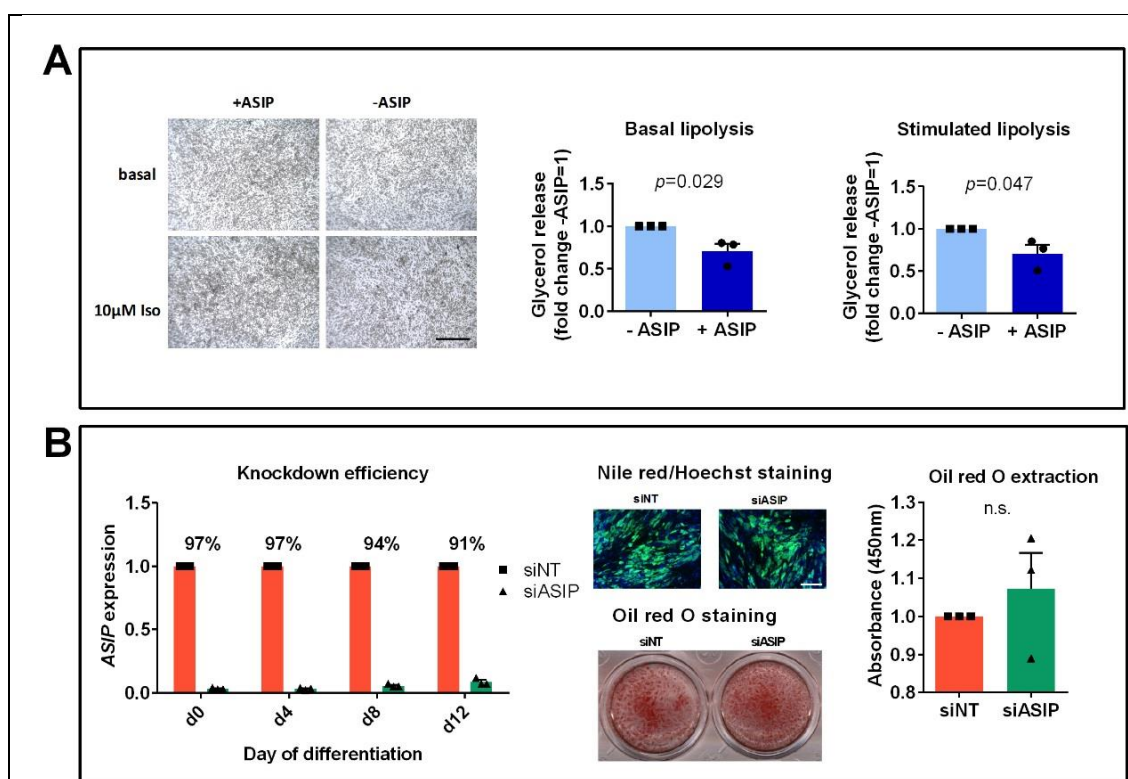


**Figure 23. Effect of ASIP on lipolysis and differentiation**

(A) For lipolysis assay, Simpson-Golabi-Behmel syndrome (SGBS) cells were differentiated into adipocytes (black scale bar: 1000  $\mu$ m), treated with agouti-signaling protein (ASIP) or left untreated, and basal and isoproterenol-stimulated glycerol release was measured (n=3). Glycerol release was normalized to cell number as assessed by protein quantification and is shown as mean fold change to untreated cells with standard error. (B) Patient SVF cells were transfected with siRNA targeting *ASIP* (siASIP) or with non-target siRNA (siNT) and were differentiated into adipocytes (n=3). *ASIP* knockdown efficiency according to gene expression is shown at days (d) 0, 4, 8 and 12 of differentiation. Differentiated cells were double-stained with Hoechst (blue) and Nile red (green) (white scale bar: 200  $\mu$ m) and stained with Oil red O. (C) Oil red O absorbance was measured. Data are shown as mean fold change to siNT with standard error. Statistical significance was assessed by student's t-test. n.s., not significant.

*Agouti* mice exhibit reduced thermogenesis [126]. Concordant with this, the resting metabolic rate of the patient was reduced, which might contribute to the development of obesity.

We assessed the bioenergetic profile of SVF cells from the patient in order to investigate if there are differences in mitochondrial respiration on SVF cell level. The maximum respiration and the spare capacity, an indicator for the ability of cells to respond to increased energetic demand, as well as the oxygen consumed due to proton leak were slightly decreased in the patient cells compared to control cells (Figure 24 A). However, *ASIP* knockdown in primary SVF cells from the patient did not have an effect on respiration in SVF cells (Figure 24 B).

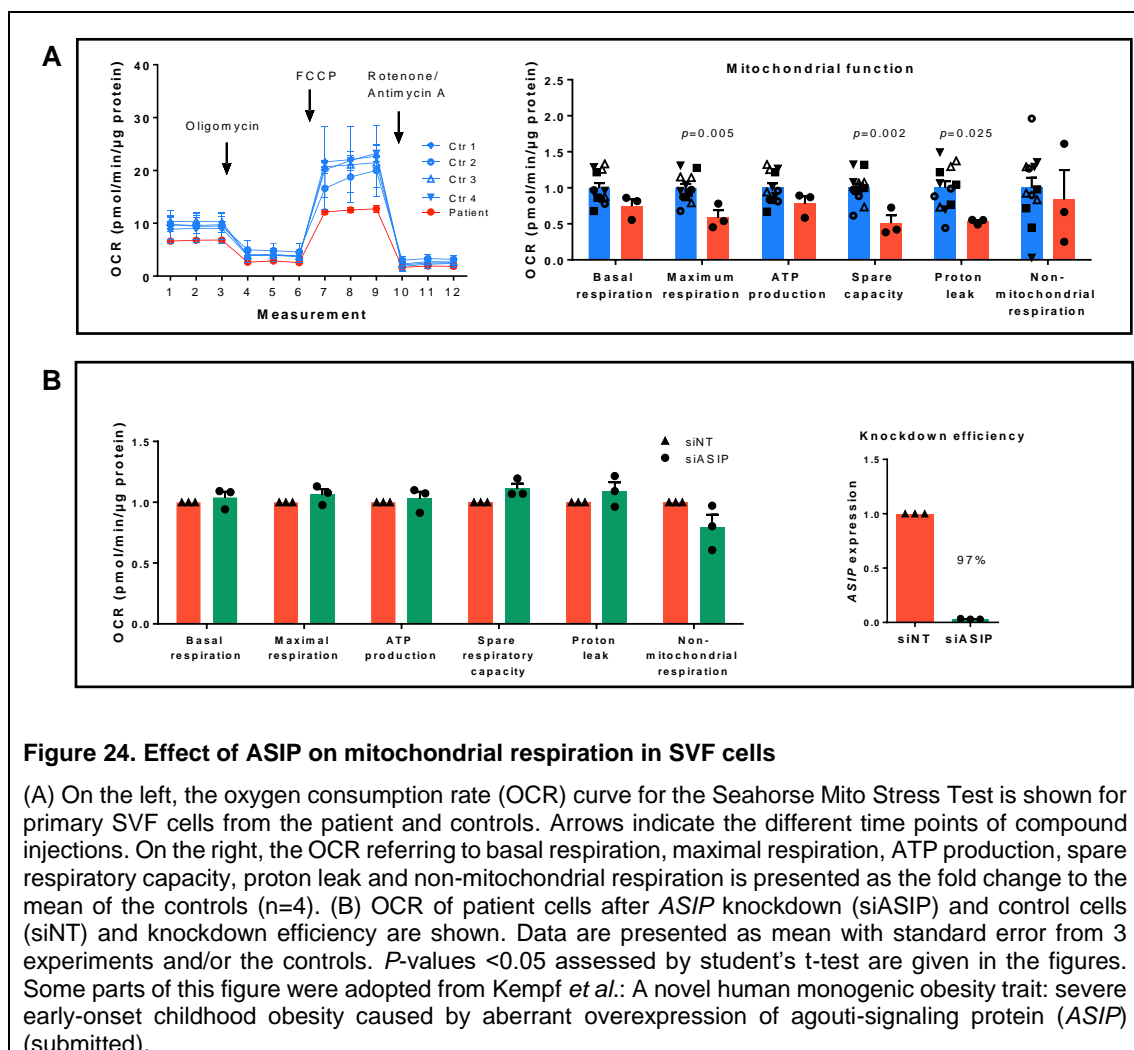


**Figure 24. Effect of ASIP on mitochondrial respiration in SVF cells**

(A) On the left, the oxygen consumption rate (OCR) curve for the Seahorse Mito Stress Test is shown for primary SVF cells from the patient and controls. Arrows indicate the different time points of compound injections. On the right, the OCR referring to basal respiration, maximal respiration, ATP production, spare respiratory capacity, proton leak and non-mitochondrial respiration is presented as the fold change to the mean of the controls (n=4). (B) OCR of patient cells after *ASIP* knockdown (siASIP) and control cells (siNT) and knockdown efficiency are shown. Data are presented as mean with standard error from 3 experiments and/or the controls. *P*-values <0.05 assessed by student's t-test are given in the figures. Some parts of this figure were adopted from Kempf *et al.*: A novel human monogenic obesity trait: severe early-onset childhood obesity caused by aberrant overexpression of agouti-signaling protein (*ASIP*) (submitted).



#### 4.3.6 Screening for additional patients with ectopic *ASIP* expression

The genomic sequence around the *ASIP* gene is characterized by the presence of high-density short interspersed elements, in particular Alu elements, which can act as a source of genetic instability and make the DNA susceptible for mutations and genetic recombination [136]. Therefore, we hypothesized that there are further patients with so far undetected *ASIP* mutations resulting in ubiquitous *ASIP* expression.

Screening already available ILLUMINA HT4v12 gene expression data from PBL from 1,020 children of the LIFE Child Cohort [86, 87], we did not identify another child with ectopic *ASIP* expression. A more targeted screening in patients with obesity, tall stature and/or red hair color in the future may enhance the probability to identify further patients with ectopic *ASIP* expression.

In summary, the novel genetic alteration here identified causes ectopic *ASIP* expression that may lead to the development of obesity by central and peripheral effects. Identification of additional patients with ectopic *ASIP* expression and might help to further understand the underlying mechanisms.

## 5 Discussion

In this thesis, we show that obesity in children and adolescents is accompanied by dynamic alterations in linear growth and in circulating levels of growth-related factors. Regarding the gene expression, AT does not seem to contribute relevantly to the elevated circulating levels of the growth-related factors GHBP and IGF-1 observed in pre-pubertal children with overweight/obesity. Instead, we found that gene expression of several growth-related factors is reduced in AT from children with overweight/obesity, which may be related to AT dysfunction. Furthermore, we identified ubiquitous *ASIP* expression as a potential novel trait for monogenetic obesity and tall stature in humans.

### 5.1 Linear growth and endocrine patterns are dynamically altered in children with obesity<sup>22</sup>

We showed that growth patterns of children with obesity deviate significantly and relevantly from those of normal-weight children with distinct dynamics across age. From early childhood on children with obesity are taller, independent of familial predisposition, whereas the pubertal growth spurt is blunted with concurrent decrease of growth velocity leading to a convergence of height curves in adolescence. After completion of linear growth, children with obesity had a normal height around 0 SDS similar to normal-weight children. A recent study [25] reported compromised adult height in relation to mid-parental height in individuals with obesity. We, instead, found a rather increased final height when corrected for mid-parental height. Those discrepancies might derive from the fact that in the previous study the parents of the subjects with obesity tended to be taller than those from normal-weight children, while in our study parents of children with obesity were slightly shorter.

We confirmed the differences in height in children with obesity in a second, independent and population-based cohort, implying a high generalizability of the results on the population.

The excess height in states of obesity in early childhood develops upon slightly increased birth length, which may imply an early predisposition for accelerated growth right from, or even before, birth. Thereafter, the observed obesity-related acceleration in growth velocity of up to 1 cm/year potentiates these differences accumulating to 7-8 cm taller height in children with obesity. This growth acceleration may be driven by growth factors, such as IGF-1 that is closely related to growth [29] and suspected to be dysregulated in obesity [29, 44, 45]. Looking into the dynamics of IGF-1 serum levels from early

---

<sup>22</sup> Most parts of the text of this subchapter were adopted literally from the discussion section of the publication: **Kempf et al., *eClinicalMedicine* 2021 [1]**.

childhood to adulthood, we found IGF-1 to be increased in pre-pubertal children with obesity, although not to a great extent, while during puberty IGF-1 levels are decreased compared to normal-weight children paralleling the dynamics of growth velocities. Unfortunately, our sample size of IGF-1 in children younger than the age of 6 years was too low for the obese group to perform more detailed statistical analyses in order to determine the associations of increased IGF-1 on growth in early childhood.

Altered IGF-1 levels in obesity may be a consequence of an increased nutritional status and/or a general dysregulation involving various other hormones [27]. Indeed, and in line with previous studies showing that during puberty testosterone and gonadotropins were lower in boys with obesity [42, 137], we found parallel divergences in growth velocity and sex hormones between obese and normal-weight groups during puberty.

Girls with obesity had an earlier onset and completion of puberty than normal-weight girls, reflected by earlier thelarche and also by earlier onset of menarche [42]. Nevertheless, this is not likely to explain the increase in early pre-pubertal growth, as girls with obesity presented accelerated growth well before puberty onset. During puberty and in line with Biro *et al.* [138], estradiol levels were reduced in our girls with obesity and corresponded with the deceleration of growth. In addition, the girls with obesity had increased testosterone levels from 8 years onwards resulting in relative hyperandrogenism, particularly when the lower SHBG [137] levels in obesity are considered. Hyperandrogenism is linked to obesity [42] and somehow resembles polycystic ovary syndrome, but again this is unlikely to be the reason for the generally increased testosterone levels in girls with obesity that have also been reported in pre-pubertal children and were reversible with weight loss [139].

It is known that sex steroids can modulate the GH axis [41], for example by intensifying the amplitudes of GH pulses, by augmenting IGF-1 levels [140] or by increasing GH receptor expression and thereby potentially enhancing GH sensitivity [41]. The low testosterone levels in boys with obesity during puberty may hence contribute to the attenuated peak of serum IGF-1 and the lack of the growth spurt. However, this does not apply to girls with similarly repressed pubertal IGF-1 levels but elevated testosterone levels (even though they do not reach the extent of male testosterone) and hence does not suffice as an explanation for blunted pubertal IGF-1 response.

Finally, the elevated insulin and leptin levels in children with obesity [141] might promote growth. Insulin has receptor cross-reactivity for IGF-1 [27] and elevated insulin was associated with catch-up growth in infants born SGA [142]. Leptin may affect bone metabolism via direct molecular interaction in growth plates [27] and thereby stimulate proliferation and differentiation of chondrocytes [27]. We observed substantially elevated levels of metabolic factors already in early childhood. However, the magnitude of the

elevation in insulin and leptin levels further increased with age, thus not exactly paralleling the altered growth in childhood obesity. Hence, increased metabolic factors may contribute to promoting growth in pre-pubertal children with obesity; however, those actions may be exceeded during puberty by the response to sex steroids and IGF-1.

Given the extensive impact of obesity at the populational level, our findings of accelerated linear growth in children with obesity during early childhood and the generation of reference values for height for children with obesity may have several implications. First, considering that growth is an important indicator of health on an individual level of health surveillance, a young child with obesity is expected to be relatively tall. Using the height reference values might avoid misinterpretation of tall stature with obesity and potentially unnecessary medical diagnostic work-up. On the other hand, relative short stature in a child with obesity may indicate underlying syndromic, (mono)genetic or another physical condition, which might be overlooked when applying reference values not tailored for the weight status. With the advance of modern genetic testing methods and potential treatment opportunities, early consideration and diagnosis of underlying disease cases may have direct and beneficial consequences for potential treatment [143-145]. It is important to mention that the height reference values for children with obesity are intended to provide additional information for assessment of growth, but that they are not intended to “normalize” the altered growth observed in children with obesity.

Second, our findings illustrate and add alterations in growth and endocrine patterns to the array of obesity-related complications emerging already early in life. Considering that early increased height gain was associated with higher adult cardiovascular risk [146, 147], this may put children with obesity-related accelerated growth at increased risk for adult morbidity and potentially mortality [22].

There are several limitations of the study. First, this is a retrospective study over a long period of time combining cross-sectional and longitudinal data. Follow-up data allowing to calculate growth velocities were available in approximately half the children. Likewise, endocrine parameters were only available in a subset of the cohort, which may limit the generalizability of the conclusions. Nevertheless, as cross-sectional data such as height, parental or endocrine data add important value to this study, we did not restrict the analyses to children with multiple visits. We confirmed that these subsets showed identical growth patterns as the entire study population. Second, despite standardized procedures for anthropometric measurements, an inter-operator inaccuracy cannot be fully excluded, but might be compensated by high sample sizes and also applies to both,

the normal-weight and obese groups. Third, height data of infants (in cm) was not adjusted for gestational age. Forth, we categorized children according to their weight status using the BMI. Although BMI is not a direct reflection of body fat, BMI is the most widely used index for assessment of obesity with the advantage of being easily recordable and existing age, sex and often ethnic-specific reference values. In this study, we categorized children into normal-weight or obese according to the current weight status of the measurement, hence a change in weight category in follow-up analyses would not be regarded. However, for children, who have obesity in early childhood, the likelihood that obesity persists into adulthood is >80 % [9]. Consistent with this assumption, in our study very few children changed from the normal-weight to the obese category (0.5 %) and vice versa (2.5 %). Fifth, from this observational study we can only speculate about the mechanisms behind alterations in growth patterns with childhood obesity. Sixth, it should be noted that the height reference values for children with obesity were generated from a German study sample. Applying population-specific, national reference values may be recommended for other ethnic backgrounds.

In conclusion, growth patterns of children with obesity deviate from those of the normal-weight peer group throughout childhood and adolescence although the directions are temporarily distinct. In early childhood, imbalances in components of growth-related and metabolic parameters may contribute to altered growth and increased height in children with obesity. During pubertal age, reductions in circulating levels of the sex and growth hormone axis might contribute to the deceleration of growth. The provided novel height reference values for children with obesity may enhance the precision of individual clinical health surveillance. Mechanisms leading to the obesity-related changes in circulating levels are still to be clarified. If AT as an endocrine organ contributes to the alterations in the circulating levels of growth-related factors was investigated in study 2.

## 5.2 Contribution of AT to alterations in the GH axis in childhood obesity and associations of growth-related factors with AT function<sup>23</sup>

In study 1 [1], we showed that linear growth deviates in children with obesity and that this is associated with changes in circulating growth factors such as IGF-1. In study 2, we more closely regarded the growth-related factors IGF-1, IGFBP-3 and GHBP in childhood overweight or obesity. We investigated the role of AT in the regulation of circulating levels of these factors and the role of these factors in AT function.

We found that circulating GHBP, and in pre-pubertal children also IGF-1 but not IGFBP-3, are increased in children with overweight/obesity and that this is accompanied by increased height. We could not confirm our hypothesis that expression of these factors in AT is relevantly contributing to the increased serum levels, but found a strong relation of serum GHBP to the amount of liver fat. We found that gene expression of *GHR*, *IGF-1* and *IGFBP-3* was reduced in AT of children with overweight/obesity and was related to parameters of AT function such as adipocyte hypertrophy (Figure 25).

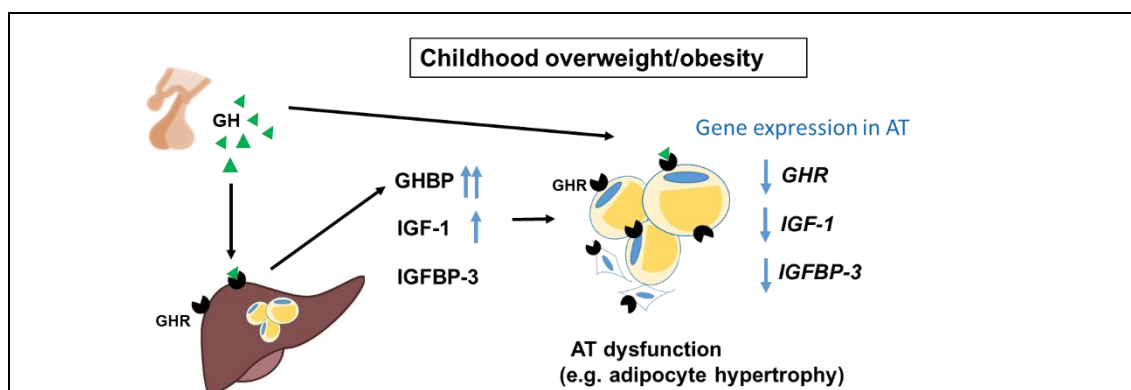


**Figure 25. Schematic overview of the proposed role of components of the GH axis in childhood obesity and adipose tissue function.**

In pre-pubertal children with overweight/obesity circulating levels of GHBP and IGF-1 are increased, while gene expression of *GHR* and *IGF-1* in AT is rather decreased. Increased liver fat content was related to increased GHBP levels. Decreased gene expression of *GHR*, *IGF-1* and *IGFBP-3* in AT may be related to parameters of AT dysfunction such as adipocyte hypertrophy. GH, growth hormone, GHR, GH receptor; GHBP, GH binding protein; IGF-1, insulin-like growth factor-1; IGFBP-3, IGF-1 binding protein-3; AT, adipose tissue. This figure was adopted and modified from Kempf *et al.*: Contribution of adipose tissue to alterations in the growth hormone axis in childhood obesity and associations with adipose tissue function (submitted).

Our results are in line with previous studies reporting that circulating GHBP was increased in children with obesity and that increased levels could be reversed by weight-loss [28, 120, 148]. We observed that serum IGF-1 and the IGF-1/IGFBP-3 molar ratio are increased in children with overweight/obesity exclusively in pre-puberty and/or early

<sup>23</sup> Most parts of the text and the figure of this subchapter were adopted literally from the discussion section of the manuscript: **Kempf et al.**: Contribution of adipose tissue to alterations in the growth hormone axis in childhood obesity and associations with adipose tissue function. **Submitted.**

puberty, which is supported by several studies [28, 29, 44, 45] and results from study 1 [1]. Previous results regarding serum IGFBP-3 levels are controversial. Some studies showed increased IGFBP-3 levels in children with obesity [149], while we (study 1) [1] and others suggest no association with BMI [28, 119]. Thus, even though GH itself was reported to be lower [44], circulating components downstream of the GH are increased in children with overweight/obesity, which might contribute to alterations in growth. This raises the question whether the increased fat mass with overweight/obesity contributes to the elevation of circulating GHBP and IGF-1.

*GHR* [51] and *IGF-1* [69] are known to be expressed in AT in humans. In this study, we further discriminated between freshly isolated human adipocytes and SVF cells and showed higher expression of *GHR* and *IGF-1* in adipocytes compared to SVF cells. We did not observe a positive correlation between gene expression in adipocytes and serum levels indicating that AT might not be the major source of circulating GHBP and IGF-1 contributing to the obesity-related elevations. Likewise, we considered the increased amount of body fat in obesity and included the parameters total adipocyte number and total body weight in our analyses, and did not see an association. Interestingly, a study investigating the relation between *GHR* expression in intra-abdominal fat and serum levels in healthy females also did not find a positive but a negative correlation with circulating GHBP [150]. Our data showing a negative association of serum GHBP with *GHR* expression in SVF cells, but not in adipocytes, suggest a cell-type-specific relation. However, based on our analyses we cannot entirely exclude that GHBP and IGF-1 released from AT contributes to obesity-related elevations in the serum levels as the amount of protein released from cells is not necessarily reflected by its gene expression. Wabitsch *et al.* showed that gene expression of *IGF-1* was not altered in differentiated SGBS cells compared to undifferentiated cells, but that secretion of the protein was enhanced with adipogenic differentiation [69]. Also, the process of GHBP shedding from GHR is complex and might depend on the abundance of different isoforms within a cell type as the truncated isoform GHR<sub>1-279</sub> was suggested to have a higher shedding rate [151].

However, our findings are supported by studies in adipocyte-specific knockout mice showing that a lack of IGF-1 in adipocytes did not alter plasma IGF-1 concentration [53, 152], while *Igf-1* expression in the liver was slightly increased. Vice versa, in liver-specific *Igf-1* knockout mice there was a trend towards an up-regulation of *Igf-1* expression in other tissues such as fat tissue [55], suggesting a compensatory feedback mechanism between tissues in order to keep circulating levels constant. Despite there are two adipocyte-specific *Ghr* knock out mouse models [153, 154], data regarding circulating

GHBP levels have not been reported. Overall, this strengthens the hypothesis that AT itself is not a relevant contributor to obesity-related elevations of circulating GHBP and IGF-1.

This implies that probably the liver as the major source of the growth factors and their binding proteins [48-50, 155] contributes to the augmentation of serum levels, particularly as the liver is affected by increased lipid load in obesity itself. Indeed, we found that serum levels of GHBP are highly associated with the percentage of liver fat in children, while the total body fat was not as relevant. Accordingly, apart from increased liver fat content, alterations in liver function tests (ALAT) and dyslipidemia, were related to elevated GHBP serum levels. Similarly, Fusco *et al.* observed an association of increased GHBP levels with adult non-alcoholic fatty liver disease [47]. Hence, at least for GHBP, the liver and not the AT may be the major source contributing to elevated serum levels with obesity. Unfortunately, associations of liver parameters with serum IGF-1 and IGFBP-3 could not be assessed due to a lack of data.

The composition of AT and its metabolic and secretory function is disturbed early in childhood obesity [21]. We observed that gene expression of *GHR* and *IGF-1* in adipocytes and expression of *IGFBP-3* in SVF cells was decreased in children with overweight/obesity compared to lean children. This follows previous findings in mice and in adult humans for *IGF-1* [53, 156] and *GHR* [157], but has not been described in children before and the previous studies in humans did not discriminate between adipocytes and SVF cells. *IGFBP-3* expression in AT has been previously shown not to be different [156] or increased after weight loss [158].

Compromised gene expression of the factors in AT might affect AT function.

Indeed, we found that low *GHR* expression in adipocytes was associated with a larger adipocyte diameter. This is in line with observations in adipocyte-specific *Ghr* knock out mice that had an increase in white AT mass and adipocyte size [153, 154]. In several studies a role of GHR in lipolysis has been confirmed [71, 159] and a lack of GHR might result in adipocyte hypertrophy. GH stimulates lipolysis in adipocytes in a GHR-dependent manner [160] via inhibition of lipoprotein lipase and stimulation of the hormone sensitive lipase [161]. In our study, *GHR* expression in adipocytes did not significantly correlate with the lipolytic rate, which might be due to the relatively small sample size.

Regarding IGF-1, we found that reduced expression in SVF cells was associated with increased adipocyte size. A potential explanation could be that proliferation of preadipocytes in AT is impaired with reduced local IGF-1 resulting in fewer and larger



adipocytes [72, 73]. In the Berlin Fat Mouse an adipocyte-specific *Igf-1* knockout resulted in a reduction of fat mass. However, the authors did not look more detailed into the AT composition in order to dissect effects on adipocyte hypertrophy or hyperplasia [152]. Effects of IGF-1 on subcutaneous adipocytes are rather mediated by INSR and not by the IGF-1R as *Insr* knockout mice had a 95 % decrease in white AT, while *Igf-1r* knockout mice only had a 25 % decrease [162]. Accordingly, we and others [163] found gene expression of *INSR*, but not *IGF-1R*, up-regulated during adipogenic differentiation.

As a modulator of bioavailability of IGF-1 IGFBP-3 is known to affect AT function via IGF-1-dependent mechanisms, but also IGF-1-independent mechanisms inhibiting adipocyte differentiation have been suggested [164, 165]. This is in line with our data showing that IGFBP-3 is rather down-regulated during differentiation of SGBS cells. We furthermore found a relation of reduced *IGFBP-3* expression in AT cells with increased AT inflammation, which fits to previously proposed anti-inflammatory and pro-apoptotic effects of IGFBP-3 [166].

A BMI-independent and inverse association of gene expression of *GHR*, *IGF-1* and *IGFBP-3* in SVF cells with fasting insulin levels implies that reduced gene expression might not only be related to AT dysfunction but also to the metabolic state in children.

A limitation of this study is that the GH status could not be assessed from circulating levels due to its nocturnal pulsatile secretion. Further, it is important to highlight again that we looked exclusively at gene expression in AT and that the secretion of the proteins might deviate. We did not perform multiple testing in this study. As some of the associations of gene expression with AT function may have not survived multiple testing, the results need to be regarded carefully.

The strength of our study is that we analyzed the role of the growth-related factors in children and not in adults, as here the regulation of growth is most important and dynamic. Furthermore, children present early stages of disease progression and are mostly free of medication and comorbidities potentially confounding the analyses. In addition and in contrast to many studies investigating obesity-related alterations in AT, we did not only look at human whole AT, but also differentiated between adipocytes and SVF cells, which might provide a more detailed insight into processes in AT.

Eventually, further studies are needed to decipher the specific role of components of the GH axis in AT function and the contribution of AT to serum levels.

In conclusion, AT may not be the major source for the obesity-related elevations in serum levels of GHBP and IGF-1 in children. However, reduced local gene expression of *GHR*, *IGF-1* and *IGFBP-3* in AT cells in children with overweight/obesity might contribute to compromised AT function.

Looking at a different family of growth factors within a collaboration with Dr. Tseng, we furthermore participated in showing that the adipokines and growth factors FGF6 and FGF9 can induce *UCP-1* in adipocytes via binding to FGFR3. The reduced expression of *FGFR3* that we observed in children with obesity might result in a blunted UCP-1 activation and might hence further disturb the energy metabolism, lead to hyperinsulinemia and deteriorate the metabolic state in children.

Thus, our data imply that components of the GH axis and other growth-related factors might be involved in WAT and BAT function in children and that a local obesity-related decrease of these factors in AT of children with obesity might contribute to AT dysfunction such as adipocyte hypertrophy or impaired thermoregulatory function. This might promote the progression of obesity and the development of obesity-associated sequelae.

### 5.3 Ubiquitous *ASIP* expression as a potential monogenic trait for human obesity and tall stature<sup>24</sup>

Using a bottom-up approach, we for the first time identified a patient with ubiquitous *ASIP* expression, which is a potential novel monogenic cause for human obesity, overgrowth and red hair. The ectopic *ASIP* expression is caused by a tandem duplication, placing a copy of the coding region of *ASIP* under control of the *ITCH* promoter. *ITCH* is supposed to be expressed ubiquitously [167] and in line with that, we found that *ITCH* is expressed in several human tissues including the hypothalamus. Therefore and as we confirmed ectopic *ASIP* expression in different cell types of the patient, we assume that *ASIP* expressed from the *ITCH-ASIP* fusion gene causes an ubiquitous *ASIP* overexpression in the patient. The tandem duplication was inherited from her father, who also suffers from obesity and has red hair color.

*ASIP* is the homologue of the murine *agouti* gene, which already has been linked to obesity in mice [127]. The coding region of the human *ASIP* gene is 85 % identical to the mouse gene [168] and there is high functional conservation [123]. Physiologically, *agouti* is expressed in dermal papilla cells of the hair follicles and antagonizes MC1R function on hair melanocytes in a paracrine manner resulting in a switch from eumelanin (darker pigments) to phaeomelanin (red pigments) synthesis [169] and yellow fur. It is supposed that *ASIP* in humans acts in a similar way [170] and variants near the *ASIP* gene have been associated with red hair color in humans [132]. Interestingly and similar to our patient, naturally occurring mice and also artificial mouse models with ubiquitous overexpression of *agouti* (*agouti* mice) exhibit overgrowth, have yellow fur and develop obesity and metabolic alterations such as hyperinsulinemia [124-127].

The obese phenotype of *agouti* mice is supposed to be the result of central effects of *agouti*, such as moderate hyperphagia and reduced thermogenesis, but also peripheral effects of *agouti* have been suggested, e.g. more efficient energy storage on adipocyte level [126, 127, 133].

Due to the high structural similarity with AGRP, ectopic *agouti* competitively antagonizes  $\alpha$ -MSH binding at the MC4R in the hypothalamus [169] leading to an impairment of the leptin-MC4R axis and to hyperphagia [80]. In line with this, during childhood our patient was reported to struggle with satiety. During teenage age, and after bariatric surgery and several years of nutrition consultations, she showed restrained eating potentially compensating for hyperphagic tendencies in order to control her weight and other eating

---

<sup>24</sup> Some parts of the text of this subchapter were adopted literally from the manuscript: **Kempf et al.**: A novel human monogenic obesity trait: severe early-onset childhood obesity caused by aberrant overexpression of agouti-signaling protein (*ASIP*). **Submitted.**

disorder psychopathology. In addition to that, increased levels of incretins after bariatric surgery may affect neuronal MC4R signaling in the patient further facilitating restrained eating [57].

Her father, carrying the same mutation, also suffers from obesity, however, to a less severe degree compared to his daughter. Regularly and intensively doing sports during adolescence as well as a potentially less obesogenic environment might have had protective effects. In fact, it was shown that the type of diet can impact the development of obesity in mice with deficiencies in the leptin-MC4R axis [171]. According to self-reported questionnaires, his eating behavior had no pathological tendencies. Importantly, hyperphagia in *agouti* mice also was reported to be only moderate compared to leptin or leptin receptor deficient mice [127] and likewise, humans ubiquitously overexpressing *ASIP* are expected to suffer from milder forms of overeating than patients with leptin or leptin receptor deficiency.

In addition to regulating food intake, ectopic *ASIP/agouti* may affect energy expenditure via central pathways and the central melanocortin system may also directly control peripheral lipid metabolism [172]. Central augmentation of the *agouti* paralogue *AGRP* resulted in reduced oxygen consumption and decreased activation of BAT [173] and it has been proposed that activation of *AGRP* neurons lead to a reduction of the sympathetic tone in AT [174]. As *agouti* can mimic *AGRP* when ectopically expressed and as *agouti* mice had a reduced core temperature [126], increased *ASIP* may have similar effects and might be related to the reduced resting metabolic rate that was observed in the patient.

Although the effects of *ASIP/agouti* are likely to be primarily mediated by central effects, ectopic *ASIP/agouti* may promote obesity additionally by affecting peripheral pathways [123, 126, 127]. *ASIP/agouti* was described to enhance insulin secretion in the pancreas [175, 176] and leptin secretion in adipocytes [177]. In particular, *ASIP/agouti* is suggested to promote obesity on AT level by enhancing energy storage [127, 133, 178], as mice with adipocyte-specific overexpression of *agouti* developed mild obesity without hyperphagia [178]. *ASIP/agouti* reduces the lipolytic activity in adipocytes in a  $Ca^{2+}$ -dependent manner, increases insulin sensitivity in adipocytes by up-regulating adipogenic transcription factors, such as *PPARG*, activates the fatty acid synthase and thereby *de novo* lipogenesis [134, 178-181] and might even have an effect on activation of BAT [182, 183]. In line with this, the patient showed hyperinsulinemia and the SVF cells from the patient showed an enhanced adipogenic capacity and a reduced maximum mitochondrial respiration than SVF cells from the controls.

As described above, *ASIP* acts via antagonizing MCRs. In AT *MCRs* are expressed in low levels, with *MC1R* showing the highest expression. It is unlikely that the obesity-

promoting effects of ASIP are mediated by MC1R as *agouti* mice carrying a dominant constitutively active variant of the *MC1R* gene became obese despite having black fur, however, it was not investigated if the degree of obesity would be even worse if the *agouti* mice carried the wildtype *MC1R* instead [184]. Besides to MC1R and MC4R, *agouti* also has a high affinity to MC3R and MC5R [185]. Interestingly, *MC3R* deficiencies in rodents and humans have been associated with obesity potentially due to a shift towards accumulation of fat over muscle mass [186-189]. *MC2R* to *MC5R* were expressed at low levels in AT and were described to be involved in the regulation of lipolysis and energy storage [190]. A previous study implies that MCR agonists can stimulate lipolysis in human AT explants but not in isolated adipocytes [180]. They propose that *MC4R* and *MC5R* expressed at nerve terminals innervating the AT mediate the release of noradrenalin that stimulates lipolysis via beta-adrenergic receptors. This would suggest that the effect of ASIP on metabolic function might be stronger *in vivo* and difficult to identify in cell culture models.

However, it was also proposed that the *agouti*-mediated increase in  $Ca^{2+}$ , leading to reduced lipolysis, is at least in part mediated by melanocortin receptor-independent mechanisms such as inhibition of  $Ca^{2+}$  channels, maybe due to a structural similarity of *agouti* to plectoxins [135]. This might explain the slight decrease in lipolytic rate upon ASIP treatment, which we observed in SGBS cells, although they did not express *MC2R* to *MC5R*. That we did not observe an effect of ASIP knockdown in the patient SVF cells on adipogenic differentiation or mitochondrial function might be due to the 3-9 % left-over ASIP expression in the cells, which still may exceed the physiological levels, and/or due to the absence of MCR expression in the cells.

As we observed an enhanced adipogenic potential of the patient's SVF cells, it might also be considered that ASIP may affect processes in SVF cells happening well before the actual adipogenic differentiation. This may be for example by shifting the composition of the SVF cells towards an increased number of adipocyte progenitor cells, as also the percentage of differentiated SVF cells was increased in the patient cells.

In summary, based on our observations and on previous studies it is likely that the severe obesity of the patient with ubiquitous ASIP expression results from a combination of moderate hyperphagia, reduced energy expenditure and potentially an enhanced capacity of adipocytes to store energy.

Besides obesity, the patient presented a prominently tall stature during childhood. Her father carries the same mutation and reported to have been taller than his peers during childhood, however, with an adult height of 185 cm, he now is within the normal range.

Unfortunately, detailed endocrine data of growth-related factors during childhood was neither available from the patient nor from the father.

Data from *agouti* mice and other mouse models with deficiencies in the leptin-MC4R pathway indicate a relation with increased growth [79-81]. However, the underlying mechanisms are not fully deciphered. In teleosts, it has been shown that AGRP-mediated suppression of MC4R appeared essential for early larval growth [191]. Also transgenic zebrafish overexpressing *asip1* showed enhanced growth compared to wildtype fish but did not become obese, indicating that deficiencies in the MC4R pathway may lead to changes in somatic growth independent from obesity and that there are interspecies differences [192]. In humans, it was shown that children with *MC4R* deficiency were taller than controls, although the control children were matched for the severity of obesity [74]. Overgrowth was also reported in children with *POMC* deficiencies [75, 193].

It was proposed that *agouti* mice showing obesity and an increased body length had reduced somatostatin expression in the periventricular nucleus in the hypothalamus, which normally inhibits GH secretion, potentially secondary to antagonism of the MC4R or decreased *NPY* expression in the arcuate nucleus, as *NPY* has stimulatory effects on somatostatin [194]. In line with this, circulating levels of GH and IGF-1 were increased in the mice.

In addition to that, in our patient hyperinsulinemia was already detectable in early childhood and might hence have contributed to the increased growth [27].

A limitation of this study is that effects of increased *AHCY* expression (due to the gene duplication) on obesity and overgrowth cannot be entirely excluded. However, so far no link between *AHCY* and obesity or increased linear growth has been described [195]. Quantification of *ASIP* in serum levels of the patient was not possible, as two commercially available enzyme-linked immunosorbent assay kits did not detect *ASIP* specifically and also a mass-spectrometry based method was not applicable due to the small size of the *ASIP* protein. Furthermore, the experiments assessing the effect of *ASIP* on AT metabolism, and in particular the *ASIP* knockdown in the patient cells, need reconsideration and validation with independent methods, e.g. generating stable *ASIP* knock out cell lines from the patient. In addition, cell lines from healthy children stably overexpressing *ASIP* would be helpful to understand the role of *ASIP* in adipogenesis and lipolysis. Although our data strongly suggest an ubiquitous expression of *ASIP* in the patient, a final proof that *ASIP* is also ectopically expressed in the hypothalamus was not available so far. Lastly, further patients with ubiquitous *ASIP* expression need to be identified in order to validate our findings.

Like in most naturally occurring *agouti* mice [125], ectopic expression in the patient is caused by a structural alteration around the *ASIP* locus. The genetic region around *ASIP* is rich in repetitive DNA elements and hence susceptible for genetic rearrangements [136]. In fact, alterations in this locus resulting in dominant gain-of-function mutations have already been described in several species and are closely linked to fur color [125, 196, 197]. Strikingly, a similar duplication resulting in an *ITCH-ASIP* fusion gene has been observed in sheep [198] and in quail [199]. Unfortunately, measures for obesity and growth were not described in those studies. Due to the genetic instability of this region and as this large duplication is not detected using routine diagnostic methods, we hypothesize that there are more humans with undiagnosed ubiquitous *ASIP* expression. Screening expression data from 1,020, though mostly lean, children, we did not identify another patient with ectopic *ASIP* expression. In future studies, screening for *ASIP* mutations specifically in obesity-enriched cohorts might be more effective in order to identify additional patients. Finding further patients is crucial in order to further understand the relation of *ASIP* with the obese and tall phenotype in humans and to provide treatment options. Recently, the novel MCR-agonist setmelanotide has been approved by the U.S. Food and Drug Administration for the treatment of patients with e.g. *POMC* or leptin receptor deficiencies [200, 201], and also is a promising treatment option for patients with ubiquitous *ASIP* expression.

In summary, ubiquitous *ASIP* expression might be a novel monogenic trait for human obesity and overgrowth, which may be treatable with melanocortin receptor agonists. Particularly in humans, the underlying pathomechanisms need further investigation.

#### 5.4 Conclusion

In conclusion, we contributed to deciphering molecular alterations causing childhood obesity, as we for the first time identified a patient with ubiquitous *ASIP* expression, a potential novel monogenic trait for human obesity. Furthermore, we found that linear growth and the endocrine profile, including components of the GH axis, sex steroids and metabolic factors, are altered in children with obesity compared to normal-weight children adding those alterations to the array of early emerging obesity-related complications. The provided height reference values for children with obesity may constitute a tool for improving the precision of individual health care.

In addition, our data imply that several growth-related factors are involved in AT function and that in children with obesity compromised gene expression of these factors in AT may promote AT dysfunction, the progression of obesity and metabolic disease.

## 6 Zusammenfassung der Arbeit<sup>25</sup>

Dissertation zur Erlangung des akademischen Grades Dr. rer. nat.

Titel: Molecular and functional alterations related to growth in childhood obesity

eingereicht von Elena Tamara Kempf

angefertigt an der Universität Leipzig, Medizinische Fakultät, Klinik und Poliklinik für Kinder- und Jugendmedizin, Pädiatrisches Forschungszentrum

betreut von Prof. Dr. Antje Körner und Dr. Kathrin Landgraf

January 2022

In 2015, 4-10 % of the children in Germany were estimated to suffer from obesity and 10-20 % from overweight. This is of major concern as first adverse health implications related to obesity are observed already at young ages during childhood. It is crucial to recognize the related health complications in children and to decipher molecular as well as functional alterations promoting obesity and the associated comorbidities.

What is often left behind is that childhood obesity can affect linear growth, however, there is uncertainty regarding the dynamics and potential causes. In particular, the role of adipose tissue (AT) in the regulation of linear growth is not fully known. Vice versa, the involvement of growth factors in AT function and obesity itself is not entirely understood. A more thorough investigation of AT biology in children may not only provide new insights into the regulation of growth, but also into the molecular and functional mechanisms causing obesity in children.

---

<sup>25</sup> Several paragraphs from this summary were adopted literally from abstracts of the manuscripts: **Kempf et al., *EClinicalMedicine* 2021** [1], **Kempf et al.**: Contribution of adipose tissue to alterations in the growth hormone axis in childhood obesity and associations with adipose tissue function. **Submitted** and **Kempf et al.**: A novel human monogenic obesity trait: severe early-onset childhood obesity caused by aberrant overexpression of agouti-signaling protein (*ASIP*). **Submitted**.



In this thesis (consisting of three studies), we investigated linear growth in children with obesity (study 1) and the role of AT in the regulation of growth (study 2). We searched for associations of growth-related factors with AT function (study 2) and, by analyzing AT function of a child with severe obesity and extremely tall stature, we searched for novel molecular alterations causing obesity and overgrowth (study 3).

**In study 1** of this thesis, we aimed

- to understand the growth dynamics of children with obesity from infancy to adolescence.
- to identify endocrine changes that are associated with alterations in growth.
- to provide height reference values specific for children with obesity.

Using data from the population-based LIFE Child study and the obesity-enriched Leipzig Obesity Childhood cohort encompassing 8,629 children (37,493 measurements), we compared height parameters, growth velocities and serum parameters between normal-weight children and children with obesity aged 0-20 years.

We found that children with obesity were significantly taller than normal-weight peers in early childhood, reaching a maximum difference of 7.6 cm (1.4 height standard deviation scores (SDS)) at ages 6-8 years. Already at birth, children with obesity were slightly taller and thereafter had increased growth velocities by up to 1.2 cm per year in early childhood. This growth acceleration was independent from parental height, but was accompanied by increased levels of insulin-like growth factor-1 (IGF-1), insulin and leptin. During puberty, children with obesity showed a catch-down in height SDS. The reduction in pubertal growth velocity by up to 25 % coincided with a decrease in levels of IGF-1 (by 17 %) and testosterone (by 62 %) in boys and estradiol (by 37 %) in girls.

As growth in children with obesity deviates from normal-weight children and as appropriate assessment of height is important for individual health surveillance, we generated height reference values specific for children with obesity from an independent cohort, the German CrescNet registry, including 12,703 children. The reference values are available publically and free-of-charge.

In conclusion, dynamics of linear growth and endocrine patterns are altered distinctively in different developmental phases in children with obesity and this study adds those alterations to the array of obesity-related complications in children. The height reference values for children with obesity may enhance the precision of clinical health surveillance.

As some of the growth-related factors showing alterations in the circulating levels in childhood obesity are expressed in AT, **in study 2**, we asked if AT itself contributes to the altered serum levels. We furthermore investigated if gene expression of these growth-related factors in AT is related to overweight and AT function.

Using the Leipzig AT Childhood Cohort (n=209) and the Atherobesity Childhood Cohort (n=97) encompassing altogether 306 children, we asked

- if serum levels of growth hormone (GH) binding protein (GHBP), IGF-1 and IGF-binding protein 3 (IGFBP-3) are altered in children with overweight/obesity.
- if AT is a relevant source for those obesity-related elevations in serum levels due to altered gene expression of these factors in AT and/or increased fat mass.
- if gene expression of these factors in subcutaneous AT cells is related to obesity, AT function and metabolic parameters in children.
- if expression of the fibroblast-growth factor (FGF) receptor 3 (*FGFR3*) in subcutaneous AT is associated with obesity and metabolic parameters (in a larger subset of the Leipzig AT Childhood Cohort: n=223).

We found that serum GHBP levels were increased in children with overweight/obesity throughout childhood, while for IGF-1 and the IGF-1/IGFBP-3 molar ratio this obesity-related elevation was only detectable until early puberty. Circulating levels of GHBP and IGF-1 did not positively correlate with gene expression of GH receptor (*GHR*) and *IGF-1* in AT cells. Increased serum GHBP, however, was associated with a higher percentage of liver fat and higher aminotransferase levels.

Expression of *GHR*, *IGF-1* and *IGFBP-3* in adipocytes and stromal vascular fraction (SVF) cells was decreased in children with overweight/obesity and independent from body mass index reduced gene expression of these factors was related to parameters of AT dysfunction, such as adipocyte hypertrophy. In addition, AT expression of *FGFR3*, a factor involved in uncoupling protein-1 activation by FGF6/9, was associated with obesity and fasting insulin levels.

Thus, in children with obesity elevations in serum GHBP and IGF-1 are unlikely to be caused by increased AT mass. Instead, the elevation in serum GHBP may be a consequence of obesity-related alterations in the liver. The diminished gene expression of the growth-related factors in AT with obesity may contribute to early AT dysfunction and a deterioration of the metabolic state in children.

In studies 1 and 2 linear growth, growth-related factors and AT function in common childhood obesity were investigated. However, there are also monogenic forms of obesity and those often are accompanied by alterations in linear growth.

**In study 3** of this thesis, we

- aimed to investigate AT function of a child with severe early-onset obesity and tall stature.
- searched for novel molecular mechanisms causing obesity und overgrowth.

Analyzing subcutaneous AT, we found that SVF cells derived from the patient showed increased adipogenesis compared to cells from four control children. Searching for mechanisms behind the enhanced adipogenesis, genome-wide expression analyses uncovered that agouti-signaling protein (*ASIP*), a melanocortin receptor antagonist, was highly overexpressed in the patient's cells. Accordingly, increased amounts of *ASIP* protein were synthesized and secreted. Detailed genetic analyses revealed that the patient carries a 183 kbp-tandem duplication resulting in an itchy E3 ubiquitin protein ligase (*ITCH*)-*ASIP* fusion gene by placing the *ASIP* coding region under the control of the *ITCH* promoter. This results in ectopic expression of an *ITCH-ASIP* fusion mRNA containing a part of the *ITCH* 5' untranslated region. Artificial reconstruction of the fusion gene confirmed that the tandem duplication causes ectopic *ASIP* protein *in vitro*. As the *ITCH* promoter drives ubiquitous expression and as *ASIP* was ectopically expressed in several cell types of the patient, *ASIP* is assumed to be ubiquitously expressed in the patient.

The murine homologue of *ASIP* is *agouti*, which has been linked to obesity in mice. Mutant mice ubiquitously overexpressing *agouti* develop obesity, exhibit overgrowth and have yellow fur. Likewise, our patient suffers from obesity and overgrowth and has a red hair color. The mutation was inherited from her father, who has a similar phenotype. As the patient did not have any other mutations in the known obesity genes, ubiquitous expression of *ASIP* in humans may be a novel monogenic trait for obesity and overgrowth.

While the influence of ectopic *ASIP/agouti* on growth is not well understood, there are proposed mechanisms on how ectopic *ASIP/agouti* promotes obesity. Centrally, ectopic *agouti* in the hypothalamus is supposed to antagonize the melanocortin 4 receptor leading to increased food intake and reduced energy expenditure in mice. In line with this, our patient was reported to struggle with hunger before bariatric surgery and her resting metabolic rate was decreased. Moreover, *ASIP/agouti* was proposed to favor obesity through peripheral effects such as enhancing insulin secretion in the pancreas and energy storage in adipocytes. Since the patient showed hyperinsulinemia as well as

a high adipogenic capacity of SVF cells, peripheral effects may additionally contribute to the obese phenotype.

Although in a first screening we did not find another patient, there may be more humans with undiagnosed ubiquitous *ASIP* overexpression. Additional studies are necessary to understand the role of *ASIP* in human obesity and linear growth and to develop therapies. Melanocortin receptor agonists may provide promising treatment options for affected patients.

To conclude, with this thesis we contribute to deciphering molecular alterations causing childhood obesity, as for the first time we identified ubiquitous *ASIP* expression as a potential novel monogenic trait for human obesity. Furthermore, we contributed to a better understanding and recognition of childhood obesity-related complications, since we report detailed differences in growth dynamics and endocrine profiles in children with obesity and provide height reference values for obesity. Additionally, our data suggest growth-related factors in AT to be related with functional alterations in AT, which may contribute to the progression of obesity and related comorbidities.

## 7 References

1. Kempf E, Vogel M, Vogel T, et al. Dynamic alterations in linear growth and endocrine parameters in children with obesity and height reference values. *EClinicalMedicine*. 2021;37:100977.
2. Shamsi F, Xue R, Huang TL, et al. FGF6 and FGF9 regulate UCP1 expression independent of brown adipogenesis. *Nat Commun*. 2020;11(1):1421.
3. NCD-RisC. Worldwide trends in body-mass index, underweight, overweight, and obesity from 1975 to 2016: a pooled analysis of 2416 population-based measurement studies in 128.9 million children, adolescents, and adults. *Lancet*. 2017;390(10113):2627-42.
4. Wang Y, Lobstein T. Worldwide trends in childhood overweight and obesity. *Int J Pediatr Obes*. 2006;1(1):11-25.
5. Ng M, Fleming T, Robinson M, et al. Global, regional, and national prevalence of overweight and obesity in children and adults during 1980-2013: a systematic analysis for the Global Burden of Disease Study 2013. *Lancet*. 2014;384(9945):766-81.
6. Kurth BM, Schaffrath Rosario A. Die Verbreitung von Übergewicht und Adipositas bei Kindern und Jugendlichen in Deutschland. *Bundesgesundheitsblatt Gesundheitsforschung Gesundheitsschutz*. 2007;50(5):736-43.
7. Keß A, Spielau U, Beger C, et al. Further stabilization and even decrease in the prevalence rates of overweight and obesity in German children and adolescents from 2005 to 2015: a cross-sectional and trend analysis. *Public Health Nutr*. 2017;20(17):3075-83.
8. Vogel M, Geserick M, Gausche R, et al. Age- and weight group-specific weight gain patterns in children and adolescents during the 15 years before and during the COVID-19 pandemic. *Int J Obes (Lond)*. 2021;23:1-9.
9. Geserick M, Vogel M, Gausche R, et al. Acceleration of BMI in early childhood and risk of sustained obesity. *N Engl J Med*. 2018;379(14):1303-12.
10. WHO. Obesity and overweight. 2016. <https://www.who.int/en/news-room/fact-sheets/detail/obesity-and-overweight>. 2020. Accessed 2020.
11. Nier H. Immer mehr stark Übergewichtige. 2019 November 10th 2020 [cited 2020 November 10th]; (4). Available from: <https://de.statista.com/infografik/17609/anteil-uebergewichtiger-in-deutschland/>.
12. Blüher M. Obesity: global epidemiology and pathogenesis. *Nat Rev Endocrinol*. 2019;15(5):288-98.
13. Beyerlein A, Kusian D, Ziegler AG, et al. Classification tree analyses reveal limited potential for early targeted prevention against childhood overweight. *Obesity (Silver Spring)*. 2014;22(2):512-7.
14. Maes HH, Neale MC, Eaves LJ. Genetic and environmental factors in relative body weight and human adiposity. *Behav Genet*. 1997;27(4):325-51.
15. Hinney A, Giuranna J. Polygenic Obesity. In: Freemark MS, editor. *Pediatric Obesity: Etiology, Pathogenesis and Treatment*. Cham: Springer International Publishing; 2018. p. 183-202.
16. Huvenne H, Dubern B, Clément K, et al. Rare genetic forms of obesity: clinical approach and current treatments in 2016. *Obes Facts*. 2016;9(3):158-73.
17. Van Gaal LF, Mertens IL, De Block CE. Mechanisms linking obesity with cardiovascular disease. *Nature*. 2006;444(7121):875-80.

18. Lauby-Secretan B, Scoccianti C, Loomis D, et al. Body Fatness and Cancer — Viewpoint of the IARC Working Group. *N Engl J Med*. 2016;375(8):794-8.
19. Strazzullo P, D'Elia L, Cairella G, et al. Excess body weight and incidence of stroke: meta-analysis of prospective studies with 2 million participants. *Stroke*. 2010;41(5):e418-26.
20. Mangner N, Scheuermann K, Winzer E, et al. Childhood obesity: impact on cardiac geometry and function. *JACC Cardiovasc Imaging*. 2014;7(12):1198-205.
21. Landgraf K, Rockstroh D, Wagner IV, et al. Evidence of Early Alterations in Adipose Tissue Biology and Function and Its Association With Obesity-Related Inflammation and Insulin Resistance in Children. *Diabetes*. 2015;64(4):1249.
22. Franks PW, Hanson RL, Knowler WC, et al. Childhood obesity, other cardiovascular risk factors, and premature death. *N Engl J Med*. 2010;362(6):485-93.
23. Kromeyer-Hauschild K, Wabitsch M, Kunze D, et al. Percentiles of body mass index in children and adolescents evaluated from different regional German studies. *Monatsschrift Kinderheilkunde*. 2001;149(8):807-18.
24. Holmgren A, Niklasson A, Nierop AF, et al. Pubertal height gain is inversely related to peak BMI in childhood. *Pediatr. Res*. 2017;81(3):448-54.
25. Brener A, Bello R, Lebenthal Y, et al. The Impact of Adolescent Obesity on Adult Height. *Horm Res Paediatr*. 2017;88(3-4):237-43.
26. Nunziata A, Funcke JB, Borck G, et al. Functional and Phenotypic Characteristics of Human Leptin Receptor Mutations. *J Endocr Soc*. 2019;3(1):27-41.
27. Shalitin S, Kiess W. Putative effects of obesity on linear growth and puberty. *Horm Res Paediatr*. 2017;88(1):101-10.
28. Ballerini MG, Ropelato MG, Domene HM, et al. Differential impact of simple childhood obesity on the components of the growth hormone-insulin-like growth factor (IGF)-IGF binding proteins axis. *J Pediatr Endocrinol Metab*. 2004;17(5):749-57.
29. Gunnell D, Oliver SE, Donovan JL, et al. Do height-related variations in insulin-like growth factors underlie the associations of stature with adult chronic disease? *J Clin Endocrinol Metab*. 2004;89(1):213-8.
30. Blum WF, Alherbish A, Alsagheir A, et al. The growth hormone-insulin-like growth factor-I axis in the diagnosis and treatment of growth disorders. *Endocr Connect*. 2018;7(6):R212-R22.
31. Roelfsema V, Clark RG. The growth hormone and insulin-like growth factor axis: its manipulation for the benefit of growth disorders in renal failure. *J Am Soc Nephrol*. 2001;12(6):1297.
32. Schilbach K, Bidlingmaier M. Growth hormone binding protein – Physiological and analytical aspects. *Best Pract Res Clin Endocrinol Metab*. 2015;29(5):671-83.
33. Zhang Y, Jiang J, Black RA, et al. Tumor necrosis factor-alpha converting enzyme (TACE) is a growth hormone binding protein (GHBP) sheddase: the metalloprotease TACE/ADAM-17 is critical for (PMA-induced) GH receptor proteolysis and GHBP generation. *Endocrinology*. 2000;141(12):4342-8.
34. Hwa V, Oh Y, Rosenfeld RG. The insulin-like growth factor-binding protein (IGFBP) superfamily. *Endocr Rev*. 1999;20(6):761-87.
35. Ranke MB. Insulin-like growth factor binding-protein-3 (IGFBP-3). *Best Pract Res Clin Endocrinol Metab*. 2015;29(5):701-11.

36. Haywood NJ, Slater TA, Matthews CJ, et al. The insulin like growth factor and binding protein family: Novel therapeutic targets in obesity & diabetes. *Mol Metab.* 2019;19:86-96.
37. Han VK, Lund PK, Lee DC, et al. Expression of somatomedin/insulin-like growth factor messenger ribonucleic acids in the human fetus: identification, characterization, and tissue distribution. *J Clin Endocrinol Metab.* 1988;66(2):422-9.
38. David A, Hwa V, Metherell LA, et al. Evidence for a continuum of genetic, phenotypic, and biochemical abnormalities in children with growth hormone insensitivity. *Endocr Rev.* 2011;32(4):472-97.
39. van der Eerden BCJ, Karperien M, Wit JM. Systemic and local regulation of the growth plate. *Endocr Rev.* 2003;24(6):782-801.
40. Argente J, Chowen JA, Pérez-Jurado LA, et al. One level up: abnormal proteolytic regulation of IGF activity plays a role in human pathophysiology. *EMBO Mol Med.* 2017;9(10):1338-45.
41. Birzniece V, Ho KKY. Sex steroids and the GH axis: implications for the management of hypopituitarism. *Best Pract Res Clin Endocrinol Metab.* 2017;31(1):59-69.
42. Reinehr T, Roth CL. Is there a causal relationship between obesity and puberty? *Lancet Child Adolesc Health.* 2019;3(1):44-54.
43. Isaia GC, D'Amelio P, Di Bella S, et al. Is leptin the link between fat and bone mass? *J Endocrinol Invest.* 2005;28(10 Suppl):61-5.
44. Argente J, Caballo N, Barrios V, et al. Multiple endocrine abnormalities of the growth hormone and insulin-like growth factor axis in prepubertal children with exogenous obesity: effect of short- and long-term weight reduction. *J Clin Endocrinol Metab.* 1997;82(7):2076-83.
45. Ong K, Kratzsch J, Kiess W, et al. Circulating IGF-I levels in childhood are related to both current body composition and early postnatal growth rate. *J Clin Endocrinol Metab.* 2002;87(3):1041-4.
46. Benyi E, Säwendahl L. The physiology of childhood growth: Hormonal regulation. *Horm Res Paediatr.* 2017;88(1):6-14.
47. Fusco A, Miele L, D'Uonno A, et al. Nonalcoholic fatty liver disease is associated with increased GHBP and reduced GH/IGF-I levels. *Clin Endocrinol (Oxf).* 2012;77(4):531-6.
48. Baruch Y, Amit T, Hertz P, et al. Decreased serum growth hormone-binding protein in patients with liver cirrhosis. *J Clin Endocrinol Metab.* 1991;73(4):777-80.
49. Haluzik M, Yakar S, Gavrilova O, et al. Insulin Resistance in the Liver-Specific IGF-1 Gene-Deleted Mouse Is Abrogated by Deletion of the Acid-Labile Subunit of the IGF-Binding Protein-3 Complex. Relative Roles of Growth Hormone and IGF-1 in Insulin Resistance. *Diabetes.* 2003;52(10):2483-9.
50. Sjogren K, Liu JL, Blad K, et al. Liver-derived insulin-like growth factor I (IGF-I) is the principal source of IGF-I in blood but is not required for postnatal body growth in mice. *Proc Natl Acad Sci U S A.* 1999;96(12):7088-92.
51. Wei Y, Rhani Z, Goodyer CG. Characterization of growth hormone receptor messenger ribonucleic acid variants in human adipocytes. *J Clin Endocrinol Metab.* 2006;91(5):1901-8.
52. Zou L, Menon RK, Sperling MA. Induction of mRNAs for the growth hormone receptor gene during mouse 3T3-L1 preadipocyte differentiation. *Metabolism.* 1997;46(1):114-8.
53. Chang HR, Kim HJ, Xu X, et al. Macrophage and adipocyte IGF1 maintain adipose tissue homeostasis during metabolic stresses. *Obesity (Silver Spring).* 2016;24(1):172-83.

54. Møller S, Fisker S, Becker U, et al. A comparison of circulating and regional growth hormone-binding protein in cirrhosis. *Metabolism*. 2001;50(11):1340-5.
55. Yakar S, Liu JL, Stannard B, et al. Normal growth and development in the absence of hepatic insulin-like growth factor I. *Proc Natl Acad Sci U S A*. 1999;96(13):7324-9.
56. Hajer GR, van Haeften TW, Visseren FLJ. Adipose tissue dysfunction in obesity, diabetes, and vascular diseases. *Eur Heart J*. 2008;29(24):2959-71.
57. Longo M, Zatterale F, Naderi J, et al. Adipose tissue dysfunction as determinant of obesity-associated metabolic complications. *Int J Mol Sci*. 2019;20(9):2358.
58. Kwok KHM, Lam KSL, Xu A. Heterogeneity of white adipose tissue: molecular basis and clinical implications. *Exp Mol Med*. 2016;48(3):e215-e.
59. Akash MSH, Rehman K, Liaqat A. Tumor necrosis factor-alpha: Role in development of insulin resistance and pathogenesis of type 2 diabetes mellitus. *J Cell Biochem*. 2018;119(1):105-10.
60. Deng Y, Scherer PE. Adipokines as novel biomarkers and regulators of the metabolic syndrome. *Ann N Y Acad Sci*. 2010;1212:e1-e19.
61. Björntorp P, Sjöström L. Number and size of adipose tissue fat cells in relation to metabolism in human obesity. *Metabolism*. 1971;20(7):703-13.
62. Ghaben AL, Scherer PE. Adipogenesis and metabolic health. *Nat Rev Mol Cell Biol*. 2019;20(4):242-58.
63. Wu H, Ballantyne Christie M. Metabolic inflammation and insulin resistance in obesity. *Circ Res*. 2020;126(11):1549-64.
64. Skurk T, Alberti-Huber C, Herder C, et al. Relationship between adipocyte size and adipokine expression and secretion. *J Clin Endocrinol Metab*. 2007;92(3):1023-33.
65. Gruzdeva O, Borodkina D, Uchasova E, et al. Leptin resistance: underlying mechanisms and diagnosis. *Diabetes Metab Syndr Obes*. 2019;12:191-8.
66. Cannon B, Nedergaard J. Nonshivering thermogenesis and its adequate measurement in metabolic studies. *J Exp Biol*. 2011;214(2):242.
67. Kajimura S, Spiegelman BM, Seale P. Brown and Beige Fat: Physiological Roles beyond Heat Generation. *Cell Metab*. 2015;22(4):546-59.
68. Alcalá M, Calderon-Dominguez M, Serra D, et al. Mechanisms of impaired brown adipose tissue recruitment in obesity. *Front Physiol*. 2019;10(94).
69. Wabitsch M, Heinze E, Debatin KM, et al. IGF-I- and IGFBP-3-expression in cultured human preadipocytes and adipocytes. *Horm Metab Res*. 2000;32(11-12):555-9.
70. Ohta H, Itoh N. Roles of FGFs as adipokines in adipose tissue development, remodeling, and metabolism. *Front Endocrinol (Lausanne)*. 2014;5:18-.
71. Kopchick JJ, Berryman DE, Puri V, et al. The effects of growth hormone on adipose tissue: old observations, new mechanisms. *Nat Rev Endocrinol*. 2020;16(3):135-46.
72. Scavo LM, Karas M, Murray M, et al. Insulin-like growth factor-I stimulates both cell growth and lipogenesis during differentiation of human mesenchymal stem cells into adipocytes. *J Clin Endocrinol Metab*. 2004;89(7):3543-53.
73. Holly J, Sabin M, Perks C, et al. Adipogenesis and IGF-1. *Metab Syndr Relat Disord*. 2006;4(1):43-50.



74. Martinelli CE, Keogh JM, Greenfield JR, et al. Obesity due to melanocortin 4 receptor (MC4R) deficiency is associated with increased linear growth and final height, fasting hyperinsulinemia, and incompletely suppressed growth hormone secretion. *J Clin Endocrinol Metab.* 2011;96(1):E181-E8.
75. Krude H, Biebermann H, Schnabel D, et al. Obesity due to proopiomelanocortin deficiency: three new cases and treatment trials with thyroid hormone and ACTH4-10. *J Clin Endocrinol Metab.* 2003;88(10):4633-40.
76. El-Sayed Moustafa JS, Froguel P. From obesity genetics to the future of personalized obesity therapy. *Nat Rev Endocrinol.* 2013;9(7):402-13.
77. Heymsfield SB, Wadden TA. Mechanisms, Pathophysiology, and Management of Obesity. *N Engl J Med.* 2017;376(3):254-66.
78. Serrenho D, Santos SD, Carvalho AL. The role of ghrelin in regulating synaptic function and plasticity of feeding-associated circuits. *Front Cell Neurosci.* 2019;13(205).
79. Yaswen L, Diehl N, Brennan MB, et al. Obesity in the mouse model of proopiomelanocortin deficiency responds to peripheral melanocortin. *Nat Med.* 1999;5(9):1066-70.
80. Huszar D, Lynch CA, Fairchild-Huntress V, et al. Targeted disruption of the melanocortin-4 receptor results in obesity in mice. *Cell.* 1997;88(1):131-41.
81. Ollmann MM, Wilson BD, Yang YK, et al. Antagonism of central melanocortin receptors in vitro and in vivo by agouti-related protein. *Science.* 1997;278(5335):135-8.
82. Blüher S, Shah S, Mantzoros CS. Leptin deficiency: clinical implications and opportunities for therapeutic interventions. *J Investig Med.* 2009;57(7):784-8.
83. Steppan CM, Crawford DT, Chidsey-Frink KL, et al. Leptin is a potent stimulator of bone growth in ob/ob mice. *Regul Pept.* 2000;92(1):73-8.
84. U.S. Food and Drug Administration. FDA approves first treatment for weight management for people with certain rare genetic conditions. 2020. <https://www.fda.gov/drugs/drug-safety-and-availability/fda-approves-first-treatment-weight-management-people-certain-rare-genetic-conditions>. Accessed 2020.
85. Clément K, van den Akker E, Argente J, et al. Efficacy and safety of setmelanotide, an MC4R agonist, in individuals with severe obesity due to LEPR or POMC deficiency: single-arm, open-label, multicentre, phase 3 trials. *Lancet Diabetes Endocrinol.* 2020;8(12):960-70.
86. Poulain T, Baber R, Vogel M, et al. The LIFE Child study: a population-based perinatal and pediatric cohort in Germany. *Eur J Epidemiol.* 2017;32(2):145-58.
87. Quante M, Hesse M, Dohnert M, et al. The LIFE child study: a life course approach to disease and health. *BMC Public Health.* 2012;12:1021.
88. Landgraf K, Friebe D, Ullrich T, et al. Chemerin as a mediator between obesity and vascular inflammation in children. *J Clin Endocrinol Metab.* 2012;97(4):E556-64.
89. Euser AM, de Wit CC, Finken MJ, et al. Growth of preterm born children. *Horm Res Paediatr.* 2008;70(6):319-28.
90. Keller E, Gausche R, Meigen C, et al. Auxological computer based network for early detection of disorders of growth and weight attainment. *J Pediatr Endocrinol Metab.* 2002;15(2):149-56.
91. Landgraf K, Klötting N, Gericke M, et al. The obesity-susceptibility gene TMEM18 promotes adipogenesis through activation of PPARG. *Cell Rep.* 2020;33(3).

92. Wabitsch M, Brenner RE, Melzner I, et al. Characterization of a human preadipocyte cell strain with high capacity for adipose differentiation. *Int J Obes Relat Metab Disord.* 2001;25(1):8-15.
93. Reinken L, van Oost G. Longitudinale Körperentwicklung gesunder Kinder von 0 bis 18 Jahren. *Klin Padiatr.* 1992;204(03):129-33.
94. Wabitsch M, Moss A. Evidence-based (S3) guideline of the Working Group on Childhood and Adolescent Obesity (AGA) of the German Obesity Society (DAG) and the German Society of Pediatrics and Adolescent Medicine (DGKJ). 2019. <https://awmf.org/leitlinien/detail/II/050-002.html>. Accessed February 8th 2021.
95. Voigt M, Rochow N, Jahrig K, et al. Dependence of neonatal small and large for gestational age rates on maternal height and weight--an analysis of the German Perinatal Survey. *J Perinat Med.* 2010;38(4):425-30.
96. Voigt M, Fusch C, Olbertz D, et al. Analyse des Neugeborenenkollektivs der Bundesrepublik Deutschland. *Geburtshilfe Frauenheilkd.* 2006;66(10):956-70.
97. Marshall WA, Tanner JM. Variations in pattern of pubertal changes in girls. *Arch Dis Child.* 1969;44(235):291-303.
98. Marshall WA, Tanner JM. Variations in the pattern of pubertal changes in boys. *Arch Dis Child.* 1970;45(239):13-23.
99. Raschpichler MC, Sorge I, Hirsch W, et al. Evaluating childhood obesity: magnetic resonance-based quantification of abdominal adipose tissue and liver fat in children. *Rofo.* 2012;184(4):324-32.
100. Matthews DR, Hosker JP, Rudenski AS, et al. Homeostasis model assessment: insulin resistance and beta-cell function from fasting plasma glucose and insulin concentrations in man. *Diabetologia.* 1985;28(7):412-9.
101. Hilbert A, Tuschen-Caffier, B. *Eating Disorder Examination-Questionnaire: Deutschsprachige Übersetzung.* Münster: Verlag für Psychotherapie.; 2006.
102. Fairburn CG. *Cognitive behavior therapy and eating disorders.* New York: Guilford Publications; 2008.
103. Hilbert A, de Zwaan M, Braehler E. How frequent are eating disturbances in the population? Norms of the eating disorder examination-questionnaire. *PLoS One.* 2012;7(1):e29125.
104. Nagl M, Hilbert A, de Zwaan M, et al. The German version of the Dutch Eating Behavior Questionnaire: psychometric properties, measurement invariance, and population-based norms. *PLOS ONE.* 2016;11(9):e0162510.
105. Körner A, Wabitsch M, Seidel B, et al. Adiponectin expression in humans is dependent on differentiation of adipocytes and down-regulated by humoral serum components of high molecular weight. *Biochem Biophys Res Commun.* 2005;337(2):540-50.
106. Xue R, Lynes MD, Dreyfuss JM, et al. Clonal analyses and gene profiling identify genetic biomarkers of the thermogenic potential of human brown and white preadipocytes. *Nat Med.* 2015;21(7):760-8.
107. Shamsi F, Tseng Y-H. Protocols for generation of immortalized human brown and white preadipocyte cell lines. *Methods Mol Biol* 2017;1566:77-85.
108. Roth V. Doubling Time Computing. 2006 <http://www.doubling-time.com/compute.php>. Accessed

109. Bernhard F, Landgraf K, Klötting N, et al. Functional relevance of genes implicated by obesity genome-wide association study signals for human adipocyte biology. *Diabetologia*. 2013;56(2):311-22.
110. Sambrook J, Russell D. *Molecular Cloning: A Laboratory Manual (3-Volume Set)*. New York: Cold Springs Harbour Press; 2001.
111. Nebenführ A, Ritzenthaler C, Robinson DG, Brefeldin A: Deciphering an enigmatic inhibitor of secretion. *Plant Physiol*. 2002;130(3):1102-8.
112. Mollenhauer HH, James Morré D, Rowe LD. Alteration of intracellular traffic by monensin; mechanism, specificity and relationship to toxicity. *Biochim Biophys Acta Biomembr*. 1990;1031(2):225-46.
113. Cole TJ, Green PJ. Smoothing reference centile curves: the LMS method and penalized likelihood. *Stat Med*. 1992;11(10):1305-19.
114. Smyth G, Thorne N, Wettenhall J. *limma: Linear models for microarray data user's guide*. Bioinformatics and computational biology solutions using R and bioconductor 2011.
115. Beger C. CrescNet. <https://crescnet.medizin.uni-leipzig.de>. Accessed June 2021.
116. Gräfe D. Ped(Z) Pediatric Calculator. <https://bmi.pedz.de>. Accessed June 2021.
117. Bussler S, Vogel M, Pietzner D, et al. New pediatric percentiles of liver enzyme serum levels (alanine aminotransferase, aspartate aminotransferase,  $\gamma$ -glutamyltransferase): Effects of age, sex, body mass index, and pubertal stage. *Hepatology*. 2018;68(4):1319-30.
118. Juul A, Dalgaard P, Blum WF, et al. Serum levels of insulin-like growth factor (IGF)-binding protein-3 (IGFBP-3) in healthy infants, children, and adolescents: the relation to IGF-I, IGF-II, IGFBP-1, IGFBP-2, age, sex, body mass index, and pubertal maturation. *J Clin Endocrinol Metab*. 1995;80(8):2534-42.
119. Yüksel B, Özbek MN, Mungan N, et al. Serum IGF-1 and IGFBP-3 levels in healthy children between 0 and 6 years of age. *J Clin Res Pediatr Endocrinol*. 2011;3(2):84-8.
120. Kratzsch J, Dehmel B, Pulzer F, et al. Increased serum GHBP levels in obese pubertal children and adolescents: relationship to body composition, leptin and indicators of metabolic disturbances. *Int J Obes Relat Metab Disord*. 1997;21(12):1130-6.
121. Johansen MJ, Gade J, Stender S, et al. The effect of overweight and obesity on liver biochemical markers in children and adolescents. *J Clin Endocrinol Metab*. 2020;105(2):430-42.
122. Hadizadeh F, Faghihimani E, Adibi P. Nonalcoholic fatty liver disease: Diagnostic biomarkers. *World J Gastrointest Pathophysiol*. 2017;8(2):11-26.
123. Yang Y-K, Ollmann MM, Wilson BD, et al. Effects of recombinant agouti-signaling protein on melanocortin action. *Mol Endocrinol* 1997;11(3):274-80.
124. Klebig ML, Wilkinson JE, Geisler JG, et al. Ectopic expression of the agouti gene in transgenic mice causes obesity, features of type II diabetes, and yellow fur. *Proc Natl Acad Sci U S A*. 1995;92(11):4728-32.
125. Duhl DM, Vrieling H, Miller KA, et al. Neomorphic agouti mutations in obese yellow mice. *Nat Genet*. 1994;8(1):59-65.
126. Moussa NM, Claycombe KJ. The yellow mouse obesity syndrome and mechanisms of agouti-induced obesity. *Obes Res*. 1999;7(5):506-14.
127. Miltenberger RJ, Mynatt RL, Wilkinson JE, et al. The role of the agouti gene in the yellow obese syndrome. *J Nutr*. 1997;127(9):1902S-7S.

128. Ericson MD, Freeman KT, Schnell SM, et al. Structure-activity relationship studies on a macrocyclic agouti-related protein (AGRP) scaffold reveal agouti signaling protein (ASP) residue substitutions maintain melanocortin-4 receptor antagonist potency and result in inverse agonist pharmacology at the melanocortin-5 receptor. *J Med Chem.* 2017;60(19):8103-14.
129. Michaud EJ, Bultman SJ, Klebig ML, et al. A molecular model for the genetic and phenotypic characteristics of the mouse lethal yellow (Ay) mutation. *Proc Natl Acad Sci U S A.* 1994;91(7):2562-6.
130. Bouchard C. Genetics of obesity: What we have learned over decades of research. *Obesity.* 2021;29(5):802-20.
131. Allard P, Delvin EE, Paradis G, et al. Distribution of fasting plasma insulin, free fatty acids, and glucose concentrations and of homeostasis model assessment of insulin resistance in a representative sample of Quebec children and adolescents. *Clin Chem.* 2003;49(4):644-9.
132. Morgan MD, Pairo-Castineira E, Rawlik K, et al. Genome-wide study of hair colour in UK Biobank explains most of the SNP heritability. *Nat Commun.* 2018;9(1):5271.
133. Mynatt RL, Stephens JM. Agouti regulates adipocyte transcription factors. *Am J Physiol Cell Physiol.* 2001;280(4):C954-61.
134. Xue B, Moustaid N, Wilkison WO, et al. The agouti gene product inhibits lipolysis in human adipocytes via a Ca<sup>2+</sup>-dependent mechanism. *FASEB J.* 1998;12(13):1391-6.
135. Kim JH, Kiefer LL, Woychik RP, et al. Agouti regulation of intracellular calcium: role of melanocortin receptors. *Am J Physiol Endocrinol Metab.* 1997;272(3):E379-E84.
136. Nakayama K, Ishida T. Alu-mediated 100-kb deletion in the primate genome: the loss of the agouti signaling protein gene in the lesser apes. *Genome Res.* 2006;16(4):485-90.
137. Nokoff N, Thurston J, Hilkin A, et al. Sex differences in effects of obesity on reproductive hormones and glucose metabolism in early puberty. *J Clin Endocrinol Metab.* 2019;104(10):4390-7.
138. Biro FM, Pinney SM, Huang B, et al. Hormone changes in peripubertal girls. *J Clin Endocrinol Metab.* 2014;99(10):3829-35.
139. Reinehr T, Kulle A, Wolters B, et al. Steroid hormone profiles in prepubertal obese children before and after weight loss. *J Clin Endocrinol Metab.* 2013;98(6):E1022-30.
140. Coutant R, de Casson FB, Rouleau S, et al. Divergent effect of endogenous and exogenous sex steroids on the insulin-like growth factor I response to growth hormone in short normal adolescents. *J Clin Endocrinol Metab.* 2004;89(12):6185-92.
141. Körner A, Kratzsch J, Gausche R, et al. New predictors of the metabolic syndrome in children-role of adipocytokines. *Pediatr Res.* 2007;61(6):640-5.
142. Soto N, Bazaes RA, Pena V, et al. Insulin sensitivity and secretion are related to catch-up growth in small-for-gestational-age infants at age 1 year: results from a prospective cohort. *J Clin Endocrinol Metab.* 2003;88(8):3645-50.
143. Kühnen P, Krude H, Biebermann H. Melanocortin-4 receptor signalling: importance for weight regulation and obesity treatment. *Trends Mol Med.* 2019;25(2):136-48.
144. Kohlsdorf K, Nunziata A, Funcke J-B, et al. Early childhood BMI trajectories in monogenic obesity due to leptin, leptin receptor, and melanocortin 4 receptor deficiency. *Int J Obes (Lond).* 2018;42(9):1602-9.

145. Voigtmann F, Wolf P, Landgraf K, et al. Identification of a novel leptin receptor (LEPR) variant and proof of functional relevance directing treatment decisions in patients with morbid obesity. *Metabolism*. 2021;116:154438.
146. Antonisamy B, Vasan SK, Geethanjali FS, et al. Weight Gain and Height Growth during Infancy, Childhood, and Adolescence as Predictors of Adult Cardiovascular Risk. *J Pediatr*. 2017;180:53-61.e3.
147. Sabo RT, Wang A, Deng Y, et al. Relationships between childhood growth parameters and adult blood pressure: the Fels Longitudinal Study. *J Dev Orig Health Dis*. 2017;8(1):113-22.
148. Seminara S, Filpo A, La Cauza F, et al. Growth hormone binding protein activity in obese children. *J Endocrinol Invest*. 1998;21(7):441-4.
149. Park MJ, Kim HS, Kang JH, et al. Serum levels of insulin-like growth factor (IGF)-I, free IGF-I, IGF binding protein (IGFBP)-1, IGFBP-3 and insulin in obese children. *J Pediatr Endocrinol Metab*. 1999;12(2):139-44.
150. Fisker S, Hansen B, Fuglsang J, et al. Gene expression of the GH receptor in subcutaneous and intraabdominal fat in healthy females: relationship to GH-binding protein. *Eur J Endocrinol*. 2004;150(6):773-7.
151. Ross RJ, Esposito N, Shen XY, et al. A short isoform of the human growth hormone receptor functions as a dominant negative inhibitor of the full-length receptor and generates large amounts of binding protein. *Mol Endocrinol*. 1997;11(3):265-73.
152. Hesse D, Trost J, Schäfer N, et al. Effect of adipocyte-derived IGF-I on adipose tissue mass and glucose metabolism in the Berlin Fat Mouse. *Growth Factors*. 2018;36(1-2):78-88.
153. List EO, Berryman DE, Buchman M, et al. Adipocyte-Specific GH Receptor-Null (AdGHRKO) Mice Have Enhanced Insulin Sensitivity With Reduced Liver Triglycerides. *Endocrinology*. 2019;160(1):68-80.
154. List EO, Berryman DE, Funk K, et al. The role of GH in adipose tissue: lessons from adipose-specific GH receptor gene-disrupted mice. *Mol Endocrinol*. 2013;27(3):524-35.
155. Phillips LS, Pao CI, Villafuerte BC. Molecular regulation of insulin-like growth factor-I and its principal binding protein, IGFBP-3. *Prog Nucleic Acid Res Mol Biol*. 1998;60:195-265.
156. Touskova V, Trachta P, Kavalkova P, et al. Serum concentrations and tissue expression of components of insulin-like growth factor-axis in females with type 2 diabetes mellitus and obesity: The influence of very-low-calorie diet. *Mol Cell Endocrinol*. 2012;361(1):172-8.
157. Glad CAM, Svensson PA, Nystrom FH, et al. Expression of GHR and downstream signaling genes in human adipose tissue-relation to obesity and weight change. *J Clin Endocrinol Metab*. 2019;104(5):1459-70.
158. Campbell KL, Foster-Schubert KE, Makar KW, et al. Gene expression changes in adipose tissue with diet- and/or exercise-induced weight loss. *Cancer Prev Res (Phila)*. 2013;6(3):217-31.
159. Blüher S, Kratzsch J, Kiess W. Insulin-like growth factor I, growth hormone and insulin in white adipose tissue. *Best Pract Res Clin Endocrinol Metab*. 2005;19(4):577-87.
160. Høyer KL, Høgild ML, List EO, et al. The acute effects of growth hormone in adipose tissue is associated with suppression of antilipolytic signals. *Physiol Rep*. 2020;8(3):e14373.
161. Carrel AL, Allen DB. Effects of growth hormone on adipose tissue. *J Pediatr Endocrinol Metab*. 2000;13 Suppl 2:1003-9.
162. Boucher J, Softic S, El Ouaamari A, et al. Differential Roles of Insulin and IGF-1 Receptors in Adipose Tissue Development and Function. *Diabetes*. 2016;65(8):2201-13.

163. Boucher J, Tseng Y-H, Kahn CR. Insulin and insulin-like growth factor-1 receptors act as ligand-specific amplitude modulators of a common pathway regulating gene transcription. *J Biol Chem.* 2010;285(22):17235-45.
164. Baxter RC, Twigg SM. Actions of IGF binding proteins and related proteins in adipose tissue. *Trends Endocrinol Metab.* 2009;20(10):499-505.
165. Chan SSY, Schedlich LJ, Twigg SM, et al. Inhibition of adipocyte differentiation by insulin-like growth factor-binding protein-3. *Am J Physiol Endocrinol Metab.* 2009;296(4):e654-e63.
166. Lee H, Kim SR, Oh Y, et al. Targeting insulin-like growth factor-I and insulin-like growth factor-binding protein-3 signaling pathways. A novel therapeutic approach for asthma. *Am J Respir Cell Mol Biol.* 2014;50(4):667-77.
167. Sjöstedt E, Zhong W, Fagerberg L, et al. An atlas of the protein-coding genes in the human, pig, and mouse brain. *Science.* 2020;367(6482), <https://www.proteinatlas.org/ENSG00000078747-ITCH/tissue>.
168. Kwon HY, Bultman SJ, Löffler C, et al. Molecular structure and chromosomal mapping of the human homolog of the agouti gene. *Proc Natl Acad Sci U S A.* 1994;91(21):9760-4.
169. Rana BK. New insights into G-protein-coupled receptor signaling from the melanocortin receptor system. *Mol Pharmacol.* 2003;64(1):1-4.
170. Suzuki I, Tada A, Ollmann MM, et al. Agouti signaling protein inhibits melanogenesis and the response of human melanocytes to alpha-melanotropin. *J Invest Dermatol.* 1997;108(6):838-42.
171. Challis BG, Coll AP, Yeo GSH, et al. Mice lacking pro-opiomelanocortin are sensitive to high-fat feeding but respond normally to the acute anorectic effects of peptide-YY(3-36). *Proc Natl Acad Sci U S A.* 2004;101(13):4695-700.
172. Nogueiras R, Wiedmer P, Perez-Tilve D, et al. The central melanocortin system directly controls peripheral lipid metabolism. *J Clin Invest.* 2007;117(11):3475-88.
173. Small CJ, Liu YL, Stanley SA, et al. Chronic CNS administration of Agouti-related protein (Agrp) reduces energy expenditure. *Int J Obes Relat Metab Disord.* 2003;27(4):530-3.
174. Cavalcanti-de-Albuquerque JP, Bober J, Zimmer MR, et al. Regulation of substrate utilization and adiposity by Agrp neurons. *Nat Commun.* 2019;10(1):311.
175. Khotskin NV, Plyusnina AV, Kulikova EA, et al. On association of the lethal yellow (A(Y)) mutation in the agouti gene with the alterations in mouse brain and behavior. *Behav Brain Res.* 2019;359:446-56.
176. Xue BZ, Wilkison WO, Mynatt RL, et al. The agouti gene product stimulates pancreatic [beta]-cell Ca<sup>2+</sup> signaling and insulin release. *Physiol Genomics.* 1999;1(1):11-9.
177. Claycombe KJ, Xue BZ, Mynatt RL, et al. Regulation of leptin by agouti. *Physiol Genomics.* 2000;2(3):101-5.
178. Mynatt RL, Stephens JM. Regulation of PPARgamma and obesity by agouti/melanocortin signaling in adipocytes. *Ann N Y Acad Sci.* 2003;994:141-6.
179. Xue B, Zemel MB. Relationship between human adipose tissue agouti and fatty acid synthase (FAS). *J Nutr.* 2000;130(10):2478-81.
180. Møller CL, Pedersen SB, Richelsen B, et al. Melanocortin agonists stimulate lipolysis in human adipose tissue explants but not in adipocytes. *BMC Research Notes.* 2015;8(1):559.

181. Claycombe KJ, Wang Y, Jones BH, et al. Transcriptional regulation of the adipocyte fatty acid synthase gene by agouti: interaction with insulin. *Physiol Genomics*. 2000;3(3):157-62.
182. Schnabl K, Westermeier J, Li Y, et al. Opposing Actions of Adrenocorticotrophic Hormone and Glucocorticoids on UCP1-Mediated Respiration in Brown Adipocytes. *Front Physiol*. 2018;9:1931.
183. Voss-Andreae A, Murphy JG, Ellacott KL, et al. Role of the central melanocortin circuitry in adaptive thermogenesis of brown adipose tissue. *Endocrinology*. 2007;148(4):1550-60.
184. Wolff GL, Galbraith DB, Domon OE, et al. Phaeomelanin synthesis and obesity in mice. Interaction of the viable yellow (Avy) and sombre (eso) mutations. *J Hered*. 1978;69(5):295-8.
185. Møller CL, Raun K, Jacobsen ML, et al. Characterization of murine melanocortin receptors mediating adipocyte lipolysis and examination of signalling pathways involved. *Mol Cell Endocrinol*. 2011;341(1-2):9-17.
186. Lee B, Koo J, Yun Jun J, et al. A mouse model for a partially inactive obesity-associated human MC3R variant. *Nat Commun*. 2016;7(1):10522.
187. You P, Hu H, Chen Y, et al. Effects of melanocortin 3 and 4 receptor deficiency on energy homeostasis in rats. *Sci rep*. 2016;6:34938-.
188. Lee YS, Poh LK, Kek BL, et al. The role of melanocortin 3 receptor gene in childhood obesity. *Diabetes*. 2007;56(10):2622-30.
189. Micioni Di Bonaventura E, Botticelli L, Tomassoni D, et al. The Melanocortin System behind the Dysfunctional Eating Behaviors. *Nutrients*. 2020;12(11):3502.
190. Jackson DS, Ramachandrappa S, Clark AJ, et al. Melanocortin receptor accessory proteins in adrenal disease and obesity. *Front Neurosci*. 2015;9:213-.
191. Zhang C, Forlano PM, Cone RD. AgRP and POMC neurons are hypophysiotropic and coordinately regulate multiple endocrine axes in a larval teleost. *Cell Metab*. 2012;15(2):256-64.
192. Godino-Gimeno A, Sánchez E, Guillot R, et al. Growth performance after agouti-signaling protein 1 (Asip1) overexpression in transgenic zebrafish. *Zebrafish*. 2020;17(6):373-81.
193. Ozsú E, Bahm A. Delayed diagnosis of proopiomelanocortin (POMC) deficiency with type 1 diabetes in a 9-year-old girl and her infant sibling. *J Pediatr Endocrinol Metab*. 2017;30(10):1137-40.
194. Martin NM, Houston PA, Patterson M, et al. Abnormalities of the somatotrophic axis in the obese agouti mouse. *Int J Obes (Lond)*. 2006;30(3):430-8.
195. Vizán P, Di Croce L, Aranda S. Functional and Pathological Roles of AHCY. *Frontiers in Cell and Developmental Biology*. 2021;9(587).
196. Chandramohan B, Renieri C, La Manna V, et al. The alpaca agouti gene: genomic locus, transcripts and causative mutations of eumelanic and pheomelanic coat color. *Gene*. 2013;521(2):303-10.
197. Girardot M, Guibert S, Laforet MP, et al. The insertion of a full-length *Bos taurus* LINE element is responsible for a transcriptional deregulation of the Normande Agouti gene. *Pigment Cell Res*. 2006;19(4):346-55.
198. Norris BJ, Whan VA. A gene duplication affecting expression of the ovine ASIP gene is responsible for white and black sheep. *Genome Res*. 2008;18(8):1282-93.

## References

---

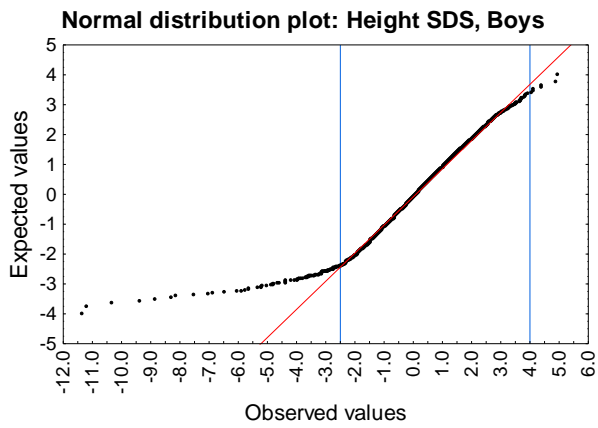
199. Robic A, Morisson M, Leroux S, et al. Two new structural mutations in the 5' region of the ASIP gene cause diluted feather color phenotypes in Japanese quail. *Genet Sel Evol.* 2019;51(1):12.
200. U.S. FDA. FDA approves first treatment for weight management for people with certain rare genetic conditions. 2020. <https://www.fda.gov/drugs/drug-safety-and-availability/fda-approves-first-treatment-weight-management-people-certain-rare-genetic-conditions>. Accessed 2020.
201. Clément K, van den Akker E, Argente J, et al. Efficacy and safety of setmelanotide, an MC4R agonist, in individuals with severe obesity due to LEPR or POMC deficiency: single-arm, open-label, multicentre, phase 3 trials. *Lancet Diabetes Endocrinol.* 2020;8(12):960-70.



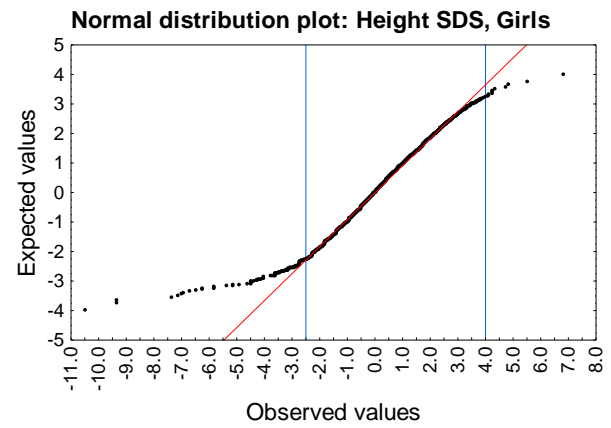
## Appendix

## I. Additional information on study populations

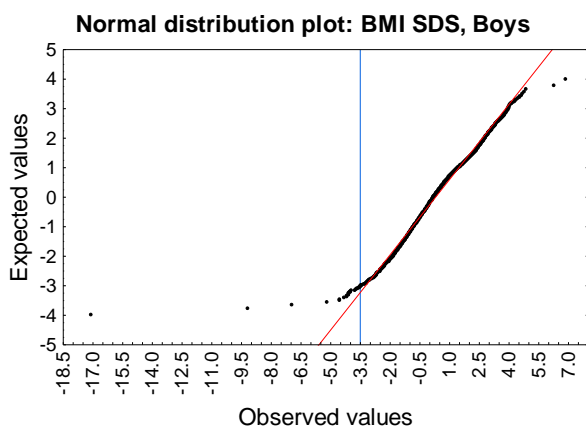
A



B



C



D

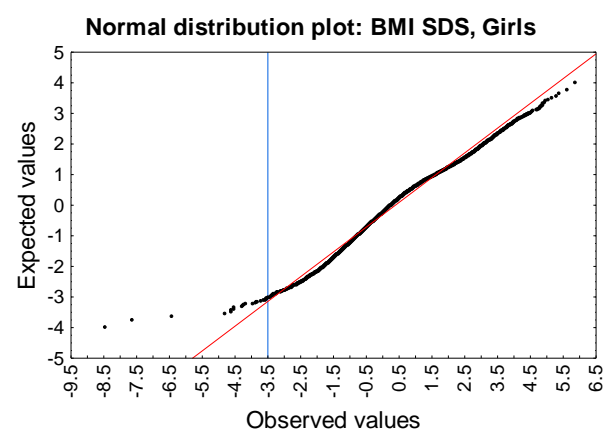


**Figure S1. Children with height standard deviation score (SDS) between -2.5 and 4.0 and a body mass index (BMI) SDS higher than -3.5 were included to the study based on linearity in normal distribution plots**

Children with diseases, manifested clinically confirmed precocious puberty and medication were already excluded in those graphs. A, B: Normal distribution plots of height SDS for boys and girls; C, D: Normal distribution plots of BMI SDS for boys and girls. This figure was adopted from Kempf *et al.*, *eClinicalMedicine* 2021 [1].

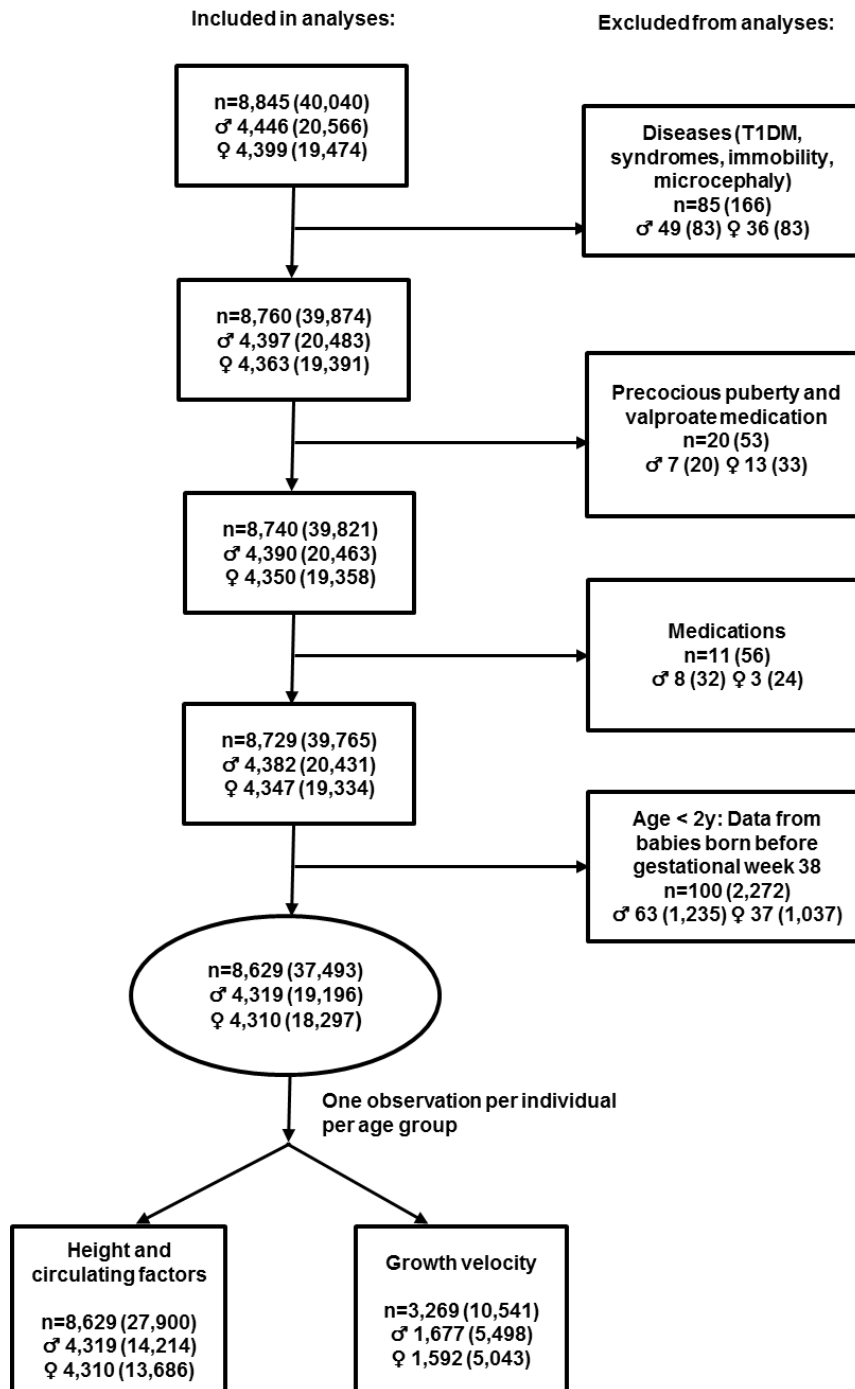


**Figure S2. Children included in the comparative analyses**

Visualization of the inclusion criteria for study 1. Children or observations were excluded due to diseases, conditions of precocious puberty, medication or premature birth (until the age of 2 years). The number of subjects (n) and observations (shown in brackets"()") are indicated for all children/observations and for boys (♂) and girls (♀) separately. Analyzing height parameters, circulating factors and growth velocities only the first observations per individual per age group was included, making altogether 27,900 observations for height and endocrine factors. Growth velocities of 3,269 children with altogether 10,541 observations (>1.5 years of mean age between the two observations) were included. This figure was adopted from Kempf *et al.*, *eClinicalMedicine* 2021 [1].

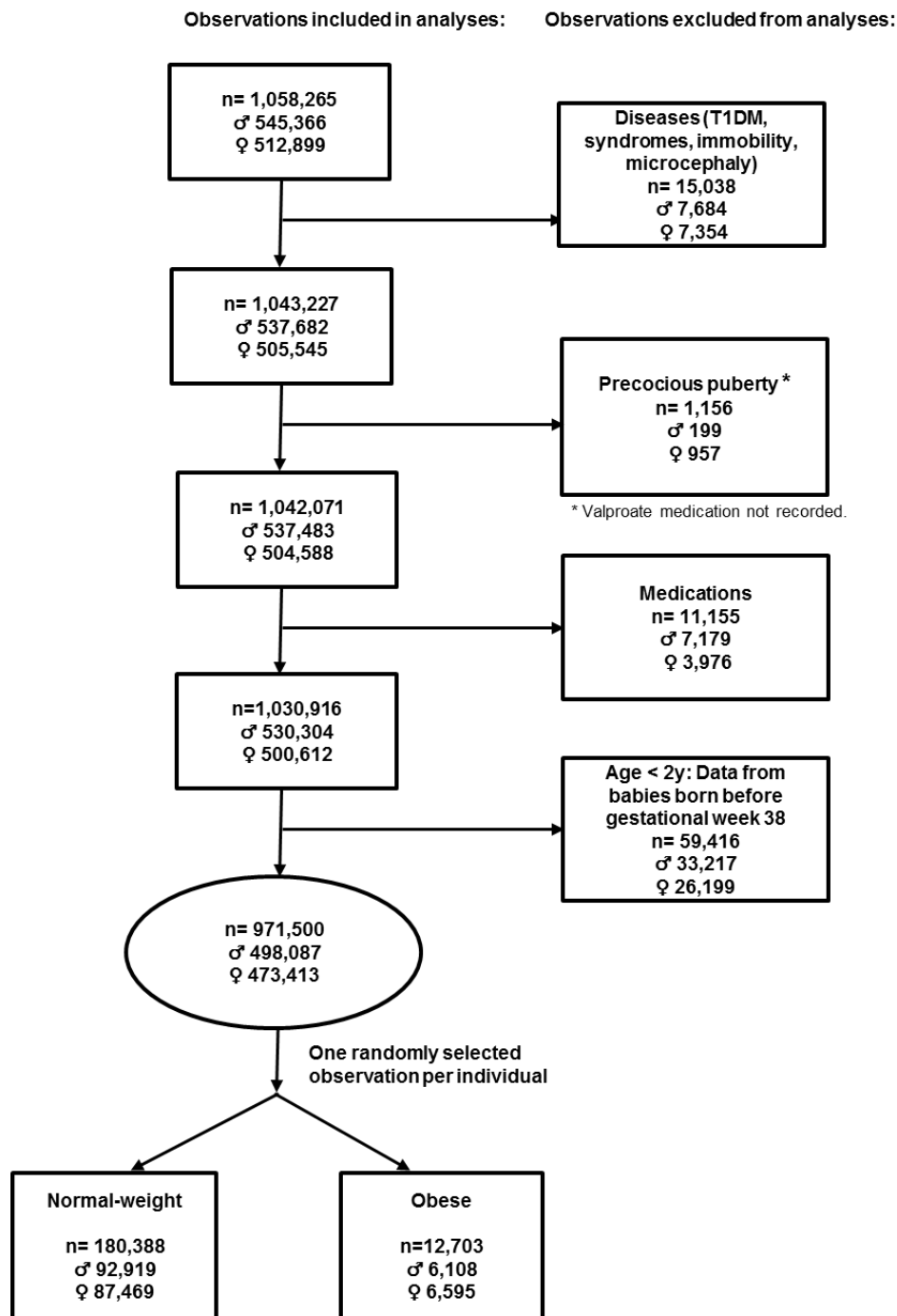


**Figure S3. Inclusion criteria for CrescNet data for the generation of height reference values for children with obesity**

Observations from children aged 0–20 years with a height standard deviation score (SDS) from -2.5 to 4.0 and a body mass index SDS higher than -3.5 were initially included. Then observations were excluded due to diseases, conditions of precocious puberty, medication or premature birth (until the age of 2 years). *n* indicates the number of observations, also separately presented for boys (♂) and for girls (♀). The asterisk indicates that valproate medication was not recorded in the registry and children were hence not excluded due to this criterion. Finally, only one randomly selected observation of each child was used for the generation of reference values. Children were classified into normal-weight and obese. Data from 6,108 boys and 6,595 girls with obesity were used for the generation of height reference values. This figure was adopted from Kempf *et al.*, *eClinicalMedicine* 2021 [1].

Table S1. Overview of the anthropometric and clinical data of the combined cohorts

Boys	UW			NW			OW			OB		
	n	Mean (SD)	Range	n	Mean (SD)	Range	n	Mean (SD)	Range	n	Mean (SD)	Range
Age, y	953	6.9 ( 5.1)	0 - 19.8	10,324	5.9 ( 5)	0 - 20.3	1,129	6.4 ( 5.6)	0 - 19	1,808	9.3 ( 5.3)	0 - 20.3
Height, cm	953	117.5 ( 34.4)	46 - 194.2	10,324	111.7 ( 37.2)	46 - 200.5	1,129	113.8 ( 44.6)	46 - 196.3	1,808	137.2 ( 41)	47 - 201
Height SDS	953	-0.2 ( 1)	-2.5 - 3.5	10,324	0.1 ( 0.9)	-2.5 - 3.9	1,129	0.3 ( 1)	-2.3 - 3.7	1,808	0.6 ( 1)	-2.5 - 3.9
BMI SDS	953	-1.7 ( 0.4)	-3.4 - -1.3	10,324	0 ( 0.6)	-1.3 - 1.3	1,129	1.6 ( 0.2)	1.3 - 1.9	1,808	2.5 ( 0.5)	1.9 - 4.9
Height <sub>parental adj</sub> SDS	559	-0.2 ( 0.9)	-2.4 - 3.4	5,960	0.1 ( 0.9)	-2.5 - 4	656	0.4 ( 1)	-2.3 - 3.6	1,132	0.8 ( 1)	-2.3 - 3.8
Growth velocity, cm/y	402	6.7 (2.2)	0.2 - 15.1	4,286	7.1 (2.3)	0 - 21.9	341	7.1 (2.7)	0 - 16.3	469	6.2 (2.6)	0 - 15
Growth velocity SDS	402	-0.2 (1.6)	-6.6 - 7	4,286	0.2 (1.5)	-6.9 - 9.8	341	0.3 (1.6)	-3.5 - 7.6	469	0.2 (1.5)	-3.5 - 9.1
TSH, mIU/L	386	2.7 (1.3)	0.4 - 9.6	3,582	2.7 (1.3)	0.3 - 14.9	365	2.7 (1.2)	0.6 - 8.7	1,009	3 (1.3)	0.4 - 8.9
FT4, pmol/L	374	16.1 (1.8)	9.7 - 21.9	3,504	16.2 (2)	8.8 - 45.4	358	15.3 (2.1)	5.8 - 24.4	1,008	15.1 (2.2)	2.8 - 24.8
LH, IU/L	318	1.5 ( 1.6)	0.1 - 8.6	3,007	1.6 ( 1.8)	0 - 10.9	346	1.7 ( 1.7)	0 - 7.6	841	1.7 ( 2)	0 - 25.1
FSH, IU/L	320	2.4 ( 1.9)	0.1 - 10.6	3,007	2.3 ( 2)	0.1 - 20	347	2.5 ( 1.6)	0.2 - 9.2	847	2.4 ( 2)	0 - 18.7
DHEA-S, µmol/L	138	3.1 (2.5)	0.1 - 15.3	1,345	3.4 (3)	0 - 20.3	136	4.8 (3)	0.3 - 15.9	194	4.4 (2.7)	0.2 - 16.3
Estradiol, pmol/L	191	50.8 (35.7)	18.4 - 164.2	1,951	55.1 (40.6)	18.4 - 259.9	232	57.6 (39.7)	0 - 277.4	437	51.5 (39.6)	0 - 200.3
Testosterone, nmol/L	136	6.2 (7.6)	0.1 - 25	1,319	6.3 (8.6)	0.1 - 35.5	180	6.1 (6.9)	0.1 - 27	501	3.8 (5)	0.1 - 21.8
SHBG, nmol/L	400	106.2 ( 50.9)	1.2 - 284.8	3,878	98 ( 54.5)	2.1 - 978.2	339	60.1 ( 44.1)	5.8 - 222.1	381	41.1 ( 30.9)	1.4 - 194
IGF-1, ng/mL	306	170.9 ( 117.4)	21.3 - 722	2,695	195.6 ( 131.9)	20 - 902	236	243.7 ( 134)	34.2 - 717	392	236.1 ( 113.3)	38.5 - 624
IGFBP3, µg/mL	283	3.8 ( 1.2)	1.3 - 8.2	2,522	4 ( 1.1)	1.2 - 7.8	213	4.4 ( 1.1)	1.3 - 7.9	372	4.5 ( 1)	1.8 - 8
Leptin, ng/mL	38	1.8 (1.2)	0.2 - 4.3	265	3.5 (3.8)	0.2 - 23.7	63	13.5 (11.7)	0.2 - 60.9	343	28.4 (15)	0.2 - 88.5
Insulin, pmol/L	138	40.7 (21)	5.1 - 113.3	1,288	49 (27.1)	3.6 - 238.2	232	79.2 (47)	4.7 - 518.1	956	111.9 (72.3)	5 - 571.7
HOMA-IR	133	1.3 (0.7)	0.2 - 3.9	1,261	1.6 (0.9)	0.1 - 8.4	227	2.7 (1.7)	0.1 - 15.7	950	3.8 (2.7)	0.1 - 28.8

Data sets were categorized according to sex and BMI SDS class. Data are presented as mean  $\pm$  standard deviation (SD) and range (minimum and maximum values) and numbers of observations (n) are provided considering only one observation per individual per age class. Data for growth velocity are shown for children  $\geq 1.5$  years (mean age between the two height observations). UW, underweight; NW, normal-weight; OW, overweight; OB, obese; BMI, Body mass index; SDS, standard deviation score; Height<sub>parental adj</sub> SDS, Height SDS relative to mid-parental height SDS; TSH, thyroid-stimulating hormone; FT4, free thyroxine; LH, luteinizing hormone; FSH, follicle-stimulating hormone; DHEA-S, dehydroepiandrosterone sulfate; SHBG, sexual hormone binding globulin; IGF-1, insulin-like growth factor-1, IGFBP-3, IGF-1 binding protein 3; HOMA-IR, homeostatic model assessment for insulin resistance. This table was adopted from Kempf *et al.*, *eClinicalMedicine* 2021 [1].

Table S1. Overview over the anthropometric and clinical data of the cohort (continued)

Girls	UW			NW			OW			OB		
	n	Mean (SD)	Range	n	Mean (SD)	Range	n	Mean (SD)	Range	n	Mean (SD)	Range
Age, y	814	6.7 ( 5.1)	0 - 19.8	9,665	6.1 ( 5.1)	0 - 19.8	1,151	6.5 ( 5.6)	0 - 18.9	2,056	9.7 ( 5.6)	0 - 20
Menarche, y	88	13 (1.2)	10 - 16	1,146	12.5 (1.1)	9 - 16	175	12.2 (1.1)	9 - 16	476	11.8 (1.3)	9 - 16
Height, cm	814	115.3 ( 34.7)	46 - 182.8	9,665	110.7 ( 36.2)	46 - 185.7	1,151	113.1 ( 43.1)	46 - 189.5	2,056	135.7 ( 39.2)	46 - 187.8
Height SDS	814	-0.2 ( 1)	-2.5 - 3.4	9,665	0 ( 0.9)	-2.5 - 3.7	1,151	0.3 ( 1.1)	-2.4 - 3.9	2,056	0.5 ( 1.1)	-2.5 - 3.9
BMI SDS	814	-1.7 ( 0.4)	-3.5 - -1.3	9,665	0 ( 0.7)	-1.3 - 1.3	1,151	1.6 ( 0.2)	1.3 - 1.9	2,056	2.6 ( 0.6)	1.9 - 5.9
Height <sub>parental adj</sub> SDS	450	0 ( 0.9)	-2.5 - 2.9	5,686	0.1 ( 0.9)	-2.5 - 3.6	690	0.4 ( 1.1)	-2.4 - 3.4	1,209	0.8 ( 1.1)	-2.4 - 3.9
Growth velocity, cm/y	318	6.2 (2.4)	0 - 18.4	3,856	6.8 (2.7)	0 - 20.2	332	6.6 (3.3)	0 - 17.1	537	4.8 (3.3)	0 - 15.6
Growth velocity SDS	318	-0.2 (1.8)	-7 - 5	3,856	0.2 (1.7)	-7.5 - 9.1	332	0.3 (1.8)	-5.8 - 9	537	0 (1.9)	-5.6 - 8.8
TSH, mIU/L	274	2.5 (1.2)	0.6 - 8	3,138	2.6 (1.2)	0.1 - 10.8	361	2.8 (1.3)	0.5 - 8.3	1,170	2.9 (1.4)	0 - 14.4
FT4, pmol/L	268	16.1 (2.1)	11.3 - 23.5	3,083	16.1 (2.1)	7.2 - 40.4	352	15.6 (2.5)	6.6 - 37.9	1,168	15.2 (2.3)	5.4 - 32.8
LH, IU/L	242	2.8 ( 5.2)	0 - 46.6	2,766	3.2 ( 6.1)	0 - 98.8	372	3.5 ( 5.2)	0 - 43.9	1,009	3.9 ( 5.3)	0 - 58.4
FSH, IU/L	243	3.9 ( 2.4)	0.1 - 11.4	2,765	3.7 ( 2.5)	0.1 - 21.7	371	3.6 ( 2.3)	0.1 - 11.8	1,016	3.7 ( 2.5)	0 - 21.3
DHEA-S, $\mu$ mol/L	119	2.8 (2.4)	0.1 - 17.4	1,215	3.1 (2.5)	0 - 18.3	128	3.7 (2.1)	0.4 - 10.5	215	4 (2.4)	0.2 - 11.5
Estradiol, pmol/L	165	134.8 (186.1)	18.4 - 1359	1,869	186.7 (274.3)	18.4 - 2518	306	163.8 (220.3)	18.4 - 1452	874	145.9 (176.3)	0 - 1649.3
Testosterone, nmol/L	119	0.5 (0.6)	0.1 - 3.8	1,190	0.5 (1)	0.1 - 17.5	178	0.6 (0.5)	0.1 - 2.5	596	0.9 (1)	0.1 - 14.7
SHBG, nmol/L	284	114.4 ( 56.9)	2.7 - 448.7	3,515	100.7 ( 52.8)	1.4 - 488.2	344	69.3 ( 54.4)	4.7 - 336.6	421	45.6 ( 43.1)	1.7 - 290.8
IGF-1, ng/mL	222	202 ( 116.6)	26.6 - 585	2,391	228.3 ( 132.8)	21.4 - 888	237	283.8 ( 141.2)	25.5 - 786	406	272.1 ( 114.6)	53 - 695
IGFBP3, $\mu$ g/mL	209	4.2 ( 1.1)	1.4 - 7	2,195	4.2 ( 1.1)	1.3 - 8.4	211	4.5 ( 1)	1.6 - 7.5	398	4.7 ( 0.9)	2 - 9.4
Leptin, ng/mL	28	3.9 (2.7)	0.2 - 9.6	295	7.6 (5.4)	0.2 - 35.2	70	18.7 (9.7)	3.1 - 53	390	38.3 (18.4)	0.2 - 109
Insulin, pmol/L	128	48.5 (25)	11.1 - 179.8	1,242	56.7 (33.9)	4.2 - 722.9	240	84.7 (39.4)	10.4 - 231.6	1,121	120.4 (70.4)	3.5 - 578.3
HOMA-IR	126	1.5 (0.8)	0.3 - 4.9	1,218	1.7 (1.2)	0.1 - 30.7	238	2.7 (1.4)	0.4 - 7.7	1,118	4 (2.5)	0.1 - 19.7

Data sets were categorized according to sex and BMI SDS class. Data are presented as mean  $\pm$  standard deviation (SD) and range (minimum and maximum values) and numbers of observations (n) are provided considering only one observation per individual per age class. Data for growth velocity are shown for children  $\geq 1.5$  years (mean age between the two height observations). UW, underweight; NW, normal-weight; OW, overweight; OB, obese; BMI, Body mass index; SDS, standard deviation score; Height<sub>parental adj</sub> SDS, Height SDS relative to mid-parental height SDS; TSH, thyroid-stimulating hormone; FT4, free thyroxine; LH, luteinizing hormone; FSH, follicle-stimulating hormone; DHEA-S, dehydroepiandrosterone sulfate; SHBG, sexual hormone binding globin; IGF-1, insulin-like growth factor-1, IGFBP-3, IGF-1 binding protein 3; HOMA-IR, homeostatic model assessment for insulin resistance. This table was adopted from Kempf *et al.*, *eClinicalMedicine* 2021 [1].

**Table S2. Numbers of observations per weight category and age group for the entire cohort (height) and subcohorts for growth velocity, IGF-1 or IGFBP-3, sex steroids, metabolic factors and thyroid hormones**

Boys	Height (entire cohort)				Growth velocity				IGF-1 or IGFBP-3				Sex steroids				Metabolic factors				Thyroid hormones			
age	UW	NW	OW	OB	UW	NW	OW	OB	UW	NW	OW	OB	UW	NW	OW	OB	UW	NW	OW	OB	UW	NW	OW	OB
0	40	1,160	223	207	-	-	-	-	8	69	9	3	0	0	0	0	0	1	0	0	15	171	13	6
1	139	1,216	104	59	-	-	-	-	18	71	3	0	24	130	5	2	0	1	0	1	27	156	8	3
2	92	1,179	113	58	25	320	20	9	9	88	6	0	10	145	15	2	1	5	0	0	11	164	16	3
3	34	550	47	21	48	642	51	35	9	130	10	2	7	167	13	5	2	6	1	4	11	188	14	7
4	97	1,104	73	62	28	473	29	21	5	112	3	6	8	160	8	7	0	4	2	7	10	171	9	9
5	88	968	65	95	71	754	55	33	12	129	6	2	15	175	7	11	1	5	1	16	21	198	8	17
6	24	295	9	36	26	298	15	16	11	154	5	11	12	188	6	26	5	66	1	26	14	206	7	27
7	28	279	14	56	14	180	4	16	14	146	6	12	17	181	8	36	4	78	2	42	18	206	9	45
8	45	411	28	82	17	199	11	18	14	191	8	23	25	307	15	58	8	121	9	54	23	244	15	61
9	45	510	43	96	21	216	11	28	22	222	10	39	33	393	29	77	11	133	16	66	26	262	17	64
10	37	345	44	124	20	200	17	37	24	200	21	35	27	269	37	91	8	144	23	98	26	254	29	95
11	55	485	75	141	23	196	17	26	32	206	21	36	42	367	53	96	13	134	41	107	34	240	39	100
12	42	374	68	135	26	186	25	48	22	212	35	46	31	296	55	96	17	147	39	105	28	242	47	99
13	50	276	63	182	27	171	27	59	28	184	28	56	35	225	54	135	16	132	43	141	38	215	48	145
14	42	267	54	148	21	163	24	40	25	164	19	56	34	206	42	104	21	123	33	109	31	213	38	116
15	47	443	52	129	15	143	19	45	27	175	20	30	44	366	36	78	28	150	20	99	25	173	17	90
16	28	276	31	88	13	94	13	23	17	149	19	23	24	219	27	62	15	111	14	60	15	158	18	59
17	14	128	13	56	6	49	3	14	7	78	8	10	10	110	10	43	5	62	5	41	10	87	7	43
18+	6	58	10	33	1	2	0	1	3	27	1	3	5	44	7	27	3	38	7	29	2	35	6	25
<b>Total</b>	953	10,324	1,129	1,808	402	4,286	341	469	307	2,707	238	393	403	3,948	427	956	158	1,460	257	1,005	385	3,583	365	1,014

Height parameters were available for the entire cohort. Subcohorts were built for observations with growth velocity (children older mean age 1.5 years), IGF-1 or IGFBP-3 measurements, sex steroid (FSH, LH, DHEA-S, SHBG, estradiol or testosterone), metabolic factor (leptin, insulin or HOMA-IR) and thyroid hormone (TSH or FT4) measurements. As also in Appendix I, for Table S1 only one observation per individual per age class was included. UW, underweight; NW, normal-weight; OW, overweight; OB, obese; IGF-1, insulin-like growth factor-1; IGFBP-3, IGF-1 binding protein 3; FSH, follicle-stimulating hormone; LH, luteinizing hormone; DHEA-S, dehydroepiandrosterone sulfate; SHBG, sexual hormone binding globulin; HOMA-IR, homeostatic model assessment for insulin resistance; TSH, thyroid-stimulating hormone; FT4, free thyroxin. This table was adopted from Kempf *et al.*, *eClinicalMedicine* 2021 [1].

**Table S2. Numbers of observations per weight category and age group for the entire cohort (height) and subcohorts for growth velocity, IGF-1 or IGFBP-3, sex steroids, metabolic factors and thyroid hormones (continued)**

Girls age	Height (entire cohort)				Growth velocity				IGF-1 or IGFBP-3				Sex steroids				Metabolic factors				Thyroid hormones			
	UW	NW	OW	OB	UW	NW	OW	OB	UW	NW	OW	OB	UW	NW	OW	OB	UW	NW	OW	OB	UW	NW	OW	OB
0	44	1,038	216	224	-	-	-	-	6	58	2	4	0	0	0	0	0	0	0	0	10	136	15	3
1	118	1,112	107	77	-	-	-	-	10	53	4	0	13	106	5	0	0	0	0	0	17	130	5	3
2	89	1,102	111	49	25	258	23	11	2	78	10	0	4	133	13	3	0	2	0	1	5	141	13	8
3	20	467	34	24	38	594	58	24	1	89	9	1	3	129	10	6	0	0	0	6	3	142	11	15
4	69	1,035	76	72	25	418	28	24	9	90	4	4	8	139	7	10	1	1	0	11	10	155	7	34
5	78	903	68	93	45	739	52	46	3	88	4	5	4	140	9	26	0	1	2	31	5	156	10	51
6	26	282	15	66	23	297	8	25	10	128	2	15	12	158	7	36	4	72	6	47	12	180	8	45
7	24	291	22	56	17	186	10	22	10	151	7	16	11	178	14	40	4	86	9	44	13	205	14	59
8	38	398	33	83	12	183	11	20	14	167	10	23	21	270	27	65	8	100	11	55	18	202	14	86
9	34	449	61	119	18	174	11	30	15	178	13	27	25	334	45	83	9	118	24	82	20	196	24	87
10	36	298	49	112	16	156	13	35	22	167	18	36	23	217	33	80	12	107	25	86	24	206	25	88
11	59	462	62	137	18	151	16	37	30	208	25	36	41	343	43	99	25	158	26	91	30	200	32	102
12	51	330	61	145	21	156	23	38	25	182	33	48	38	256	49	100	23	145	38	106	33	202	35	120
13	24	278	54	151	23	153	28	46	12	185	27	43	16	217	39	112	12	129	35	117	17	210	41	116
14	24	265	53	154	14	146	19	45	15	161	25	44	16	209	38	117	12	139	34	123	18	199	38	110
15	34	498	62	162	13	123	13	57	11	169	19	40	23	378	52	117	8	149	26	124	14	176	29	110
16	22	250	43	148	7	78	15	40	11	132	19	23	16	199	28	107	9	123	20	112	10	157	27	87
17	18	133	18	112	3	43	4	28	12	78	6	23	15	103	14	82	10	70	12	88	12	100	10	57
18+	6	74	6	72	0	1	0	9	4	37	1	18	5	54	5	55	4	44	4	64	3	46	3	0
<b>Total</b>	814	9,665	1,151	2,056	318	3,856	332	537	222	2,399	238	406	294	3,563	438	1,138	141	1,444	272	1,188	274	3,139	361	1,181

Height parameters were available for the entire cohort. Subcohorts were built for observations with growth velocity (children older mean age 1.5 years), IGF-1 or IGFBP-3 measurements, sex steroid (FSH, LH, DHEA-S, SHBG, estradiol or testosterone), metabolic factor (Leptin, Insulin or HOMA-IR) and thyroid hormone (TSH or FT4) measurements. As also in Appendix I, Table S1 only one observation per individual per age class was included. UW, underweight; NW, normal-weight; OW, overweight; OB, obese; IGF-1, insulin-like growth factor-1; IGFBP-3, IGF-1 binding protein 3; FSH, follicle-stimulating hormone; LH, luteinizing hormone; DHEA-S, dehydroepiandrosterone sulfate; SHBG, sexual hormone binding globulin; HOMA-IR, homeostatic model assessment for insulin resistance; TSH, thyroid-stimulating hormone; FT4, free thyroxin. This table was adopted from Kempf *et al.*, *eClinicalMedicine* 2021 [1].

**Table S3. Data from the patient and control children**

available	Data from AT					Gene expression data from PBL				
	Patient	Ctr 1	Ctr 2	Ctr 3	Ctr 4	Patient	Ctr 5	Ctr 6	Ctr 7	Ctr 8
<b>Anthropometric data</b>										
Age (years)	12.4	17.4	13.3	11.8	12.7	14.1	16	12.8	12.3	15.0
Sex	female	female	male	female	female	female	female	female	female	female
Height (cm) / Height SDS	181 / 3.4	176 / 1.3	156 / 0.0	158 / 0.7	160 / 0.3	183 / 2.9	167 / 0.1	186 / 3.8	163 / 1.0	183 / 2.7
BMI (kg/m <sup>2</sup> ) / BMI SDS	47.6 / 3.7	40.5 / 3.7	25.5 / 1.8	31.4 / 2.7	29.7 / 2.4	37.8 / 3.2	33.1 / 2.8	44.7 / 3.6	31.0 / 2.6	38.6 / 3.3
Surgery	gastric bypass	gastric bypass	remov al 8P	implan- tation 8P	implan- tation 8P	---	---	---	---	---
Location	abdome n	abdome n	femur	knee	knee	---	---	---	---	---

Ctr, control; SDS, standard deviation score; BMI, body mass index; 8P, eight plate; PBL, peripheral blood leukocytes, gDNA, genomic deoxyribonucleic acid; RNA, ribonucleic acid; AT, adipose tissue; SVF, stromal vascular fraction. This table was adopted from Kempf *et al.*: A novel human monogenic obesity trait: severe early-onset childhood obesity caused by aberrant overexpression of agouti-signaling protein (*ASIP*), (submitted) and modified.



## II. Additional methods

**Table S4. Evaluation of pubertal stage according to Tanner criteria**

Boys and girls were categorized into five pubertal stages according to pubic hair and testicular volume or breast stage according to Tanner.

Pubertal group	Boys		Girls	
	Pubic hair	TV (cm <sup>3</sup> )	Pubic hair	Breast
1	PH=1	TV≤3	PH=1	B=1
2	PH≤2	4≤TV≤10	PH≤3	B=2
	PH≥2	TV≤3		B=1
3	PH=3	TV≥4	2≤PH≤4	B=3
4	PH=4	TV≥4	PH≥3	B=4
5	PH≥5	TV≥7	PH≥4	B=5

PH, pubic hair; TV, testicular volume; B, breast stage. This table was adopted from Kempf *et al.*, *eClinicalMedicine* 2021 [1].

**Table S5. Methods for the measurement of serum parameters**

Serum parameter	Measurement method	Source
Insulin-like growth factor (IGF-1)*	Immunoluminometric assay	Advantage, Nichols Institute Diagnostics, San Clemente, CA, USA
	Enzyme-linked immunosorbent assay (ELISA)	Mediagnost, Reutlingen, Germany
	Automated chemiluminescence immunoassay (CLIA) iSYS	IDS, Boldon/Tyne & Wear, UK
IGF-binding protein 3 (IGFBP-3)*	Immunoluminometric assay	Advantage, Nichols Institute Diagnostics, San Clemente, CA, USA
	ELISA	Mediagnost, Reutlingen, Germany
	CLIA iSYS	IDS, Boldon/Tyne & Wear, UK
Adiponectin	ELISA	Mediagnost, Reutlingen, Germany
Leptin	ELISA	Mediagnost, Reutlingen, Germany
Glucose	Photometric measurement	Cobas Roche, Mannheim, Germany
High sensitivity c-reactive protein (hsCRP)	Photometric measurement	Cobas Roche, Mannheim, Germany
Total cholesterol	Photometric measurement	Cobas Roche, Mannheim, Germany
High density lipoprotein (HDL)	Photometric measurement	Cobas Roche, Mannheim, Germany
Low-density lipoprotein (LDL)	Photometric measurement	Cobas Roche, Mannheim, Germany
Triglycerides	Photometric measurement	Cobas Roche, Mannheim, Germany
Alanine aminotransferase (ALAT)	Photometric measurement	Cobas Roche, Mannheim, Germany
Aspartate aminotransferase (ASAT)	Photometric measurement	Cobas Roche, Mannheim, Germany
Insulin	CLIA	Liaison, DiaSorin, Dietzenbach, Germany
	Electro CLIA (ECLIA)	Cobas Roche, Mannheim, Germany
Glycated haemoglobin (hbA1c)	High performance liquid chromatography	Tosoh, Sysmex Deutschland GmbH
Estradiol	ECLIA	Elecsys 2010, Roche, Mannheim, Germany
		Cobas, Roche, Mannheim, Germany
Testosterone	ECLIA	Elecsys 2010, Roche, Mannheim, Germany
		Cobas Roche, Mannheim, Germany
Sex-hormone binding globulin (SHBG)	ECLIA	Cobas, Roche, Mannheim, Germany
Luteinizing hormone (LH)	ECLIA	Cobas, Roche, Mannheim, Germany
Follicle-stimulating hormone (FSH)	ECLIA	Cobas, Roche, Mannheim, Germany
Dehydroepiandrosterone sulfate (DHEA-S)	ECLIA	Cobas, Roche, Mannheim, Germany
Thyroid-stimulating hormone (TSH)	ECLIA	Cobas, Roche, Mannheim, Germany
Free thyroxin (FT4)	ECLIA	Cobas, Roche, Mannheim, Germany
Growth hormone receptor-binding protein (GHBP)	ELISA	DSL, Sinsheim, Germany
Tumor necrosis factor alpha (TNF- $\alpha$ )	ELISA	R&D, Minneapolis, Canada

\* We obtained qualitatively comparable results if each method was analyzed separately

### III. Additional results

#### A. Study 1

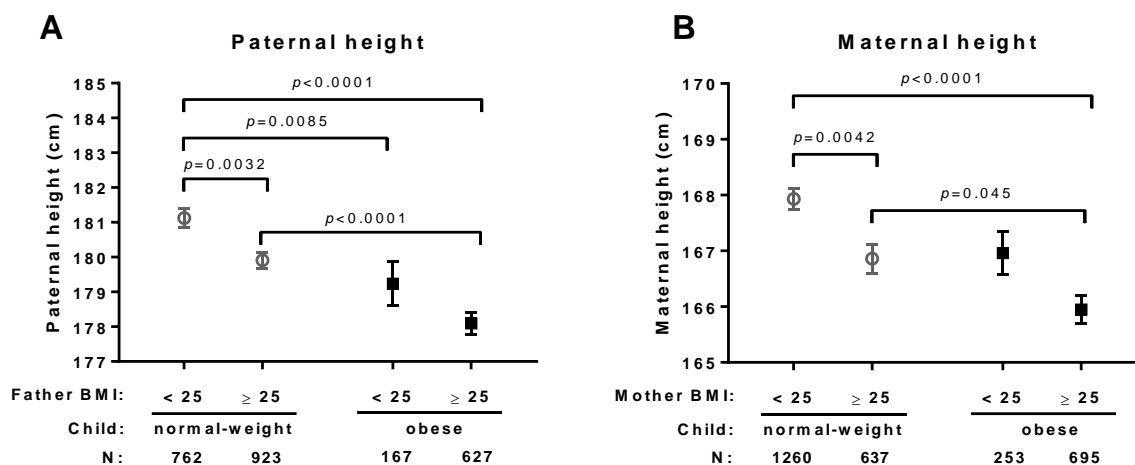


**Figure S4. Comparison of parental height in children with normal-weight or obesity**

Parental height of children aged 0-18+ years was compared between normal-weight (NW) and obese (OB) children. Only the first observation of a child was used. The weight status of the father and mother was categorized according to the BMI in kg/m<sup>2</sup> in BMI<25 and BMI≥25. A: Paternal height; B: Maternal height. Data are shown as mean with standard error; *p*-values corrected for multiple comparison are given for significant differences (*p*<0.05) as assessed by two-way ANOVA and Fishers Least Significant Difference test combined with a Holm-Šidák multiple comparison test. This figure was adopted from Kempf *et al.*, *eClinicalMedicine* 2021 [1].

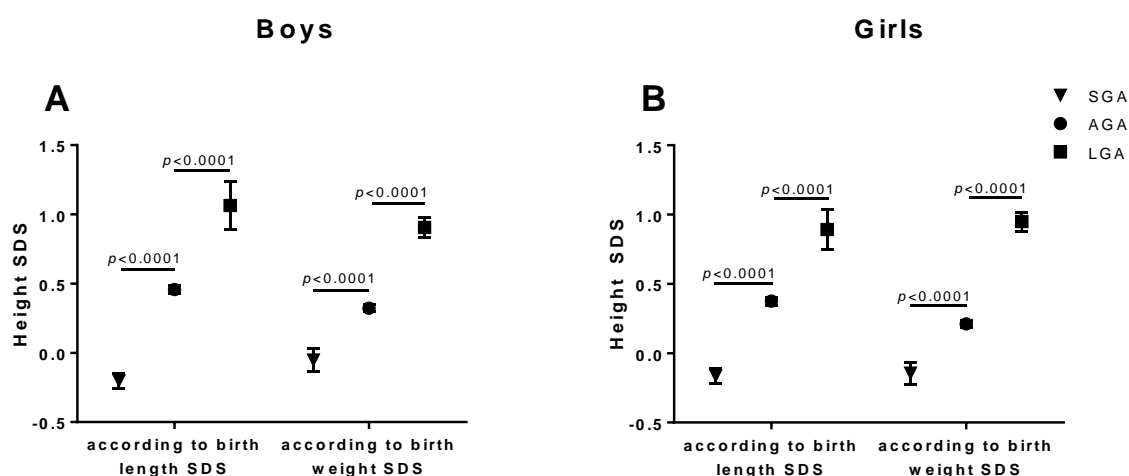


**Figure S5. The impact of birth length and birth weight on later height standard deviation scores (SDS)**

Newborns were categorized into born small for gestational age (SGA), appropriate for gestational age (AGA) and large for gestational age (LGA) according to the body length and body weight. A, B: Mean height SDS of boys and girls between the ages 4-14.99 years are depicted. Data are shown as mean with standard error; *p*-values corrected for multiple comparison are given for significant differences (*p*<0.05) as assessed by two-way ANOVA and Fisher's Least Significant Difference test combined with a Holm-Šidák multiple comparison test. This figure was adopted from Kempf *et al.*, *eClinicalMedicine* 2021 [1].

**Table S6. Comparison of birth and parental parameters between children with normal-weight and obesity ages 4-14 years**

Boys (4-14 years)	NW children		OB children		p-value
	Mean (SEM)	n	Mean (SEM)	n	
Birth weight, g	3579.06 (14.26)	1,034	3627.68 (23.45)	494	0.064
Birth weight SDS	0.03 (0.03)	1,034	0.09 (0.05)	494	0.36
Birth length, cm	51.11 (0.07)	1,024	51.36 (0.11)	489	0.039
Birth length SDS	-0.50 (0.03)	1,024	-0.44 (0.04)	489	0.23
Paternal BMI, kg/m <sup>2</sup>	25.94 (0.15)	578	29.42 (0.36)	271	<b>&lt;0.0001</b>
Maternal BMI, kg/m <sup>2</sup>	24.15 (0.18)	654	29.91 (0.4)	304	<b>&lt;0.0001</b>
Paternal height, cm	180.56 (0.29)	636	178.84 (0.42)	345	<b>0.00059</b>
Maternal height, cm	167.90 (0.25)	673	166.28 (0.34)	366	<b>0.00012</b>
Girls (4-14 years)	NW children		OB children		p-value
	Mean (SEM)	n	Mean (SEM)	n	
Birth weight, g	3434.72 (14.24)	968	3547.54 (25.45)	480	<b>&lt;0.0001</b>
Birth weight SDS	0.02 (0.03)	968	0.27 (0.06)	480	<b>&lt;0.0001</b>
Birth length, cm	50.11 (0.07)	962	50.62 (0.12)	479	<b>&lt;0.0001</b>
Birth length SDS	-0.62 (0.03)	962	-0.41 (0.05)	479	<b>0.00021</b>
Paternal BMI, kg/m <sup>2</sup>	26.06 (0.16)	539	29.31 (0.36)	235	<b>&lt;0.0001</b>
Maternal BMI, kg/m <sup>2</sup>	24.24 (0.18)	626	30.71 (0.44)	297	<b>&lt;0.0001</b>
Paternal height, cm	180.1 (0.29)	605	177.96 (0.46)	310	<b>&lt;0.0001</b>
Maternal height, cm	167.71 (0.26)	642	166.46 (0.37)	354	<b>0.0047</b>

Birth-related, parental and socioeconomic parameters of children who were obese (OB) or normal-weight (NW) between ages of 4-14.99 years were compared using unpaired t-test (two-sided) with Holm-Šidák correction for multiple comparison. Data are presented as mean with standard error of the mean (SEM). Unadjusted *p*-values are shown. *P*-values are highlighted in bold when remaining <0.05 after adjustment for multiple testing. SEM, standard error of the mean; n, number of individuals; SDS, standard deviation score; BMI, body mass index. This table was adopted from Kempf *et al.*, *eClinicalMedicine* 2021 [1].

**Table S7. Mean age of pubertal stages and onset of menarche in children with underweight, normal-weight, overweight or obesity older than 5 years**

	UW		NW		OW		OB		NW vs. UW	NW vs. OW	NW vs. OB	
Pubertal stage/ menarche	Age, y (SEM)	n	Age, y (SEM)	n	Age, y (SEM)	n	Age, y (SEM)	n	p-value	p-value	p-value	
<b>Boys</b>	P1	8.75 (0.2)	129	8.36 (0.06)	1133	9.55 (0.19)	11	8.96 (0.11)	29	<b>&lt; 0.0001</b>	<b>&lt; 0.0001</b>	<b>&lt; 0.0001</b>
	P2	11.82 (0.3)	43	11.03 (0.1)	320	11.33 (0.17)	85	11.58 (0.12)	18	<b>&lt; 0.0001</b>	<b>0.00070</b>	<b>&lt; 0.0001</b>
	P3	14.16 (0.52)	7	13.22 (0.15)	86	13.12 (0.39)	21	13.16 (0.14)	83	<b>&lt; 0.0001</b>	0.63	<b>0.0079</b>
	P4	15.58 (0.35)	13	14.77 (0.1)	140	14.46 (0.24)	19	14.35 (0.15)	74	<b>&lt; 0.0001</b>	<b>0.00053</b>	<b>&lt; 0.0001</b>
	P5	15.59 (0.16)	20	15.48 (0.05)	300	15.23 (0.17)	36	15.33 (0.13)	10	0.0075	<b>&lt; 0.0001</b>	<b>&lt; 0.0001</b>
<b>Girls</b>	P1	8.51 (0.20)	100	7.64 (0.06)	952	8.42 (0.18)	80	7.82 (0.11)	23	<b>&lt; 0.0001</b>	<b>&lt; 0.0001</b>	0.094
	P2	11.53 (0.14)	50	10.71 (0.07)	344	10.04 (0.15)	81	9.95 (0.14)	16	<b>&lt; 0.0001</b>	<b>&lt; 0.0001</b>	<b>&lt; 0.0001</b>
	P3	12.54 (0.39)	10	12.14 (0.09)	195	11.53 (0.18)	47	11.76 (0.13)	91	0.3368	<b>0.0039</b>	<b>0.0069</b>
	P4	15.02 (0.23)	19	13.96 (0.13)	188	12.92 (0.30)	26	13.59 (0.14)	10	<b>0.0098</b>	<b>0.0039</b>	0.031
	P5	15.75 (0.19)	30	15.31 (0.05)	492	15.13 (0.13)	80	15.10 (0.09)	30	<b>0.0241</b>	0.17	<b>0.00046</b>
menarche	13.13 (0.22)	39	12.55 (0.05)	466	12.20 (0.15)	71	11.81 (0.07)	31	<b>0.0037</b>	0.023	<b>&lt; 0.0001</b>	

Data are presented as mean age in years (y) with standard error of the mean (SEM) and the number of subjects (n). For each pubertal stage mean ages of normal-weight children were compared with mean ages of children with underweight, overweight or obesity using multiple unpaired t-tests (two-sided) with Holm-Šidák correction for multiple comparison. Unadjusted *p*-values are shown. *P*-values are highlighted in bold when remaining <0.05 after adjustment for multiple testing. UW, underweight; NW, normal-weight; OW, overweight; OB, obese; vs. – versus; SEM, standard error of the mean; y, years; P1-5, Pubertal stage 1-5. This table was adopted from Kempf *et al.*, *eClinicalMedicine* 2021 [1].

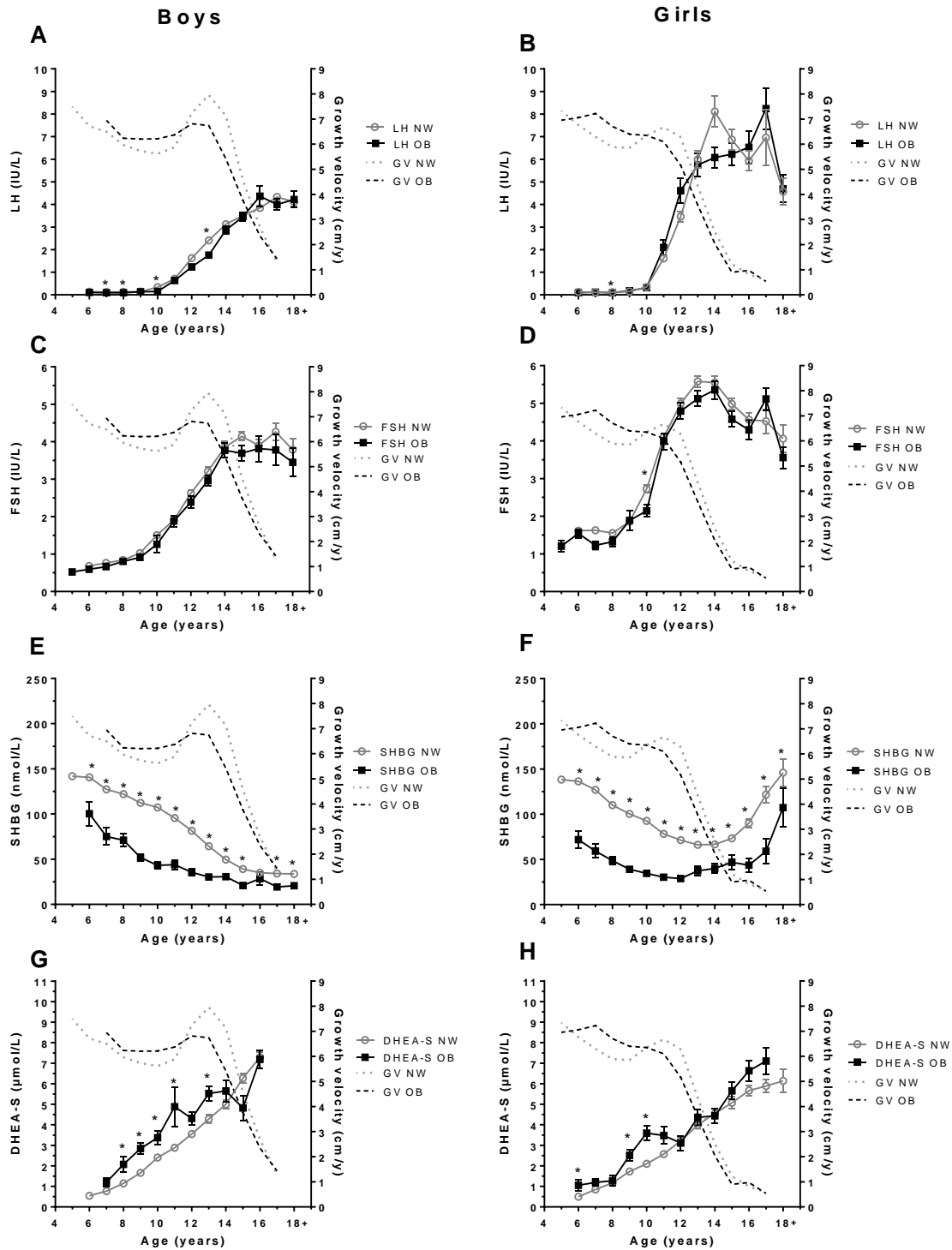


**Figure S6. Serum levels of sex hormones in children with normal-weight and obesity in relation to growth velocities**

Serum sex hormone levels of children with obesity (OB, full black squares) and normal-weight (NW, open grey circles) are presented. The dotted- and dashed-lined curves present the growth velocities (GV) in cm per year for individuals with normal-weight and obesity, respectively, from whom sex steroid measurements were available. Sample sizes are provided in Appendix I, Table S2. A, B: Serum luteinizing hormone (LH); C, D: Serum follicle stimulating hormone (FSH); E, F: Serum sex hormone-binding globulin (SHBG); G, H: Dehydroepiandrosterone sulfate (DHEA-S). Data are shown as mean with standard error; Asterisks (\*) mark significant ( $p < 0.05$ ) differences between NW and OB children assessed by multiple t-tests combined with a Holm-Šidák multiple comparison test. This figure was adopted from Kempf *et al.*, *eClinicalMedicine* 2021 [1].

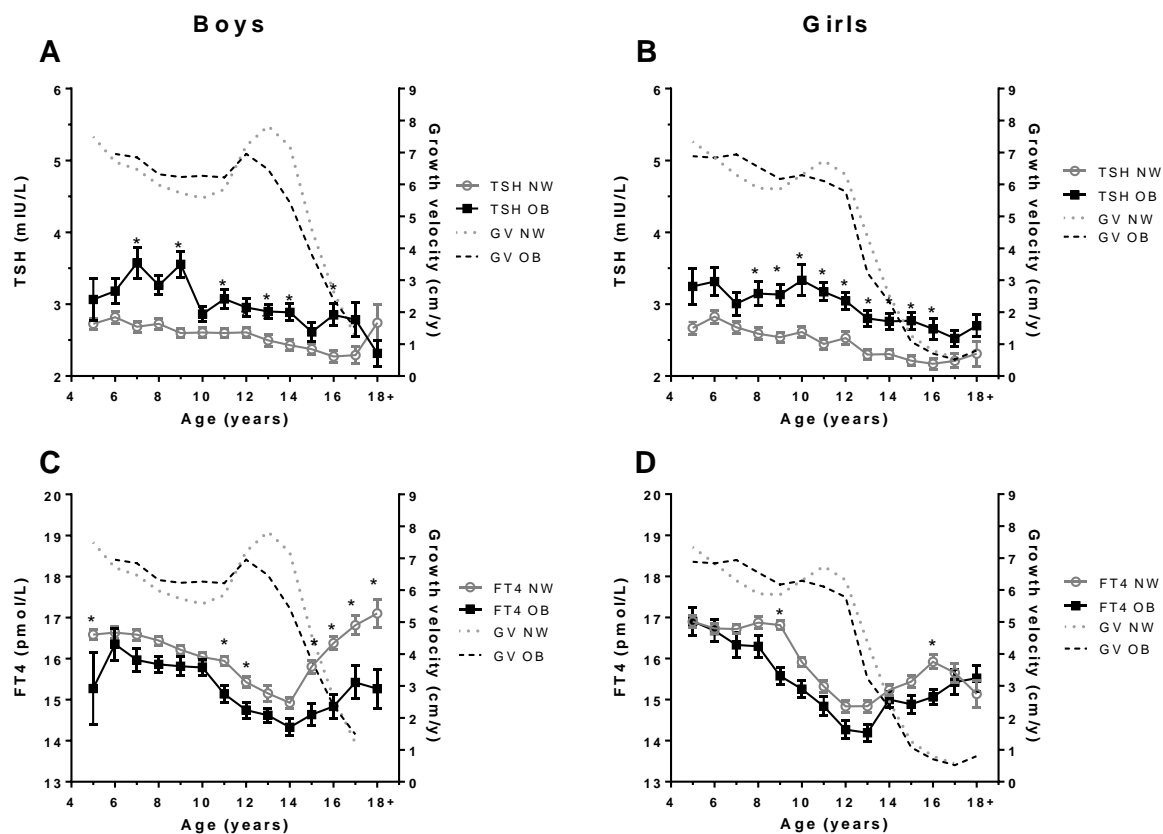


**Figure S7. Serum levels of thyroid hormones in children with normal-weight and obesity in relation to growth velocities**

Serum thyroid hormone levels of children with obesity (OB, full black squares) and normal-weight (NW, open grey circles) are presented. The dotted- and dashed-lined curves present the growth velocities (GV) in cm per year for individuals with normal-weight and obesity, respectively, from whom thyroid hormone measurements were available. Data are shown as mean with standard error; Asterisks (\*) mark significant ( $p < 0.05$ ) differences between NW and OB children assessed by multiple t-tests combined with a Holm-Šidák multiple comparison test. Sample sizes are provided in Appendix I, Table S2. A, B: Serum thyroid-stimulating hormone (TSH); C, D: Serum free thyroxin (FT4). This figure was adopted from Kempf *et al.*, *eClinicalMedicine* 2021 [1].

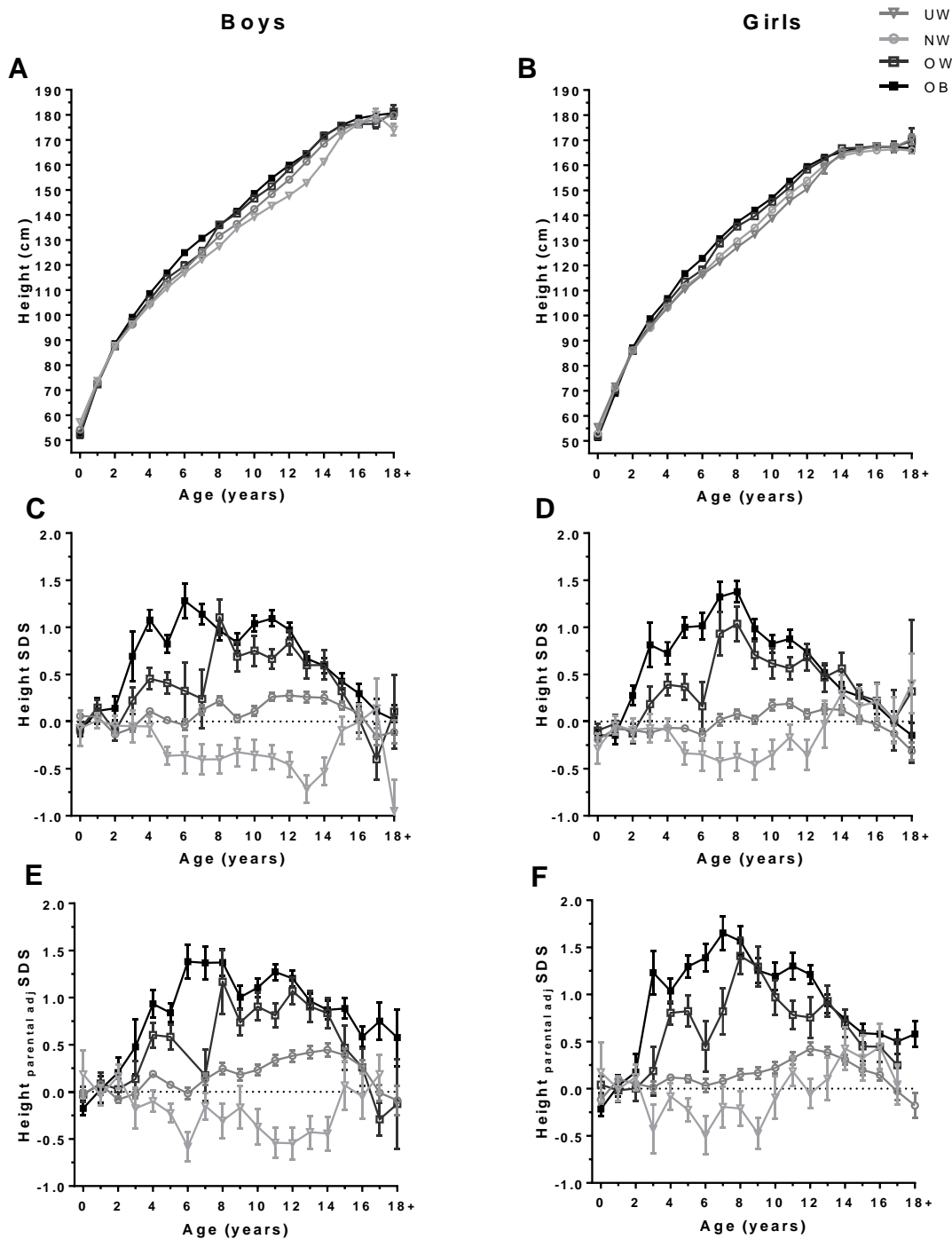


**Figure S8. Height parameters of children with underweight, normal-weight, overweight or obesity**

Parameters of height for children with underweight (UW, grey empty triangles), normal-weight (NW, empty grey circles), overweight (OW, dark grey empty squares) or obesity (OB, full black squares) in the ages from 0-18+ are shown. Sample sizes are provided in Appendix I, Table S2. A, B: Total height; C, D: Height standard deviation score (SDS); E, F: Height SDS relative to mid-parental height SDS ( $\text{Height}_{\text{parental adj}} \text{SDS}$ ). Data are shown as mean with standard error. This figure was adopted from Kempf *et al.*, *eClinicalMedicine* 2021 [1].



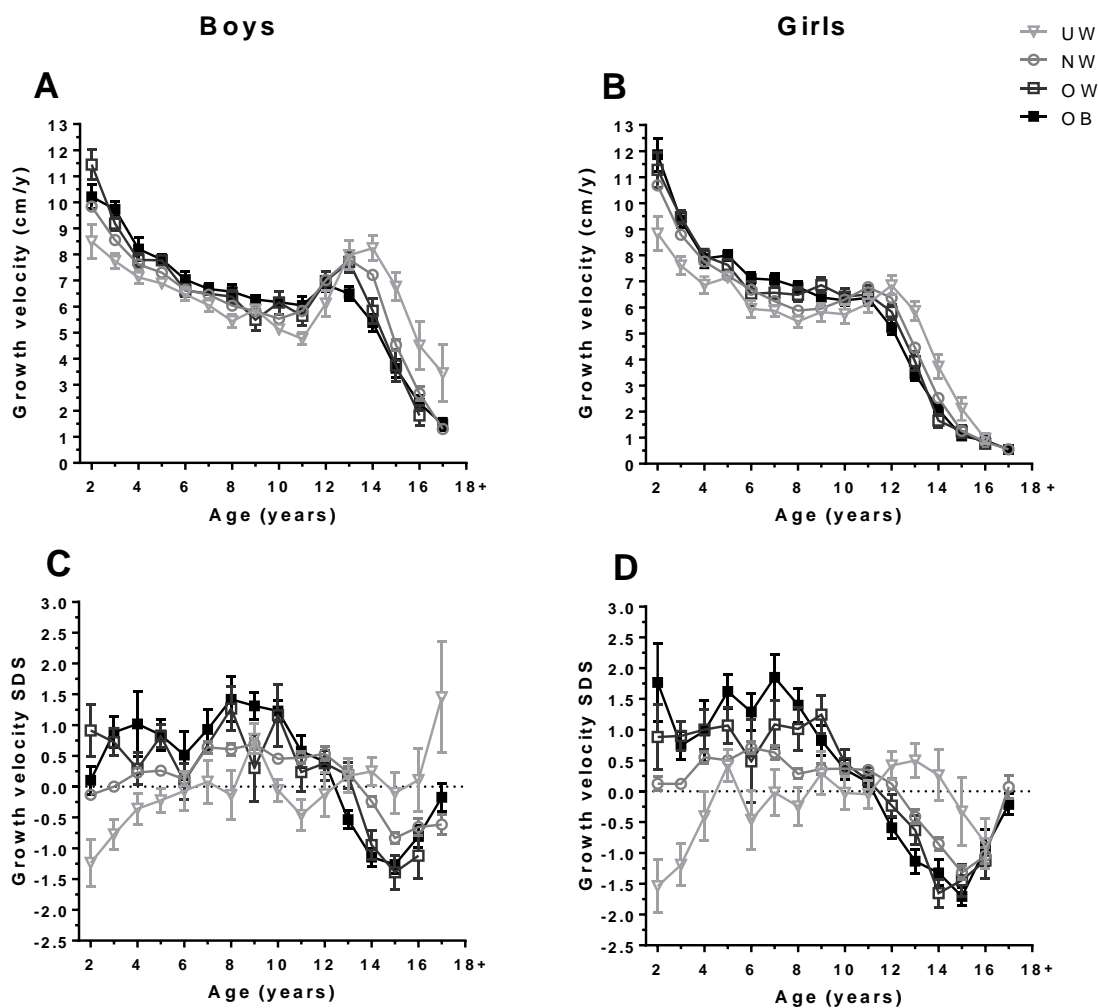


**Figure S9. Growth velocities of children with underweight, normal-weight, overweight or obesity**

Growth velocities for children with underweight (UW, grey empty triangles), normal-weight (NW, empty grey circles), overweight (OW, dark grey empty squares) or obesity (OB, full black squares) are presented. Sample sizes are provided in Appendix I, Table S2. A, B: Growth velocities in cm per year between the ages of 2-18+ years; C, D: Growth velocity standard deviation score (SDS). Data are shown as mean with standard error. This figure was adopted from Kempf *et al.*, *eClinicalMedicine* 2021 [1].

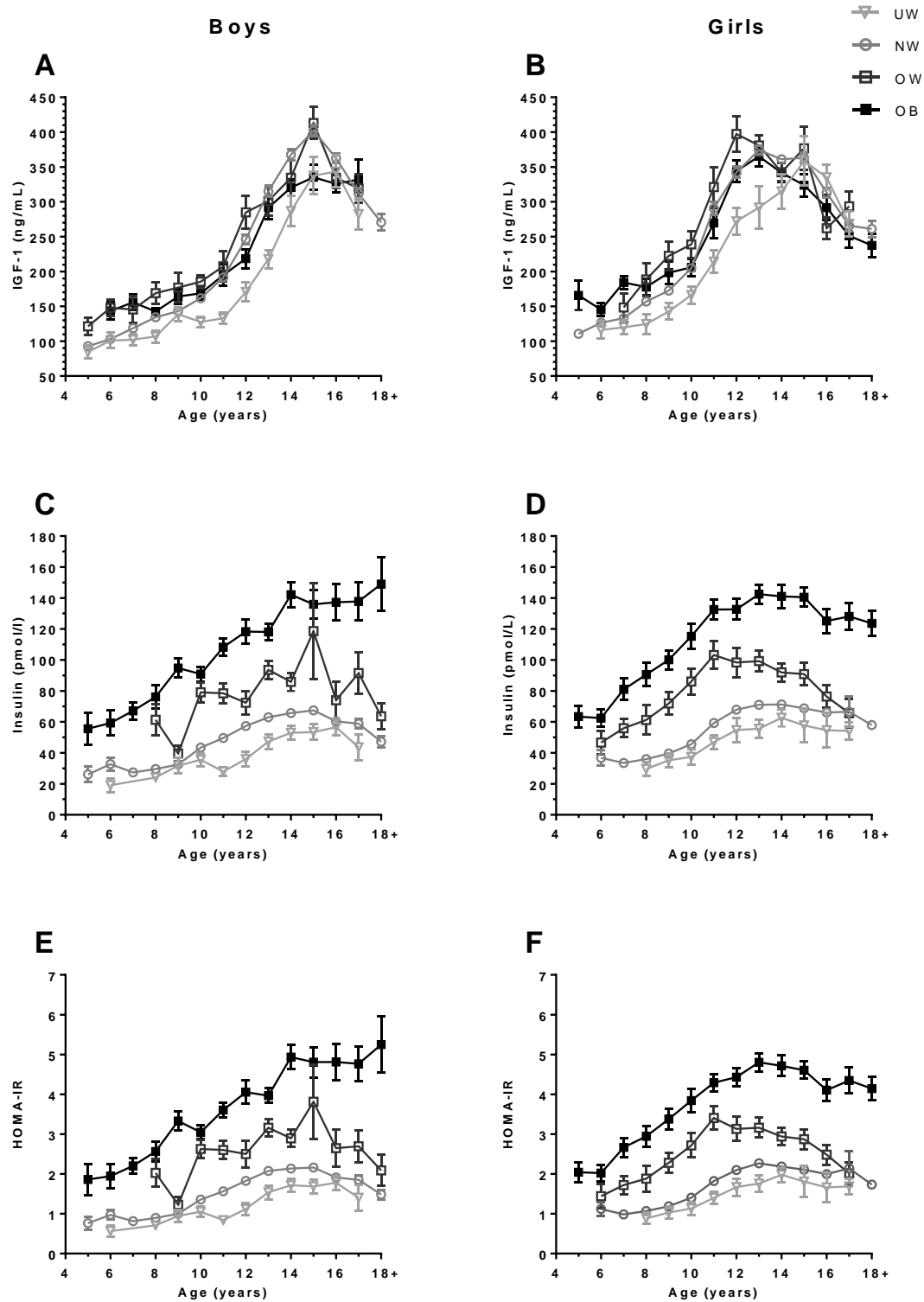


**Figure S10. Serum IGF-1 and metabolic parameters of children with underweight, normal-weight, overweight or obesity**

Serum hormone levels of children with underweight (UW, bright grey open triangle), normal-weight (NW, grey open circles), overweight (OW, dark grey open squares) or obesity (OB, black full squares) aged 5-18 years are presented. Sample sizes are provided in Appendix I, Table S2. A, B: Serum insulin-like growth factor-1 (IGF-1); C, D: Fasting serum insulin; E, F: Homeostatic Model Assessment for Insulin Resistance (HOMA-IR). Data are shown as mean with standard error. This figure was adopted from Kempf *et al.*, *eClinicalMedicine* 2021 [1].

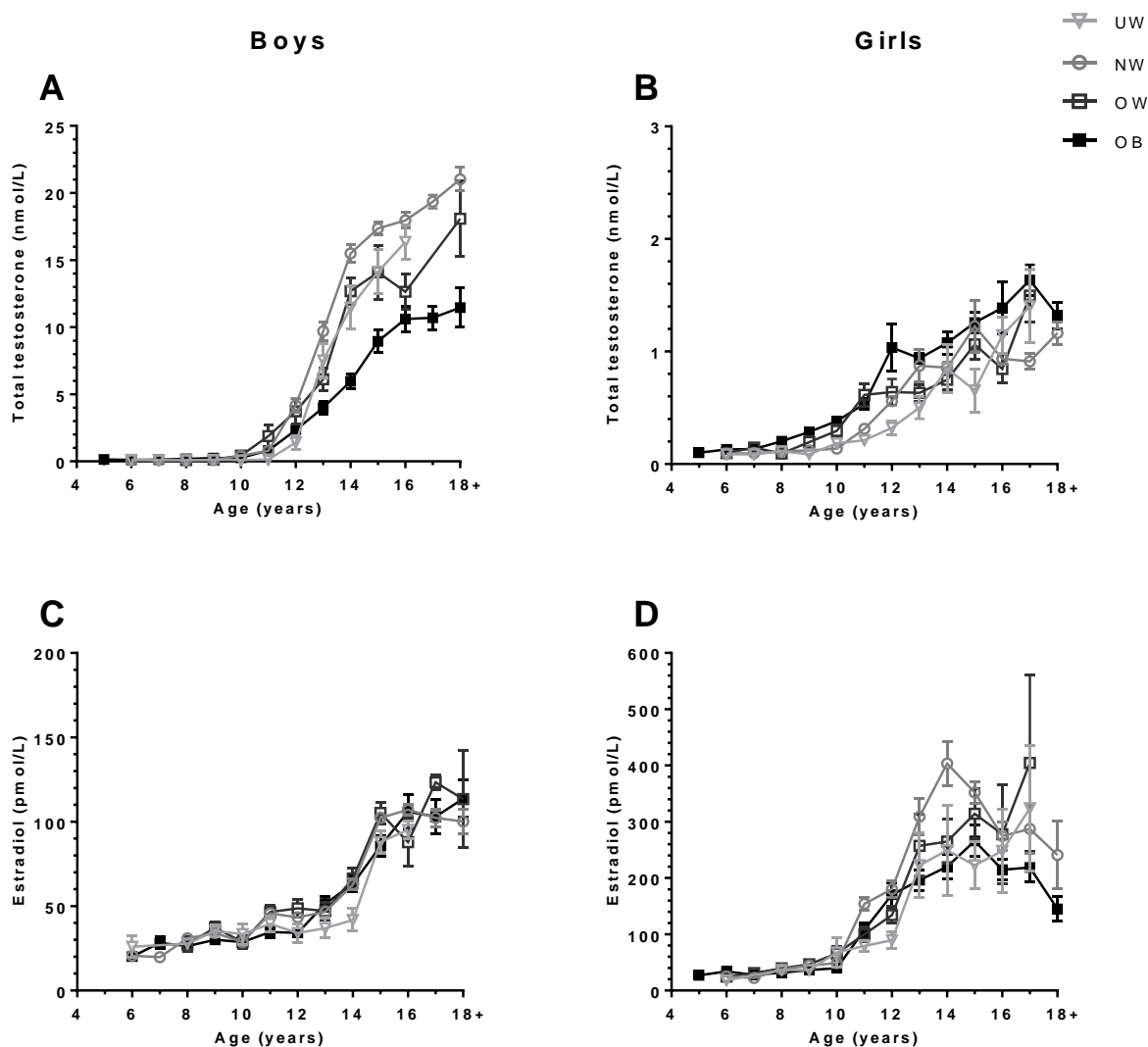


**Figure S11. Serum sex hormone levels of children with underweight, normal-weight, overweight or obesity (I)**

Serum hormone levels of children with underweight (UW, bright grey open triangle), normal-weight (NW, grey open circles), overweight (OW, dark grey open squares) or obesity (OB, black full squares) aged 5-18 years are presented. Sample sizes are provided in Appendix I, Table S2. A, B: Serum testosterone; C, D: Serum estradiol. Data are shown as mean with standard error. This figure was adopted from Kempf *et al.*, *eClinicalMedicine* 2021 [1].

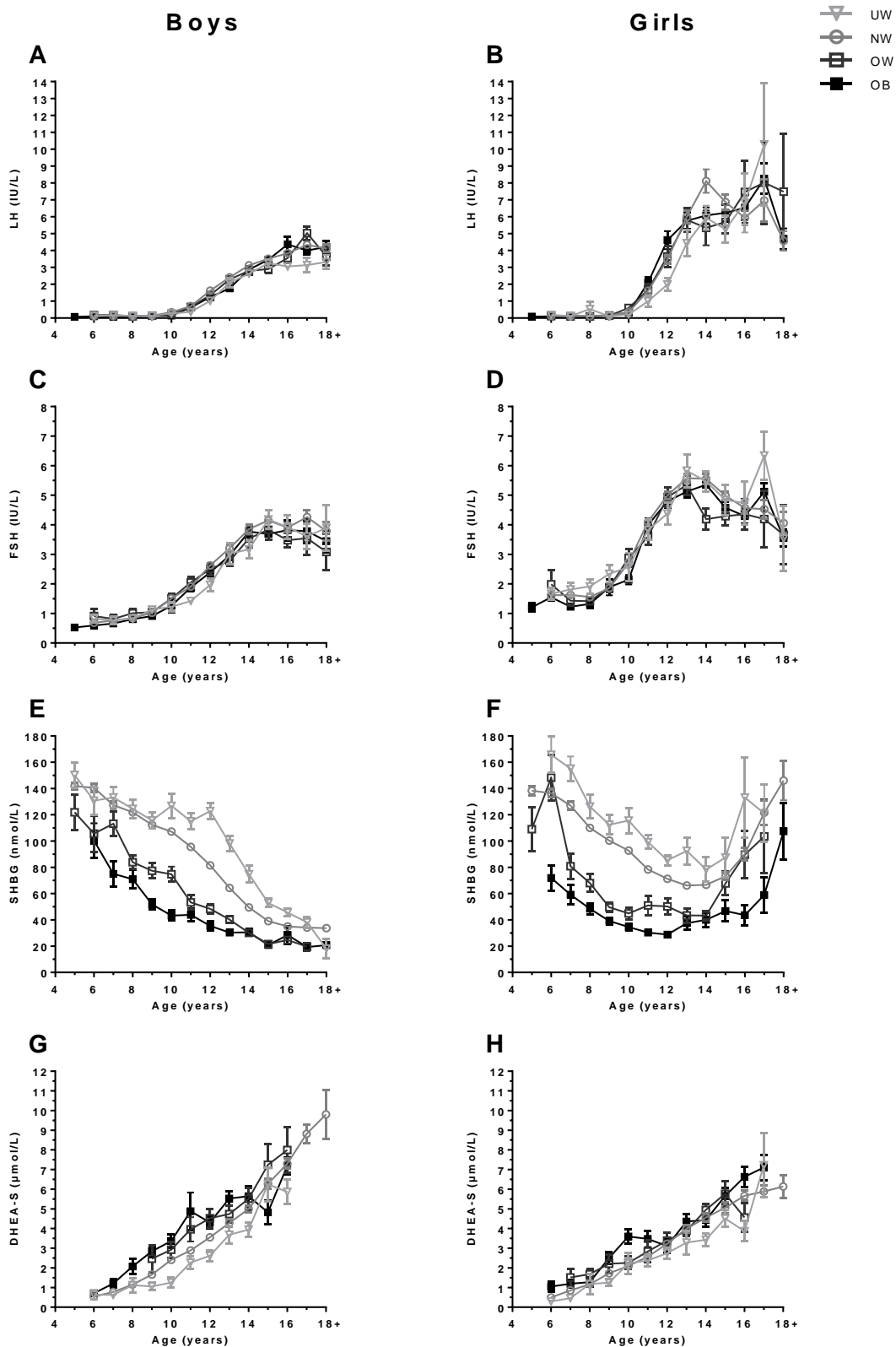


**Figure S12. Serum sex hormone levels of children with underweight, normal-weight, overweight or obesity (II)**

Serum sex hormone levels of children with underweight (UW, bright grey open triangle), normal-weight (NW, grey open circles), overweight (OW, dark grey open squares) or obesity (OB, black full squares) aged 5-18 years are presented. Sample sizes are provided in Appendix I, Table S2. A, B: Serum luteinizing hormone (LH); C, D: Serum follicle stimulating hormone (FSH); E, F: Serum sex hormone-binding globulin (SHBG); G, H: Dehydroepiandrosterone sulfate (DHEA-S). Data are shown as mean with standard error. This figure was adopted from Kempf *et al.*, *eClinicalMedicine* 2021 [1].

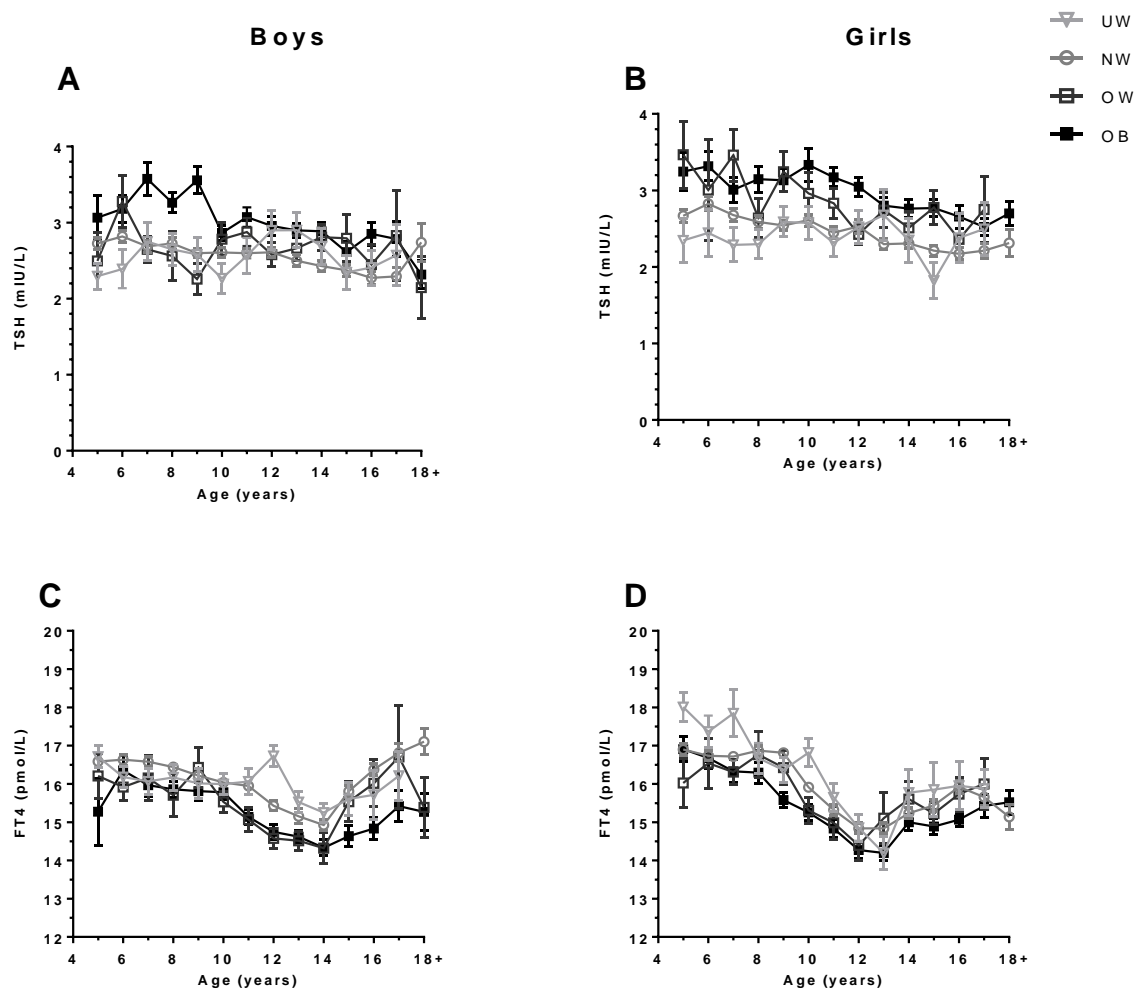


**Figure S13. Serum thyroid hormone levels of children with underweight, normal-weight, overweight or obesity**

Serum thyroid hormone levels of children with underweight (UW, bright grey open triangle), normal-weight (NW, grey open circles), overweight (OW, dark grey open squares) or obesity (OB, black full squares) aged 5-18+ years are presented. Sample sizes are provided in Appendix I, Table S2. A, B: Serum thyroid-stimulating hormone (TSH); C, D: Serum free thyroxine (FT4). Data are shown as mean with standard error. This figure was adopted from Kempf *et al.*, *eClinicalMedicine* 2021 [1].

## B. Study 2

Table S8. Characteristics of the cohort (N=306) and comparison of different parameters between lean children and children with overweight/obesity

Anthropometry	Lean				Overweight/obese				p
	n	mean	SD	range	n	mean	SD	range	
Sex	157	female: 75 (47.8 %), male : 82 (52.2 %)			149	female: 74 (48.7 %), male : 75 (51.3 %)			0.740 <sup>a</sup>
Age	157	11.05	4.80	2 - 18.72	149	12.89	3.63	2.35 - 18.71	<0.001
Height SDS	157	0.03	1.10	-2.47 - 3.07	149	0.65	1.08	-2.23 - 3.3	<0.001
BMI SDS	157	-0.16	0.82	-1.8 - 1.24	149	2.37	0.63	1.32 - 4.34	<0.001
Body weight, kg	157	40.42	18.43	9 - 82.45	149	77.08	24.46	14 - 137.6	<0.001
Pubic hair stage	139	2.75	1.69	1 - 5	139	3.35	1.57	1 - 5	0.001 <sup>a</sup>
Liver fat, % (MRI)	24	1.20	0.64	0.1 - 2.45	28	9.63	12.32	0.3 - 47.78	<0.001 *
Total body fat, % (MRI)	24	20.35	11.09	7.36 - 58.64	27	34.34	8.13	13.42 - 46.21	<0.001
AT mass, kg	81	10.02	6.71	1.94 - 31.25	66	26.61	10.86	4.16 - 60	<0.001 *
Total number of adipocytes x10 <sup>9</sup>	20	23.16	14.78	8.12 - 58.45	30	50.61	20.18	22.13 - 107.14	<0.001 *
Total number of AT-derived SVF cells x10 <sup>9</sup>	18	13.10	11.20	1.83 - 49.46	21	31.49	21.78	7.99 - 95.11	<0.001 *
<b>Serum parameters</b>									
<b>GH axis</b>									
GHBP, ng/mL	145	13.55	2.21	7.66 - 18.92	140	16.01	3.83	8.9 - 28.18	<0.001
IGF-1, ng/mL	107	198.87	117.51	32.3 - 484.6	81	284.19	124.94	38.5 - 549.4	<0.001
IGFBP-3, µg/mL	107	3.97	1.07	1.47 - 6.12	81	4.67	1.01	1.96 - 6.96	<0.001
IGF-1/IGFBP3 molar ratio	107	0.17	0.07	0.06 - 0.36	81	0.21	0.08	0.07 - 0.37	<0.001
<b>Metabolic factors</b>									
Triglycerides, mmol/L	37	0.91	0.47	0.43 - 2.25	56	1.22	0.68	0.5 - 3.74	0.015*
Cholesterol, mmol/L	144	3.88	0.72	2.46 - 6.45	141	4.00	0.80	2.25 - 6.27	0.240*
HDL cholesterol, mmol/L	144	1.35	0.32	0.71 - 2.44	141	1.15	0.27	0.47 - 2.02	<0.001 *
LDL cholesterol, mmol/L	144	2.18	0.55	1 - 3.8	142	2.35	0.65	0.95 - 4.1	0.016*
hsCRP, mg/L	106	0.69	0.75	0.08 - 4.5	75	1.22	0.99	0.08 - 4.5	<0.001 *
TNF-α, pg/mL	104	2.08	0.91	0.52 - 6.02	79	1.98	0.76	0.6 - 4.78	0.511*
ALAT, µkat/L	38	0.26	0.09	0.07 - 0.52	59	0.47	0.35	0.13 - 1.77	<0.001 *
ASAT, µkat/L	38	0.43	0.10	0.24 - 0.73	59	0.46	0.16	0.19 - 0.98	0.233*
Adiponectin, mg/L	106	8.61	4.41	2.1 - 25.6	81	6.10	3.07	1.7 - 15.9	<0.001 *
Leptin, ng/mL	109	6.06	5.25	0.2 - 24.1	84	28.38	22.11	0.6 - 99	<0.001 *
Glucose, mmol/L	107	4.57	0.53	2.47 - 6.06	83	4.66	0.62	3.14 - 6.23	0.280
Insulin, pmol/L	103	43.16	32.89	4.1 - 159.6	79	108.28	70.66	5 - 309.8	<0.001 *
HOMA-IR	103	1.26	1.04	0.13 - 5.64	79	3.22	2.28	0.14 - 10.12	<0.001 *

Differences within each parameter between lean children and children with overweight/obesity have been analysed using student's t-test. Categorical parameters have been compared using the Chi<sup>2</sup>-Test as indicated with <sup>a</sup>. A parameter has been log<sub>10</sub>-transformed for analyses if the *p*-value is marked with an asterisk (\*). *P*-values <0.05 are highlighted in bold. SD, standard deviation; SDS, SD score; AT, adipose tissue; GHBP, growth hormone binding protein; IGF-1, insulin-like growth factor-1; IGFBP-3, IGF-1 binding protein-3; ALAT, alanine aminotransferase; ASAT, aspartate aminotransferase; hsCRP, high sensitive C-reactive protein; HDL, high-density lipoprotein; LDL, low density lipoprotein; TNF-α, tumor necrosis factor alpha; HOMA-IR, Homeostasis Model Assessment for Insulin Resistance; GHR, growth hormone receptor; SVF, stromal vascular fraction. This table was adopted from Kempf *et al.*: Contribution of adipose tissue to alterations in the growth hormone axis in childhood obesity and associations with adipose tissue function. submitted.

**Table S9. Comparison of different parameters regarding the subcutaneous AT between lean children and children with overweight/obesity**

Gene expression levels, [A.U.]	Lean				Overweight/obese				p
	n	mean	SD	range	n	mean	SD	range	
Adipocytes <i>GHR</i>	31	1.20	0.42	0.52 - 1.98	40	0.83	0.37	0.26 - 1.89	<b>&lt;0.001*</b>
Adipocytes <i>IGF-1</i>	31	0.25	0.11	0.07 - 0.51	40	0.16	0.08	0.05 - 0.39	<b>&lt;0.001*</b>
Adipocytes <i>IGFBP-3</i>	31	0.01	0.01	0 - 0.02	40	0.01	0.01	0 - 0.02	0.375*
SVF <i>GHR</i>	31	0.13	0.05	0.05 - 0.26	40	0.10	0.04	0.03 - 0.22	<b>0.036*</b>
SVF <i>IGF-1</i>	31	0.06	0.02	0.03 - 0.14	40	0.06	0.03	0.03 - 0.16	0.390*
SVF <i>IGFBP-3</i>	31	0.11	0.05	0.02 - 0.25	40	0.07	0.04	0.02 - 0.22	<b>&lt;0.001*</b>
Total adipocyte <i>GHR</i> expression *10 <sup>9</sup> per kg BW	15	0.64	0.39	0.26 - 1.45	22	0.59	0.51	0.13 - 1.85	0.712*
Total adipocyte <i>IGF-1</i> expression x10 <sup>9</sup> per kg BW	15	0.12	0.09	0.03 - 0.4	22	0.11	0.07	0.03 - 0.35	0.649*
<b>AT function</b>									
Adipocyte diameter , $\mu\text{m}$	20	114.24	12.01	90.91 - 131.2	29	127.14	13.4 <sub>3</sub>	98.01 - 146.2	<b>0.001</b>
Number of adipocytes per g ATx10 <sup>6</sup>	20	2.19	0.62	1.20 - 3.69	29	1.82	0.52	1.00 - 3.01	<b>0.031*</b>
Macrophages per 100 adipocytes	25	12.12	8.97	0 - 29	32	22.59	22.2 <sub>2</sub>	0 - 115	<b>0.032*</b>
Crown-like structures	25	absent: 20 (80.0%), present: 5 (20.0 %)			32	absent: 12 (37.5 %), present: 20 (62.5 %)			<b>0.001<sup>a</sup></b>
Basal lipolysis of adipocytes	7	0.47	0.19	0.2 - 0.71	11	0.38	0.21	0.18 - 0.74	0.351
Stimulated lipolysis of adipocytes	7	2.07	0.98	0.6 - 3.77	12	2.23	1.32	0.99 - 5.08	0.819*
Doubling time of cells, hours	13	146.20	97.44	30.8 - 366.79	20	110.77	91.6 <sub>8</sub>	17.8 - 303.6	0.181*
Differentiation of SVF cells, %	11	23.85	16.29	4 - 46.62	19	21.76	14.1 <sub>5</sub>	0.24 - 57.65	0.713

Differences within each parameter between lean children and children with overweight/obesity have been analyzed using student's t-test. Categorical parameters have been compared using the Chi<sup>2</sup>-Test as indicated with <sup>a</sup>. A parameter has been log<sub>10</sub>-transformed for analyses if the *p*-value is marked with an asterisk (\*). *P*-values <0.05 are highlighted in bold. SD, standard deviation; SDS, SD score; AT, adipose tissue; GHR, growth hormone receptor; IGF-1, insulin-like growth factor-1; IGFBP-3, IGF-1 binding protein-3; SVF, stromal vascular fraction; BW, body weight. This table was adopted from Kempf *et al.*: Contribution of adipose tissue to alterations in the growth hormone axis in childhood obesity and associations with adipose tissue function. submitted.

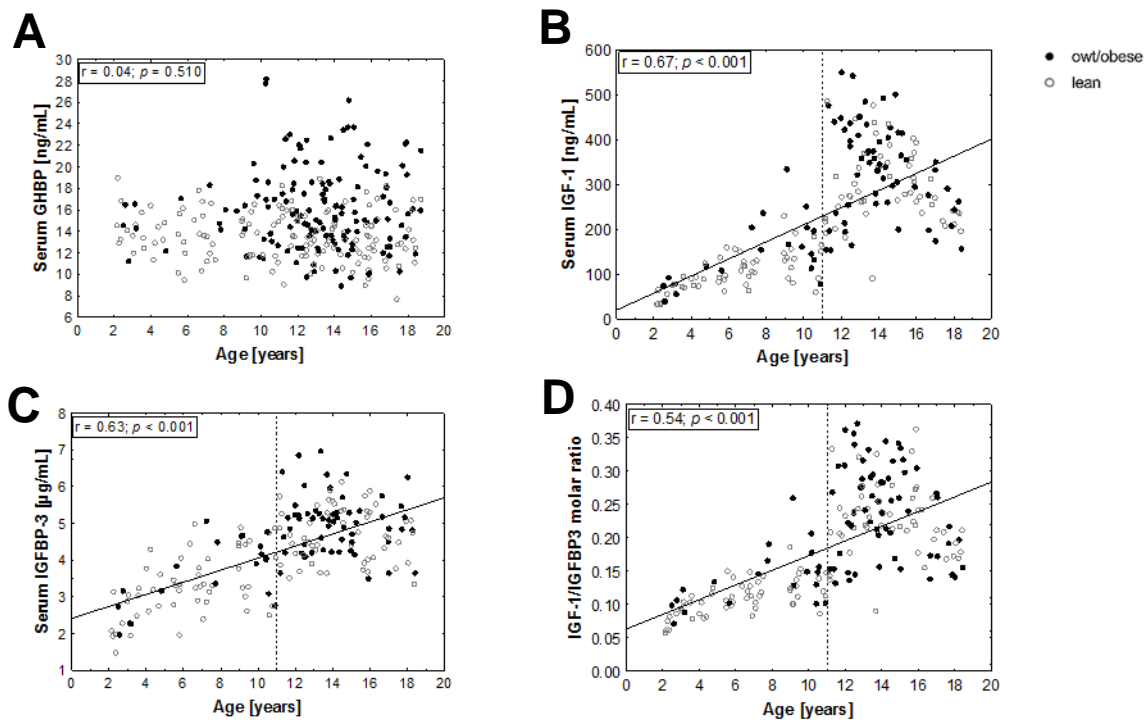


**Figure S14. Serum levels of lean children and children with overweight/obesity across the age**

(A) Growth hormone binding protein (GHBP), (B) insulin-like growth factor 1 (IGF-1), (C) IGF binding protein-3 (IGFBP-3) and (D) the molar ratio of IGF-1 and IGFBP-3 (IGF-1/IGFBP-3) are shown. Regression coefficient  $r$  and  $p$ -value are given and significant correlations with age are marked with a regression line (solid line). For B-D, serum levels showed an approximately linear increase until the age of 10.999 years (identified by visual inspection) and the age cut-off is indicated by dotted lines. This figure was adopted from Kempf *et al.*: Contribution of adipose tissue to alterations in the growth hormone axis in childhood obesity and associations with adipose tissue function. submitted.

**Table S10. Multiple regression analyses on the impact of sex, age and height SDS on serum GHBP, IGF-1 and IGFBP-3 in lean children**

Ages included (years)	Dependent variable	Step	Independent variable	$\Delta r^2$	$\beta \pm SE$	$p$
2-18	<b>Serum GHBP</b> ( $r^2=0.015$ ; $p=0.146$ ; $n=145$ )	1	Age	0.015	$-0.121 \pm 0.083$	0.146
2-10	<b>Serum IGF-1</b> ( $r^2=0.480$ ; $p<0.001$ ; $n=54$ )	1	Age	0.442	$0.662 \pm 0.105$	<b>&lt;0.001</b>
		2	Sex	0.024	$-0.161 \pm 0.105$	0.131
		3	Height SDS	0.014	$0.117 \pm 0.102$	0.255
2-10	<b>Serum IGFBP-3</b> ( $r^2=0.373$ ; $p<0.001$ , $n=54$ )	1	Age	0.302	$0.488 \pm 0.115$	<b>&lt;0.001</b>
		2	Sex	0.56	$-0.244 \pm 0.115$	<b>0.039</b>
		3	Height SDS	0.015	$0.121 \pm 0.112$	0.287
2-10	<b>IGF-1/IGFBP-3</b> ( $r^2=0.382$ ; $p<0.001$ , $n=54$ )	1	Age	0.382	$0.618 \pm 0.109$	<b>&lt;0.001</b>

As independent variables age, sex and height SDS were included. For IGF-1, IGFBP-3 and IGF-1/IGFBP-3, exclusively serum levels of children until the age of 10 years were included to the statistical analyses as until this age serum levels followed an approximately linear pattern (Appendix IIIB, Figure S14).  $P$ -values  $<0.05$  are highlighted in bold. SDS, standard deviation score; GHBP, growth hormone binding protein; IGF-1, insulin-like growth factor-1; IGFBP-3, IGF-1 binding protein-3; IGF-1/IGFBP-3, IGF-1 IGFBP-3 molar ratio;  $\Delta r^2$ ,  $r$  square change;  $\beta \pm SE$ , standardized beta and standard error. This table was adopted from Kempf *et al.*: Contribution of adipose tissue to alterations in the growth hormone axis in childhood obesity and associations with adipose tissue function. submitted.



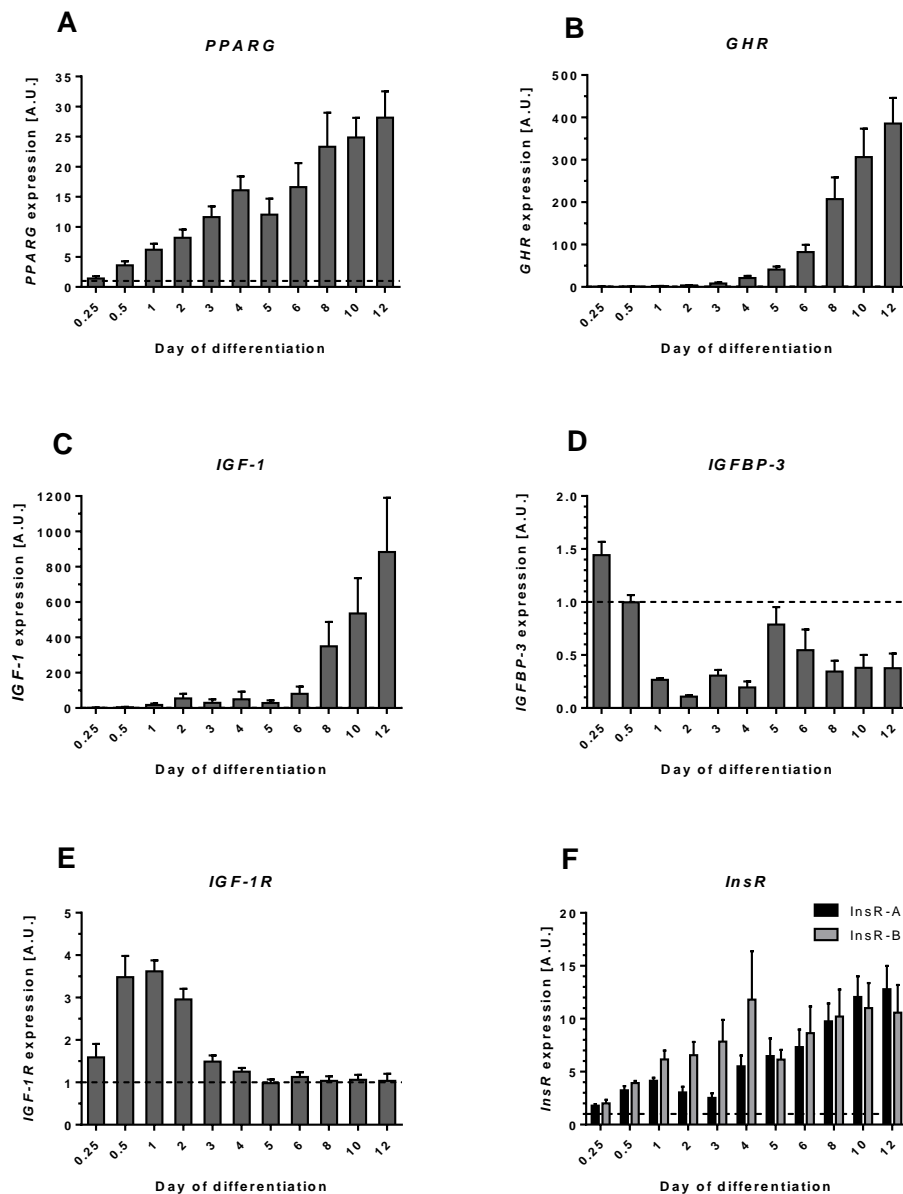


### Figure S15. Gene expression of components of the GH axis during adipocyte differentiation

Gene expression of (A) peroxisome proliferator-activated receptor gamma (*PPARG*), (B) growth hormone receptor (*GHR*), (C) insulin-like growth factor-1 (*IGF-1*), (D) IGF-1 binding protein-3 (*IGFBP-3*), (E) IGF-1 receptor (*IGF-1R*) and (F) insulin receptor isoforms A (*INSR-A*) and B (*INSR-B*) in Simpson-Golabi-Behmel syndrome cells during adipocyte differentiation. Results are given as mean fold change with SEM compared to day 0 of differentiation (dashed line) ( $n=4$ ). Experiments were measured in three technical replicates. One-way ANOVA was performed to identify statistical differences between the different time points of differentiation. For all genes gene expression of at least one time point of differentiation was different to another time point ( $p < 0.0001$ ). This figure was adopted from Kempf *et al.*: Contribution of adipose tissue to alterations in the growth hormone axis in childhood obesity and associations with adipose tissue function. submitted.

**Table S11. Multiple stepwise regression analyses on the impact of sex, age and height SDS on gene expression levels of *GHR*, *IGF-1* and *IGFBP-3* in AT cells in lean children (n=31)**

	Dependent variable	Step	Independent variable	$\Delta r^2$	$\beta \pm SE$	<i>p</i>
<b><i>GHR</i></b>	<b>Adipocytes</b> ( $r^2=0.132$ ; $p=0.044$ )	1	Sex	0.132	$0.363 \pm 0.173$	<b>0.044</b>
	<b>SVF</b> ( $r^2=0.285$ ; $p=0.026$ )	1	Age	0.178	$-0.444 \pm 0.166$	<b>0.013</b>
		2	Height SDS	0.067	$0.280 \pm 0.164$	0.099
		3	Sex	0.041	$-0.208 \pm 0.167$	0.222
<b><i>IGF-1</i></b>	<b>Adipocytes</b> ( $r^2=0.113$ ; $p=0.065$ )	1	Height SDS	0.113	$-0.336 \pm 0.175$	0.065
	<b>SVF</b> ( $r^2=0.194$ ; $p=0.049$ )	1	Age	0.110	$-0.389 \pm 0.173$	<b>0.032</b>
		2	Sex	0.084	$-0.296 \pm 0.173$	0.098
<b><i>IGFBP-3</i></b>	<b>Adipocytes</b> ( $r^2=0.307$ ; $p=0.001$ )	1	Age	0.307	$-0.554 \pm 0.155$	<b>0.001</b>
	<b>SVF</b> ( $r^2=0.301$ ; $p=0.007$ )	1	Age	0.211	$-0.519 \pm 0.161$	<b>0.003</b>
		2	Sex	0.090	$-0.305 \pm 0.1161$	0.068

As independent variables age, sex and height SDS were included. *P*-values <0.05 are highlighted in bold. In contrast to the serum levels, patterns of gene expression in AT cells across age appeared linear for all three genes (data not shown), hence gene expression data from children at ages 2-18 years were analyzed. Gene expression data was  $\log_{10}$ -transformed for analyses. *GHR*, growth hormone receptor; *IGF-1*, insulin-like growth factor-1; *IGFBP-3*, *IGF-1* binding protein-3; *SVF*, stromal vascular fraction;  $\Delta r^2$ , *r* square change;  $\beta \pm SE$ , standardized beta and standard error. This table was adopted from Kempf *et al.*: Contribution of adipose tissue to alterations in the growth hormone axis in childhood obesity and associations with adipose tissue function. submitted.

**Table S12. Correlation between BMI SDS and gene expression levels of *GHR*, *IGF-1* and *IGFBP-3* in adipocytes and *SVF* cells adjusted for age and sex (n=71)**

BMI SDS vs. gene expression of:	<b><i>GHR</i></b>		<b><i>IGF-1</i></b>		<b><i>IGFBP-3</i></b>	
In cell types:	<i>r</i>	<i>p</i>	<i>r</i>	<i>p</i>	<i>r</i>	<i>p</i>
<b>Adipocytes</b>	-0.431	<b>&lt;0.001</b>	-0.417	<b>&lt;0.001</b>	0.088	0.471
<b>SVF</b>	-0.210	0.084	-0.028	0.820	-0.324	<b>0.007</b>

Children from ages 2-18 have been included for all three genes. Gene expression data have been  $\log_{10}$ -transformed for analyses. As the gene expression levels in part were related to age and/or sex in lean children (Appendix IIIB, Table S11) analyses were adjusted to age and sex. *P*-values <0.05 are highlighted in bold. BMI SDS, body mass index standard deviation score; *GHR*, growth hormone receptor; *IGF-1*, insulin-like growth factor-1; *IGFBP-3*, *IGF-1* binding protein-3; *SVF*, stromal vascular fraction. This table was adopted from Kempf *et al.*: Contribution of adipose tissue to alterations in the growth hormone axis in childhood obesity and associations with adipose tissue function. submitted.

## C. Study 3

Table S13. Genetic variants associated with red hair in the patient and her father

Gene	Variant ID	Effect	Associated with red hair	Patient	Father
<i>MC1R</i>	rs1805006	D84E	A	C/C	C/C
<i>MC1R</i>	rs1805007	R151C	T	C/C	C/C
<i>MC1R</i>	rs1110400	I155T	C	T/T	T/T
<i>MC1R</i>	rs1805009	D294H	C	G/G	G/G
<i>MC1R</i>	rs1805008	rg160Trp R160W or	T	C/C	C/C
<i>MC1R</i>	rs34357723	97 kbp from the 5' end of <i>MC1R</i>	T	C/C	C/C
<i>MC1R</i>	rs368507952	R306H	A	G/G	G/G
<i>MC1R</i>	rs200000734	R213W	T	C/C	C/C
<i>MC1R</i>	rs201326893	Y152X	A	C/C	C/C
<i>MC1R</i>	rs11547464	R142H	A	G/G	G/G
<i>MC1R</i>	rs3212379	upstream	T	C/C	C/C
<i>MC1R</i>	rs34474212	S83P	C	T/T	T/T
<i>MC1R</i>	rs34158934	T95M	T	C/C	C/C
<i>MC1R</i>	rs555179612	I182Hfs	TC	C/C	C/C
<i>RALY/ASIP</i>	rs6059655	non-coding	A	G/G	G/G

The affected gene, variant ID, effect and the allele associated with red hair are shown together with the genotypes of patient and her father. *MC1R*, melanocortin receptor 1; *RALY*, RALY heterogeneous nuclear ribonucleoprotein; *ASIP*, agouti-signaling protein. This table was adopted from Kempf *et al.*: A novel human monogenic obesity trait: severe early-onset childhood obesity caused by aberrant overexpression of agouti-signaling protein (*ASIP*), (submitted).

**List of Figures**

Figure 1. The GH axis ..... 3

Figure 2. The leptin-MC4R axis ..... 8

Figure 3. Aims of this thesis ..... 9

Figure 4. Taconic expression vector .....27

Figure 5. Height SDS curves of children with normal-weight and obesity .....34

Figure 6. Growth velocities of children with normal-weight and obesity .....35

Figure 7. Serum IGF-1 and IGFBP-3 levels of children with normal-weight and obesity .....36

Figure 8. Sex hormone levels of children with normal-weight and obesity .....37

Figure 9. Metabolic parameters of children with normal-weight and obesity .....38

Figure 10. Height percentiles for children with obesity compared to population-based reference values.....40

Figure 11. Height, age and serum parameters stratified for pubertal stage in lean children and children with overweight/obesity .....42

Figure 12. Associations of gene expression of *GHR* and *IGF-1* in adipocytes and SVF cells with serum levels.....44

Figure 13. Gene expression of *GHR*, *IGF-1* and *IGFBP-3* in adipose tissue cells in lean children and children with overweight/obesity .....47

Figure 14. Association of *FGFR3* expression in adipose tissue with metabolic parameters ..49

Figure 15. SVF cells from the patient show increased adipogenic potential .....51

Figure 16. *ASIP* expression in the patient and in human tissues.....53

Figure 17. Detection of the ASIP protein .....55

Figure 18. A heterozygous tandem duplication at the *ASIP* locus.....57

Figure 19. Increased ASIP protein is generated from the *ITCH-ASIP* fusion gene.....59

Figure 20. Phenotypic characterization of the patient and her father .....60

Figure 21. Liver and metabolic parameters of the patient .....62

Figure 22. Gene expression of melanocortin receptors in human tissues .....64

Figure 23. Effect of ASIP on lipolysis and differentiation.....65

Figure 24. Effect of ASIP on mitochondrial respiration in SVF cells .....66

Figure 25. Schematic overview of the proposed role of components of the GH axis in childhood obesity and adipose tissue function.....72

**List of Tables**

Table 1. Cells used in this work .....	12
Table 2. Culture media used in this work.....	13
Table 3. Enzymes used in this work .....	14
Table 4. Reagents used in this work.....	15
Table 5. Plasmids used in this work.....	16
Table 6. TaqMan Assays used for quantitative real-time PCR .....	16
Table 7. Primer sequences for quantitative real-time PCR .....	17
Table 8. Primers used for colony PCR or sequencing .....	17
Table 9: Equipment and software used in this work.....	18
Table 10. PCR programs for the 5'-RACE PCR.....	26
Table 11. Primers used for amplification and cloning of <i>ITCH</i> and <i>ASIP</i> sequences.....	27
Table 12. Multiple regression analysis on the effect of BMI SDS on serum levels of GHBP, IGF-1 and IGFBP-3 .....	43
Table 13. Multiple stepwise regression analysis in order to identify predictors for GHBP serum levels.....	45
Table 14. Association of serum GHBP with metabolic and liver parameters .....	46
Table 15. Association of <i>GHR</i> , <i>IGF-1</i> and <i>IGFBP-3</i> expression in adipocytes and SVF cells with AT function.....	48

## **Specification of own scientific contribution**

### Study 1: Alterations in linear growth and endocrine parameters in childhood obesity

**Kempf E**, Vogel M, Vogel T, Kratzsch J, Landgraf K, Kühnapfel A, Gausche R, Gräfe D, Sergejev E, Pfäffle R, Kiess W, Stanik J, Körner A. Dynamic alterations in linear growth and endocrine parameters in children with obesity and height reference values. ***EClinicalMedicine***. 2021; 37:100977

I contributed to the manuscript, under guidance and with help and contribution of all co-authors, by:

- Performing literature research
- Combining data from different study cohorts
- Performing quality control of cohort data
- Defining inclusion and exclusion criteria for the study
- Calculating anthropometric parameters
- Performing statistical analyses (Comparison of children of different weight categories)
- Coordinating the additional statistical analyses with the co-authors
- Preparing of figures and tables
- Writing and revising of the manuscript

Study 2: Growth-related factors and adipose tissue function in childhood obesity

**Kempf E**, Landgraf K, Vogel T, Spielau U, Stein R, Raschpichler M, Kratzsch J, Kiess W, Stanik J, Körner A. Contribution of adipose tissue to alterations in the growth hormone axis in childhood obesity and associations with adipose tissue function. **Submitted.**

I contributed to the manuscript, under guidance and with help and contribution of all co-authors, by:

- Performing literature research
- Defining inclusion and exclusion criteria for the study
- Performing cell culture experiments:
  - Adipogenic differentiation of SGBS cells
  - Isolation of RNA from SGBS cells and reverse transcription into cDNA
- Performing gene expression measurements:
  - In already available cDNA samples from AT, adipocytes and SVF cells from children
  - In cDNA from SGBS cells at different time points during adipogenic differentiation
- Calculating additional variables (total gene expression of adipocytes per kg body weight)
- Performing the statistical analyses
- Preparing of figures and tables
- Writing of the manuscript

Shamsi F, [6 authors], **Kempf E**, [17 authors], Tseng YH. FGF6 and FGF9 regulate *UCP1* expression independent of brown adipogenesis. **Nat Commun.** 2020; 11(1):1421

I spent 6 months in the research group of Prof. Dr. Yu-Hua Tseng (Harvard Medical School, Joslin Diabetes Center Section on Integrative Physiology and Metabolism, Boston, MA, USA). Besides learning how to immortalize SVF cells, I participated in the project investigating FGF6/9 in AT tissue function.

I contributed to the manuscript, under guidance and with help and contribution of all co-authors, by:

- Helping to establish cell culture and animal experiments
- Statistically analyzing gene expression data (preprocessed by Dr. Andreas Kühnapfel (University of Leipzig, Medical Faculty, Institute for Medical Informatics, Statistics and Epidemiology, Leipzig, Germany) from AT from the Leipzig AT Childhood Cohort and preparing figures

Study 3: Ubiquitous *ASIP* expression as a potential novel monogenic trait for obesity and tall stature

**Kempf E**, Stein R, Hilbert A, Jamra RA, Kühnapfel A, Tseng YH, Schöneberg T, Kühnen P, Rayner W, Zeggini E, Kiess W, Blüher M, Landgraf K, Körner A. A novel human monogenic obesity trait: severe early-onset childhood obesity caused by aberrant overexpression of agouti-signaling protein (*ASIP*). **Submitted.**

I contributed to the manuscript, under guidance and with the help and contribution of all co-authors, by:

- Performing literature research
- Planning and performing experiments and statistical analyses:
  - Isolation and cultivation of SVF cells from adipose tissue
  - Immortalization of SVF cells
  - Assessment of proliferation and differentiation capacity of SVF cells
  - Assessment of mitochondrial function
  - Gene expression analyses
  - gDNA copy number analyses
  - 5'-RACE-PCR
  - Molecular cloning and generation of plasmids
  - Transfection of cells
  - Dual luciferase reporter assays
  - Inhibition of the secretory pathway in SVF cells
  - Immunoblotting
- Coordinating additional experiments and analyses with the co-authors
- Preparing of figures and tables
- Writing of the manuscript



## Selbstständigkeitserklärung

### Erklärung über die eigenständige Abfassung der Arbeit

Hiermit erkläre ich, dass ich die vorliegende Arbeit selbstständig und ohne unzulässige Hilfe oder Benutzung anderer als der angegebenen Hilfsmittel angefertigt habe. Ich versichere, dass Dritte von mir weder unmittelbar noch mittelbar eine Vergütung oder geldwerte Leistungen für Arbeiten erhalten haben, die im Zusammenhang mit dem Inhalt der vorgelegten Dissertation stehen, und dass die vorgelegte Arbeit weder im Inland noch im Ausland in gleicher oder ähnlicher Form einer anderen Prüfungsbehörde zum Zweck einer Promotion oder eines anderen Prüfungsverfahrens vorgelegt wurde. Alles aus anderen Quellen und von anderen Personen übernommene Material, das in der Arbeit verwendet wurde oder auf das direkt Bezug genommen wird, wurde als solches kenntlich gemacht. Insbesondere wurden alle Personen genannt, die direkt an der Entstehung der vorliegenden Arbeit beteiligt waren. Die aktuellen gesetzlichen Vorgaben in Bezug auf die Zulassung der klinischen Studien, die Bestimmungen des Tierschutzgesetzes, die Bestimmungen des Gentechnikgesetzes und die allgemeinen Datenschutzbestimmungen wurden eingehalten. Ich versichere, dass ich die Regelungen der Satzung der Universität Leipzig zur Sicherung guter wissenschaftlicher Praxis kenne und eingehalten habe.

.....  
Datum

.....  
Unterschrift

**Curriculum Vitae**

due to data protection reasons removed

**Curriculum Vitae**

due to data protection reasons removed

## Publications and conference contributions

### JOURNAL PUBLICATIONS

Hanschkow M, Boulet N, **Kempf E**, Bouloumié A, Kiess W, Stein R, Körner A, Landgraf K. Expression of the adipocyte progenitor markers MSCA1 and CD36 is associated with adipose tissue function in children. *JCEM*. 2021; dgab630; Epub ahead of print.

**Kempf E**, Vogel M, Vogel T, Kratzsch J, Landgraf K, Kühnapfel A, Gausche R, Gräfe D, Sergejev E, Pfäffle R, Kiess W, Stanik J, Körner A. Dynamic alterations in linear growth and endocrine parameters in children with obesity and height reference values. *EClinicalMedicine*. 2021; 37:100977

Shamsi F, Xue R, Huang TL, Lundh M, Liu Y, Leiria LO, Lynes MD, **Kempf E**, Wang CH, Sugimoto S, Nigro P, Landgraf K, Schulz T, Li Y, Emanuelli B, Kothakota S, Williams LT, Jessen N, Pedersen SB, Böttcher Y, Blüher M, Körner A, Goodyear LJ, Mohammadi M, Kahn CR, Tseng YH. FGF6 and FGF9 regulate UCP1 expression independent of brown adipogenesis. *Nat Commun*. 2020; 11(1):1421

Vogel T, **Kempf E**, Stanik J, Körner A. Unterschiedliche Wachstumsverläufe von Kindern mit Übergewicht im Vergleich zu normalgewichtigen Kindern. *Kinder- und Jugendmedizin*. 2018; 18(03):182-189

### UNPUBLISHED MANUSCRIPTS

**Kempf E**, Stein R, Hilbert A, Jamra RA, Kühnapfel A, Tseng YH, Schöneberg T, Kühnen P, Rayner W, Zeggini E, Kiess W, Blüher M, Landgraf K, Körner A. A novel human monogenic obesity trait: severe early-onset childhood obesity caused by aberrant overexpression of agouti-signaling protein (*ASIP*). **Submitted**.

**Kempf E**, Landgraf K, Vogel T, Spielau U, Stein R, Raschpichler M, Kratzsch J, Kiess W, Stanik J, Körner A. Contribution of adipose tissue to alterations in the growth hormone axis in childhood obesity and associations with adipose tissue function. **Submitted**.

## CONFERENCE CONTRIBUTIONS

### Talks:

A new stromal vascular cell line from white adipose tissue exhibits enhanced adipogenesis; **2nd International Symposium of the CRC 1052 “Obesity Mechanisms”**, Leipzig, Germany; 2019.

### Poster presentations:

Characterization of subcutaneous stromal vascular cells in order to establish new cell models for human adipogenesis; **Keystone Symposia: Obesity and Adipose Tissue Biology (J7)**, Banff, Alberta, Canada; 2019

A new stromal vascular cell line from white adipose tissue exhibits enhanced adipogenesis; **EMBO Workshop, Organ crosstalk in energy balance and metabolic disease**, Sancti Petri, Chiclana, Cádiz, Spain; 2019.

Children with obesity are taller in early childhood with subsequent catch-down growth until adolescence; **European Society for Paediatric Endocrinology, 57th Annual ESPE Meeting 2018**, Athens, Greece; 2018

## **Acknowledgement**

First, I would like to thank, Prof. Dr. Antje Körner, for the opportunity to work on those highly interesting projects, the constant guidance, support, motivation, patience and trust. I also want to express my sincere gratitude and appreciation to Dr. Kathrin Landgraf for her continuous guidance, support, encouragement and her invaluable advice and expertise in all stages. This entire work would not have been possible without their input and mentoring, not only in terms of scientific work, but also in terms of personal development.

I also want to express gratitude to Dr. Juraj Stanik for his guidance and encouragement and thank in particular Antje Berthold as well as Nathan Fekade and Roy Tauscher, for their profound help in the lab and with questions of all issues. I also want to thank Dr. Robert Stein for his advice regarding medical aspects, Dr. Ulrike Spielau, Martha Hanschkow, Tim Vogel and Paula Boczki for their support, input and help. I furthermore want to thank all colleagues from the Pediatric Research Center and specifically AG Kiess.

I want to thank all collaborators and co-authors of the manuscripts, with particular emphasis on Prof. Dr. Wieland Kiess, Dr. Mandy Vogel, Dr. Andreas Kühnapfel, Prof. Dr. Jürgen Kratzsch, Ruth Gausche, Dr. Daniel Gräfe and Prof. Dr. Anja Hilbert, who enriched the studies a lot with data, genetic and statistical analyses and their expertise and advice.

Special thanks to Prof. Dr. Yu-Hua Tseng and her group, with sincere gratitude to Dr. Farnaz Shamsi, for supervising and teaching me during my research stay at the Joslin Diabetes Center.

I thank the physicians, researchers, bioinformaticians and technical assistants in the LIFE Child Study, the Leipzig Obesity Childhood Cohort, the Leipzig Atherobesity Childhood Cohort, the Leipzig Adipose Tissue Childhood Cohort and the CrescNet registry, who performed the clinical examinations, data collection, laboratory measurements and who provided the data. I sincerely thank all children and parents, who participated in the studies.

For financial support I thank the European Society for Pediatric Endocrinology (ESPE) for receiving the Early Career Scientific Development Award and the European Foundation for the Study of Diabetes (EFSD) for receiving the Albert Renold Travel Fellowship.

Finally, I would like to thank my family and friends and all the people, whom I did not mention here, but who contributed to this work in a scientific way or who supported me during this time.